

INFORMATION TO USERS

This manuscript has been reproduced from the microfilm master. UMI films the text directly from the original or copy submitted. Thus, some thesis and dissertation copies are in typewriter face, while others may be from any type of computer printer.

The quality of this reproduction is dependent upon the quality of the copy submitted. Broken or indistinct print, colored or poor quality illustrations and photographs, print bleedthrough, substandard margins, and improper alignment can adversely affect reproduction.

In the unlikely event that the author did not send UMI a complete manuscript and there are missing pages, these will be noted. Also, if unauthorized copyright material had to be removed, a note will indicate the deletion.

Oversize materials (e.g., maps, drawings, charts) are reproduced by sectioning the original, beginning at the upper left-hand corner and continuing from left to right in equal sections with small overlaps.

Photographs included in the original manuscript have been reproduced xerographically in this copy. Higher quality 6" x 9" black and white photographic prints are available for any photographs or illustrations appearing in this copy for an additional charge. Contact UMI directly to order.

**ProQuest Information and Learning
300 North Zeeb Road, Ann Arbor, MI 48106-1346 USA
800-521-0600**

UMI[®]

NOTE TO USERS

Page(s) not included in the original manuscript and are unavailable from the author or university. The manuscript was microfilmed as received.

116-120

This reproduction is the best copy available.

UMI[®]

**SORPTIVE DYNAMICS AND FLUORESCENCE PROPERTIES OF
ORGANIC CARBON WITHIN
COASTAL SEDIMENTARY ENVIRONMENTS**

by

TOMOKO KOMADA

**A Dissertation submitted to the
Graduate School-New Brunswick
Rutgers, The State University of New Jersey
in partial fulfillment of the requirements**

for the degree of

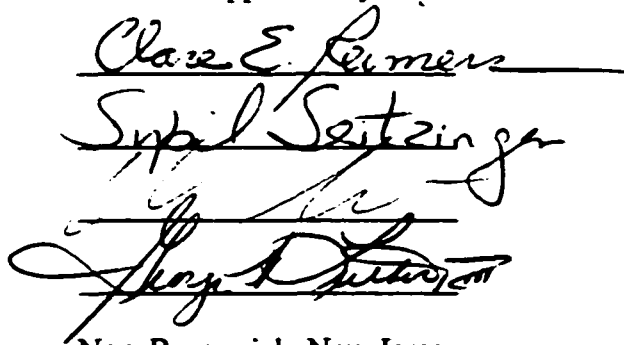
Doctor of Philosophy

Graduate Program in Oceanography

written under the direction of

Clare E. Reimers

and approved by

Three handwritten signatures are stacked vertically. The top signature is 'Clare E. Reimers', the middle is 'Sybil Seitzinger', and the bottom is 'Roy D. Anderson'. Each signature is written in black ink and is positioned above a horizontal line.

New Brunswick, New Jersey

January, 2002

UMI Number: 3046750

**Copyright 2002 by
Komada, Tomoko**

All rights reserved.

UMI[®]

UMI Microform 3046750

**Copyright 2002 by ProQuest Information and Learning Company.
All rights reserved. This microform edition is protected against
unauthorized copying under Title 17, United States Code.**

**ProQuest Information and Learning Company
300 North Zeeb Road
P.O. Box 1346
Ann Arbor, MI 48106-1346**

© 2002

Tomoko Komada

ALL RIGHTS RESERVED

ABSTRACT OF THE DISSERTATION

**Sorptive dynamics and fluorescence properties of
organic carbon within coastal sedimentary environments**

by TOMOKO KOMADA

Dissertation Director:

Clare E. Reimers

Sorptive behavior and fluorescence characteristics of organic carbon (OC) were examined in Hudson River Estuary and Inner New York Bight sediments, with the overall goal of understanding the nature and biogeochemical role of the fraction of particulate OC (POC) that readily exchanges with dissolved OC (DOC). In two studies, the significance of sorption and fundamental properties of the readily-exchangeable POC fraction were investigated under laboratory conditions simulating bottom resuspension. In the third study, the role of sorption in controlling pore-water DOC cycling was evaluated within the sediment column.

In order to simulate resuspension, surface sediments were dispersed in bottom water from the same locations for 30 seconds to 2 hours. After resuspension, DOC

concentration generally exceeded the value predicted by conservative mixing of pore and bottom waters, indicating net release of OC from POC. Regression analyses between the amount of OC released and the POC content of sediment density fractionates suggest that $\leq 0.3\%$ of the mineral-bound POC pool may be readily releasable into solution across the estuarine gradient

In the second study, chemical characteristics of the OC released into solution during the resuspension experiments were explored through excitation-emission matrix (EEM) fluorescence spectroscopy. Examination of EEMs revealed that relative to values predicted by conservative mixing, resuspension resulted in: (1) more intense humic-like fluorescence; and (2) proportionally greater fluorescence in the longer wavelength region of the electromagnetic spectrum. Trends in the literature data strongly suggest fluorophores that emit at longer wavelengths to be increasingly degraded. The data therefore imply that resuspension results in net release of degraded, mineral-bound organic matter from the sediment matrix into solution.

In order to evaluate the significance of sorptive processes within the sediment column, a diagenetic model was applied to DOC profiles determined within the study area. OC was assumed to undergo linear equilibrium adsorption, with a coefficient that was estimated from the results of the first study. Model calculations show that sorption is unlikely to be a major factor controlling pore-water DOC accumulation patterns. Rather, redox-dependent microbial processes and sediment mixing most often dominate DOC cycling within the benthos.

ACKNOWLEDGEMENTS

This work would have been impossible without the support, guidance, and friendship of many people. First and foremost, I wish to thank my advisor Clare Reimers for her unending support during my years as a graduate student. Ever since I became interested in the idea of sorptive preservation (as a result of reading two papers Clare picked for a journal club meeting), she continued to encourage me to pursue my own ideas, and helped me stay on the right track. I am also indebted to the dissertation committee members, Sybil Seitzinger, Oscar Schofield, and George Luther, III, for their support, many helpful discussions, insightful comments and ideas, and words of encouragement.

Many people provided help and taught me new techniques both in the laboratory and in the field: Wei Wang, Renée Styles, Char Fuller, Ron Lauck, Jay Cullen, Paul Field, Michal Koblizek, Kevin Wyman, Brian Lettini, Jeff Pace, Maria Calisto, Martial Taillefert (Univ. Georgia) and Tim Rozan (Univ. Delaware). M. Buchholz ten Brink (USGS) provided ship-time in the Inner New York Bight, and taught me the ins and outs of handling a sediment core. With my rusty calculus, it would have been impossible to solve diagenetic equations without the help of Enrique Curchitser, Byoung-Ju Choi, and Fadli Syamsudin. I am also grateful to David Burdige (Old Dominion Univ.) for kindly providing me with his pore-water DOM model.

My life as a graduate student would have been very different if it were not for Hilairy Hartnett and Susan Boehme, who provided invaluable support in various ways – both in and out of the lab – particularly in the last two years. Tracy Wiegner was always

willing to listen and helped me get over some tough times. Finally, I thank my family for their continued support, Caza and Hoss for reminding me to go out and play, and Tim Otto for always being my true and very best friend.

This research was funded by the National Undersea Research Program, Hudson River Foundation, and the Office of Naval Research, and the Institute of Marine and Coastal Sciences at Rutgers.

TABLE OF CONTENTS

ABSTRACT OF THE DISSERTATION	ii
ACKNOWLEDGEMENTS	iv
LIST OF TABLES	ix
LIST OF FIGURES	xi
CHAPTER 1: INTRODUCTION	1
CHAPTER 2: RESUSPENSION-INDUCED PARTITIONING OF ORGANIC CARBON BETWEEN SOLID AND SOLUTION PHASES FROM A RIVER-OCEAN TRANSITION	6
Abstract	6
Introduction	7
Materials and methods	9
Sample site description	9
Sample collection	10
Resuspension experiments	11
Analyses	14
Diffusive flux calculations	15
Results	16
Biogeochemical characteristics of the study area	16
Resuspension experiment results	19
Discussion	20

Sources for the OC released during resuspension	20
Geochemical significance of resuspension-induced OC release	22
CHAPTER 3: FLUORESCENCE CHARACTERISTICS OF ORGANIC MATTER RELEASED FROM	
COASTAL SEDIMENTS DURING RESUSPENSION	45
Abstract	45
Introduction	46
Materials and methods	49
Sample collection	49
Analyses	50
Resuspension experiments	52
Results	54
Fluorescence characteristics of non-experimental bottom and pore waters	54
Fluorescence characteristics of organic matter released from the solid phase....	56
Discussion	59
Nature of the long-wavelength peak fluorophore	59
Possible source for the long-wavelength peak fluorophore	62
Geochemical implications	63
CHAPTER 4: FACTORS AFFECTING DISSOLVED ORGANIC MATTER DYNAMICS IN SUBOXIC TO	
ANOXIC COASTAL SEDIMENTS	77
Abstract	77
Introduction	78
Development of a coupled DOC-DIC model	80
Data set	83

Station locations, sampling, and analyses	83
Pore water and solid phase profiles	84
Partitioning of OC between pore water and sediment particles	88
Model application and discussion	89
Model fit to a non-bioturbated/irrigated sediment (Shelf-3)	90
Application to bioturbated sediments	93
Significance of adsorption/desorption on sediment DOC cycling	95
Additional controls on pore-water DOC distribution: Potential role of Fe	96
Concluding remarks	98
CHAPTER 5: SUMMARY	116
APPENDICES	121
BIBLIOGRAPHY	125
CURRICULUM VITA	133

LIST OF TABLES

TABLE 2.1	Summary of station locations and bottom characteristics	28
TABLE 2.2	Summary of resuspension experiment conditions	29
TABLE 2.3	POC and total nitrogen content and specific mineral surface area of homogenized surficial sediments	30
TABLE 2.4	Calculated molecular diffusive fluxes by sediment diagenesis and measured net DOC releases during sediment resuspension experiments	31
TABLE 2.5	Linear regression coefficient R^2 and P value among various environmental parameters	32
TABLE 2.6	Derivation of estimated sediment resuspension rates and associated release of OC into Lower New York-Raritan Bay complex and the Hudson River Estuary	33
TABLE 3.1	Fluorescence peak types and corresponding ranges in Ex/Em-max as reported by Coble et al. (1998)	65
TABLE 3.2	Fluorescence peak positions that lie to the red of the visible humic-like region C	66
TABLE 4.1	List of symbols used in the coupled DOC-DIC model	99
TABLE 4.2	Summary of station locations and general characteristics	100
TABLE 4.3	Estimated equilibrium partition coefficients of DOC in surficial (uppermost 2 cm) sediments	101

TABLE 4.4 Parameter values used to calculate DOC-DIC model outputs for stations

Shelf-3 and Bay-3 (6/97) 102

LIST OF FIGURES

FIGURE 2.1	Sampling region and station locations	34
FIGURE 2.2	DOC concentrations observed in pore water and bottom water control tubes	35
FIGURE 2.3	OC to total nitrogen ratios of the different density fractionates of surface sediments	36
FIGURE 2.4	Plot of POC content in the high-density fraction against corresponding specific mineral surface area of surface sediments	37
FIGURE 2.5	Depth profiles of measured and expected high-density phase POC for station Bay-3	38
FIGURE 2.6	Pore-water profiles of DIC, DOC and NH_4^+	39
FIGURE 2.7	Net amount of OC released over the course of each extraction period in continuous and series extractions	40
FIGURE 2.8	DOC concentration in the supernatant during 10-minute series extractions	41
FIGURE 2.9	Differences between the observed and predicted concentrations of NH_4^+ and NO_3^- in the supernatant during continuous extractions	42
FIGURE 2.10	Correlation between OC released during 1-hr continuous extractions and POC present in the high-density fraction	43
FIGURE 2.11	A proposed model of the interrelationships among different reservoirs of dissolved and particulate C, applicable to both the sediment and the water column	44

FIGURE 3.1	Visible humic-like peak intensities observed in bottom-water and pore-water control tubes	67
FIGURE 3.2	EEMs of 2-hour test experiment samples after subtraction of predicted EEMs for station Riv-2 and Shelf-2	68
FIGURE 3.3	Contour and surface representations of EEMs of bottom- and pore-water samples from stations Riv-2 and Shelf-1 that were collected and analyzed independently for the extraction experiments	69
FIGURE 3.4	Peak positions observed in various EEMs	70
FIGURE 3.5	Fluorescence intensity of the visible humic-like peak plotted against DOC concentration of bottom and pore waters	71
FIGURE 3.6	Net changes in DOC concentration and humic-like peak intensity in the sample supernatant during continuous extraction experiments	72
FIGURE 3.7	Net changes in DOC concentration and humic-like peak intensity in the sample supernatant during series extraction experiments	73
FIGURE 3.8	Measured, predicted and residual EEMs of 2-hour extraction samples from stations Bay-2 and Shelf-2	74
FIGURE 3.9	Increases in fluorescence intensities of the humic-like peak and the long-wavelength peak against increases in DOC in the sample supernatant ...	75
FIGURE 3.10	Variations in emission ratio, R, with extraction time in continuous experiments and with extraction number in series experiments	76
FIGURE 4.1	A diagrammatic representation of the coupled DOC-DIC model modified after the pore-water DOC model developed by Burdige (in press).....	103

FIGURE 4.2	A schematic describing the relative positioning of the suboxic-anoxic boundary and L in the sediment column	104
FIGURE 4.3	Sampling locations in the Raritan-Lower New York Bay complex and the Inner New York Bight	105
FIGURE 4.4	Short (< 15 cm) pore-water and solid-phase profiles from stations Bay-1, 2, and 3	106
FIGURE 4.5	Short (< 7 cm) pore-water profiles of NH₄, DOC and PO₄ for stations Bay-4 and Bay-5	108
FIGURE 4.6	Long (> 15 cm) pore-water and solid-phase profiles from stations Bay-3 (7/99 and 6/97) and Shelf-3	109
FIGURE 4.7	Diffusive fluxes of DIC, NH₄ and DOC calculated using the Fick's first law as described by Berner (1980)	111
FIGURE 4.8	Maximum intensity of humic-like fluorescence versus DOC concentration of pore waters	112
FIGURE 4.9	Measured profiles of DIC, DOC and humic-like fluorescence and model-derived profiles of DOC, pLMW-DOC, and DIC for station Shelf-3 ...	113
FIGURE 4.10	Measured and model-derived profiles of DIC and DOC for stations Bay-3 (6/97)	114
FIGURE 4.11	Measured DOC and humic-like fluorescence profiles at station Shelf-3, and pLMW-DOC profiles calculated using different partition Coefficients	115

CHAPTER 1: INTRODUCTION

Organic carbon (OC) found in the marine environment is chemically heterogeneous, ranging from identifiable biochemicals to compounds that are not readily characterized at the molecular level using currently available analytical techniques (Henrichs, 1992; Hedges et al., 2000). Naturally occurring OC is also physically heterogeneous, ranging in size, density and shape. The different components that comprise this complex and heterogeneous pool may originate from diverse sources and be subjected to varying modes of transport and reaction conditions (Mannino and Harvey, 1999, 2000a; Benner and Opsahl, 2001). Therefore, in order to study the dynamics of OC in the marine environment, it is necessary to identify biogeochemically meaningful ways of characterizing and following discrete fractions of the OC pool, either by size, specific chemical compounds/elements, isotopic composition, or lability (e.g., Alperin et al., 1994; Amon and Benner, 1996; Wang et al., 1998; Raymond and Bauer, 2001c). This dissertation examines the dynamics of OC in a coastal environment through investigations of its sorptive behavior and fluorescence characteristics.

BIOGEOCHEMICAL SIGNIFICANCE OF SORPTION

Similar to many dissolved constituents found in the aquatic environment, natural assemblages of OC partition between solid and solution phases through adsorption and desorption. As expected from the heterogeneity of the OC pool as well as the physicochemical nature of mineral surfaces, the strength of associations between OC and mineral surfaces can vary widely. For example, the amount of OC preserved in marine

sediments increases with increasing mineral surface area, indicating that OC is associated with mineral particles (Mayer, 1994a,b; Keil et al., 1994b), and that such associations are strong enough to last over geologic time scales (Henrichs, 1995).

In contrast, several lines of evidence also point to the presence of a much more dynamic fraction of the sorbed OC that can be desorbed over shorter time scales. Laboratory studies directly examining the sorptive behavior of dissolved OC (DOC) present in pore waters along with extracts of sediment particulate OC (POC) demonstrate that OC partitions between these two phases in the sediment column through adsorption and desorption (Thimsen and Keil, 1998; Arnarson and Keil, 2000). These findings, along with a previous report that 20-50 % of the POC preserved in marine sediments can be desorbed (by repetitive extractions with UV-oxidized seawater, KCl, and distilled water; Keil et al., 1994) led to the hypothesis that sediment POC can buffer pore-water DOC concentrations through phase partitioning (Hedges and Keil, 1995; Thimsen and Keil, 1998). Meanwhile, the results of several field-oriented studies suggest that resuspended particles in the bottom nepheloid layer release OC that may be diagenetically altered, and/or of terrigenous origin (Bianchi et al., 1997; Guo and Santchi, 2000; Mitra et al., 2000). Therefore, in contrast to surface estuarine and oceanic waters that are relatively enriched in fresh and labile DOC (Kirchman et al., 1991; Santchi et al., 1995, 1998), the benthic nepheloid layer may serve as a source of degraded DOC to the ocean's interior (Guo and Santchi, 2000).

All of the above findings imply that the boundary between the operationally defined POC and DOC pools is elastic, and that mass transfer across these pools may play a significant role in the marine OC cycle. Furthermore, because the majority of the

OC preserved in sediments is of marine origin (Emerson et al., 1987; Emerson and Hedges, 1988) while mineral particles originate in large part from continental erosion, some strong OC-mineral associations must form in the marine environment, presumably through the more active, or loosely-sorbed pool of the mineral associated OC. However, the nature and dynamics of the loosely-sorbed pool, in particular, the relationship between this dynamic fraction and the more strongly-sorbed pool that persists over geologic time, are unknown.

GOALS AND STRUCTURE OF THIS DISSERTATION

The overall objective of this dissertation was to better understand the nature and the biogeochemical role of the loosely-sorbed POC pool and how it impacts DOC cycling in a coastal environment, with the long-term goal of understanding how and when strong OC-mineral associations form. In addition to investigating short-term adsorption-desorption behavior of DOC, fluorescence measurements were also conducted as a means to track the behavior of, and distinguish gross compositional variations in, the humic-like component of the DOC pool. The coastal ocean was an ideal setting for this research mainly for the reason that exchanges between particulate and dissolved OC are likely to be high relative to other oceanic regions; the active biological and physical processes superimposed on high input rates of (both terrigenous and marine) POC and DOC results in extensive alteration and degradation of the source material.

I assessed the sorptive behavior of OC and its biogeochemical significance using sediment and water samples collected within the Hudson River Estuary and the Inner New York Bight under two contrasting physical settings: in Chapters 2 and 3, I evaluate

the significance of sorptive processes under conditions meant to simulate bottom resuspension; whereas in Chapter 4, I examine the role of sorptive processes on DOC dynamics within the sediment column. The goal of Chapter 2 was to determine the size of the loosely-sorbed fraction of the sediment POC relative to the more tightly-sorbed fraction, and also to identify the source within the sediment matrix that releases OC to solution during resuspension events. The goal of Chapter 3 was to investigate the chemical characteristics of the humic component of the loosely-sorbed POC pool through fluorescence measurements, and thereby further advance a conceptual model that was formulated based on the results of Chapter 2. Humic-like substances were targeted for several reasons: first for their abundance in natural waters (typically 30-50 % of the total DOC pool; Thurman, 1985) and in coastal sediments (~30 % of total POC; Romankevich, 1984); second for their tendency to undergo phase partitioning (Rashid et al., 1972; Preston and Riley, 1982); and third, because the fluorescent nature of humics is readily detectable by standard spectrofluorometry (Coble, 1996).

The focus of Chapter 4 was to test the hypothesis that POC-DOC interactions are quantitatively significant within the sediment column, such that pore water DOC is controlled in large part by physicochemical in addition to microbial processes (Hedges and Keil, 1995; Thimsen and Keil, 1998). In order to test this hypothesis, it was first necessary to develop a pore-water DOC model that accounts for the impact of linear equilibrium adsorption in addition to reaction, diffusion, and advection. Of the currently existing pore-water DOC models (Alperin et al., 1994; Burdige, in press), I adopted the model developed by Burdige (in press) which is the first to take into account the potential effects of varying redox conditions and bioturbation/irrigation that are commonly

encountered in coastal sediments. To this model, I further included the effects of linear adsorption (using a partition coefficient estimated by interpreting the data from Chapter 2 in the context of linear equilibrium adsorption), and dissolved inorganic carbon (DIC) as an additional variable. The latter modification not only allowed for an additional check on the model fit to the pore-water data, but also made it possible to constrain some unknown parameters solely based on the DIC data.

The three studies outlined above are discussed in detail in the following pages (Chapters 2-4). In Chapter 5, I summarize the main findings of each study and discuss their implications in the broader context of the marine C cycle.

CHAPTER 2: RESUSPENSION-INDUCED PARTITIONING OF ORGANIC CARBON BETWEEN SOLID AND SOLUTION PHASES FROM A RIVER-OCEAN TRANSITION¹

ABSTRACT

Laboratory experiments were conducted to evaluate the net exchange of organic carbon (OC) between sediments and overlying water during episodes of resuspension. Surface sediment samples collected from six locations within the Hudson River Estuary and the Inner New York Bight were resuspended in their respective bottom waters for periods ranging from 30 seconds to 2 hours. After resuspension, dissolved organic carbon (DOC) concentration generally reached levels greater than that predicted by conservative mixing of pore-water and bottom water, indicating net release of OC from the sediment particles. The amount of OC released during the extractions comprised $\leq 0.3\%$ of the total sediment pool, but correlated positively ($R^2 = 0.65$, $P < 0.052$) with the amount of particulate organic carbon (POC) found in the high-density fraction of the sediment matrix. This suggests that the mineral-bound fraction of sedimentary OC was the major source for the excess DOC released into solution, and that across various sedimentary environments, only a small (but fairly constant) fraction of the total sedimentary POC may be poised for rapid transfer to the water column.

¹ Komada, T., Reimers, C. E., 2001. *Marine Chemistry* 176, 155-174.

1. INTRODUCTION

Much of the particulate organic carbon (POC) found in soils, river suspensions, as well as marine sediments is sorbed to mineral grains (Keil et al., 1994b, 1997; Mayer, 1994a,b; Bergamaschi et al., 1997; Ransom et al., 1998). However, variation in the ratio between organic carbon and mineral surface area across different aquatic environments (Hedges and Keil, 1995; Keil et al., 1997; Hedges et al., 1999) and reversible adsorption observed in a variety of laboratory sorption experiments (Henrichs and Sugai, 1993; Wang and Lee, 1993; Gu et al., 1995, 1996; Thimsen and Keil, 1998) indicate that natural organic matter-mineral associations are rarely permanent. Non-permanent adsorption implies that organic compounds once disassociated from particles in aquatic environments may be subject to more rapid degradation or greater dispersal compared to adsorbed counterparts (Keil et al., 1994a; Hedges and Keil, 1999). If these differences in fate are significant it becomes important to understand what aquatic processes may undo natural organic-mineral associations.

The objective of this study was to examine the partitioning behavior of organic carbon (OC) between natural sediment particles and water in riverine and coastal marine surface sediments under simulated resuspension conditions. Resuspension-deposition cycles - an ubiquitous process in the coastal ocean (Naudin and Cauwet, 1997) - subject particles to abrupt changes in surroundings due to the large gradients in chemical and physical properties which exist at the sediment-water interface. Previous sorption studies of OC sources collected from the marine environment have focused on bulk behavior, or identifying reaction mechanisms under experimental conditions that were approaching

steady-state (e.g., Rashid et al., 1972; Tomaic and Zutic, 1988; Thimsen and Keil, 1998; Arnarson and Keil, 2000). For example, Thimsen and Keil (1998) determined adsorption isotherms for organic-free minerals mixed with seawater solutions of dissolved organic carbon (DOC) that originated from the pore-water of a coastal sediment and from extracts of sediment POC. The similarity in the bulk sorptive behavior of the two OC fractions led to the conclusion that there exists in the sedimentary POC, an easily extractable fraction which may ordinarily undergo reversible exchange with DOC present in pore solutions. Their findings, if viewed in a context of sorption models and theory (Stumm, 1992), suggest that fluctuations in environmental conditions (such as pH, solute concentration, redox potential, nature and availability of surface area) must significantly influence the partitioning of OC between POC and DOC, and possibly the composition of the POC and DOC pools. To our knowledge, however, no studies have been conducted to investigate the influences on the partitioning of OC of natural processes that abruptly change environmental conditions. Further, the size of the readily extractable POC pool has not been rigorously constrained.

We conducted laboratory experiments and field work to determine the amount of POC that is easily extracted by brief resuspension of suboxic to anoxic surface sediment into oxic bottom water; and secondly, to identify the possible source within the sediment matrix that releases OC to solution. We use our experimental results to consider whether or not resuspension-induced OC partitioning is an important aspect of the marine C cycle.

2. MATERIALS AND METHODS

2.1. Sample Site Description

Six locations along an estuarine gradient were selected as sediment sources for resuspension studies and a seventh end member was also characterized. These sites ranged from the freshwater reaches of the Hudson River to the Raritan-Lower New York Bay complex and the Inner New York Bight (Fig. 2.1, Table 2.1). At all stations, bottom water was at least 50 % saturated with atmospheric levels of oxygen. The Hudson River is generally characterized as a net heterotrophic system fueled by non-phytoplanktonic allochthonous organic matter (Findlay et al., 1991b; Howarth et al., 1996). The river bottom is frequently resuspended by both tidal and freshwater flow, and exhibits an average turbidity of 30 mg L^{-1} within the entire tidal portion of the river (between the Battery and the dam at Troy, Fig. 2.1a) (Bokuniewicz and Arnold, 1984). The dominant source of freshwater to the Bay complex is the Hudson River, whose annual mean discharge is an order of magnitude greater than that of the Raritan River (Duedall et al., 1979). The Bay complex is currently accumulating sediment supplied by fluvial (Hudson River) and marine sources (Bokuniewicz and Ellsworth, 1986), mainly in the recurrently dredged shipping channels (Olsen et al., 1984). All sediment samples were collected away from the dredged channels where little sedimentation is occurring (1.5 mm yr^{-1}) as a result of continuous resuspension (Olsen et al., 1984).

The shelf stations chosen for this study were located at the head of the Hudson Shelf Valley on the eastern boundary of a former dredge spoil dumpsite (closed in 1997;

Shelf-1), and in the axis of the Hudson Shelf Valley (Shelf-2; Fig. 2.1c). Although there is rapid sediment accumulation in the Hudson Shelf Valley (Bopp et al., 1995), distributions of near-bottom suspended particulates show evidence for bottom resuspension of fine particles from this area (Meade et al., 1975; Biscaye and Olsen, 1976).

2.2. Sample Collection

Short cores (8.5 cm in diameter) of surface sediment were collected for resuspension experiments by subcoring from a Peterson grab sampler. At least three cores were collected at each station from multiple grabs, and bottom water was renewed over the sediment surface. The cores were then placed over ice, and the overlying water was gently bubbled with air until transported back to the laboratory in New Brunswick, NJ. Additional bottom water samples (3-5 L) were collected by a Niskin bottle and stored in the dark over ice in pre-combusted glass jugs.

Once in the laboratory, the cores from site Riv-2 were frozen whereas all others used in resuspension experiments were incubated (Table 2.2). When incubated, cores were stored up to 16 days in the dark at laboratory temperatures of 22-24 deg.C. The overlying water was gently bubbled at all times and the water level was adjusted periodically for evaporation by addition of distilled water. Bottom water samples were filtered (0.45 μm polysulfone) and stored at 4 deg.C in the dark.

Sediment cores were also collected to determine pore-water profiles of various dissolved species. These data are presented in this study as a measure of site to site

variability and used to estimate molecular diffusive fluxes of DOC across the sediment-water interface for comparison with exchange rates associated with resuspension. The pore-water cores were collected using either a push corer (mounted on a ROV; Luther et al., 1999), gravity corer, or a Peterson grab sampler as described above. These cores were sectioned (at intervals of 0.5, 1 cm, or greater) within 12 hours of retrieval under a N₂ atmosphere. Pore solution was collected both by centrifugation (at 1500 g for 10 minutes at 4 deg.C) and by gentle suction using sippers modified after Alperin et al. (1999). Sippers were employed to avoid pressurization during centrifugation which can artificially elevate pore-water DOC concentration (Martin and McCorkle, 1993; Alperin et al., 1999). However, in this study there was no significant difference in DOC concentrations in samples retrieved by sipper versus centrifuging from the same sediments. Extracted pore-water was immediately filtered through 0.45 µm polysulfone membrane filters that were pre-rinsed with deionized distilled water. The first 1 to 2 mL of the filtrate was discarded. Aliquots for DOC were frozen immediately in pre-combusted glass vials with Teflon-lined caps. Samples for NH₄ and other analyses of nutrients (not reported here) were acidified to pH of about 2 and refrigerated. DIC samples were poisoned with HgCl₂ and sealed in 1.5 mL serum bottles and refrigerated.

2.3. Resuspension Experiments

Prior to each experiment, the uppermost 2 cm of three cores from each site were extruded in a N₂-filled glove bag. Shells and visible plant/faunal remains were removed with forceps, and the three sediment aliquots were combined and homogenized.

Approximately 3.5 g of the homogenized sediment were then placed into 8 acid-cleaned 50 mL polyethylene centrifuge tubes. The remaining homogenized sediment was set aside for further solid phase analyses (section 2.4.2.). The tubes were capped, removed from the glove bag, and weighed.

These sediment aliquots were subjected to two types of resuspension-mimicking extractions: continuous and series. By design these treatments were much milder than previously reported procedures in which sorbed organic matter was extracted by repetitive desorption using UV-oxidized seawater, 2N KCl and distilled water (Keil et al., 1994a). Here, 35 mL of filtered air-saturated bottom water were added to each tube of sediment (resulting in particle concentrations of approximately 100 g L^{-1}), and the slurries were vortex mixed for a few seconds. In the continuous extraction, the sealed tubes were shaken continuously in air for 30 seconds, 10 minutes, 1 hour, or 2 hours (Table 2.2). At the end of each extraction period, two tubes were centrifuged and the supernatant removed and filtered ($0.45 \mu\text{m}$ polysulfone) for analyses. The 10-minute treatment tubes were further subjected to series extraction. At the end of the first 10-minute extraction, a fresh aliquot of bottom water was added back into the tubes and the procedure was repeated up to 3 times. In all experiments, the supernatant was analyzed for DOC. When extracting sediment from the bay and shelf stations, NH_4 , NO_3 , PO_4 and total dissolved Fe were also analyzed to supply evidence for processes other than OC desorption (Table 2.2).

Controls containing either only bottom water or sediment were run in duplicate in all extractions; the results for DOC are shown as an example in Fig. 2.2. DOC concentrations varied little with time, but those in sediment controls were generally

higher than what was observed in the cores sectioned within 12 hours of retrieval to derive pore-water depth-distributions (Fig. 2.2a; see also Fig. 2.6). These differences were most likely due to effects of storage or the homogenization step, and storage by freezing was discontinued after observing the first control samples from Riv-2 were exceptionally high (Fig. 2.2a).

In extraction samples, the amount of OC released from the solid phase was calculated by comparing the DOC concentration detected in the supernatant to that which would have been obtained if pore-water and seawater had mixed conservatively. The latter value was predicted from the average DOC concentrations in the seawater and pore-water control tubes (Fig. 2.2) and the respective volumes present in the sample tube. The pore-water volume initially present in the sample tube was estimated from porosity and wet sediment density (section 2.4.2.), and the mass of sediment placed in the tube. The volume of residual solution present in the tube at the end of each series extraction was determined by weight difference.

To verify the establishment of solution and sediment mass, a check experiment was conducted using chloride as a tracer. Sediment from station Bay-1 and bottom water diluted five fold with distilled water were mixed for 30 seconds using the same procedure as described above. Chloride was determined using a AgNO_3 titration method after Gieskes and Peretsman (1986) with precision of 1 % or better. Measured and predicted chloride concentrations from triplicate runs agreed generally within analytical precision (data not shown), demonstrating that mass balance was established for the solution phase. Comparison of sediment mass at the beginning and at the end of 4 extractions also showed less than 2 % loss in the solid phase.

2.4. Analyses

2.4.1. Aqueous phase samples

DOC was determined by high-temperature catalytic oxidation (Sugimura and Suzuki, 1988) using a Shimadzu 5000A TOC Analyzer according to Sharp et al. (1993). When required, samples were diluted up to 10 times with distilled deionized water prior to analysis. DOC reference materials prepared in the laboratory of Dr. J. H. Sharp, Univ. of Delaware, were used on each day of analysis ($n = 39$). The average value for the blank reference was $0.2 \pm 1.6 \text{ :M}$ (assigned value $0.0 \pm 1.5 \text{ :M}$) and for the deep ocean reference $48 \pm 4 \text{ :M}$ (assigned value $44.0 \pm 1.5 \text{ :M}$). Precision was typically within 5 %. Pore-water DIC was quantified by flow injection analysis (Hall and Aller, 1992), with precision of about 3 %. NH_4 , NO_3 and PO_4 were determined with an automated analyzer (Quick Chem AE, Lachat Instruments) with precision of 3 % or better. Total dissolved Fe was determined by a modified method of Stookey (1970).

2.4.2. Solid phase samples

The fraction of sedimentary organic carbon associated with the mineral phase was determined by density fractionation using saturated CsCl (having density of 1.9 g mL^{-1}) (Mayer et al., 1993). Approximately 4 g of wet sediment was vortex mixed in 10 mL of the CsCl solution. The slurry was then centrifuged (7000 g for 30 minutes at 10 deg.C) and the supernatant containing the low-density particles removed with a Pasteur pipette. This wash cycle was repeated up to five times until the supernatant became free of visible suspended particles. The low-density fraction was pooled, filtered onto a pre-weighed

polysulfone membrane (0.45 μm), rinsed thoroughly with distilled water, and dried in air. The high-density fraction was rinsed four times with 1:10 seawater-distilled water mixture and freeze-dried.

OC, inorganic carbon and total nitrogen content of bulk as well as the low- and high-density fractions were determined using a Carlo Erba CNS Analyzer following the method of Hedges and Stern (1984). Precision was typically within 3 %. All reported values have been corrected for salt content. Mineral surface area was determined by 5 point BET method (Brunauer et al., 1938) using a Coulter SA 3100 surface area analyzer. Samples were outgassed for 15 minutes at 250-350 deg.C according to Mayer (1994b). Prior to surface area analysis, organic matter was removed from the sediments by gentle heating according to Keil et al. (1997). Porosity and wet sediment density was calculated from the wet and dry masses and the pore-water salinity of a known volume of sediment. Four replicate determinations gave better than 2 % precision.

2.5. Diffusive Flux Calculations

Molecular diffusive fluxes of DOC, DIC, and NH_4 across the sediment-water interface were calculated using pore-water gradients and the Fick's First Law as described in Berner (1980). The concentration gradient of the dissolved species across the sediment-water interface was approximated by the concentration change between the bottom water and the uppermost pore-water value divided by the mid-depth of the interval (0.25 or 0.5 cm depth in sediment). Sediment diffusion coefficients were calculated according to the modified Weissberg relation (Boudreau, 1997) using porosity

and the molecular diffusion coefficient for each species corrected for temperature and salinity (Li and Gregory, 1974). The molecular diffusion coefficient for DOC (approximately $2 \times 10^{-6} \text{ cm}^2 \text{ sec}^{-1}$) was estimated from the Stokes-Einstein relationship with an assigned average molecular weight of 5000 Da (Burdige et al., 1992; Alperin et al., 1994).

Theoretically, if a system is at steady-state and molecular diffusion and burial are the only solute transport mechanisms that operate, the diffusive flux across the sediment-water interface is equal to the depth-integrated production rate of that solute, less its loss through burial (Bernier 1980). However, benthic fluxes may also be enhanced by bioturbation and bioirrigation which were not determined in this study. Therefore, diffusive fluxes calculated as given above will be considered minimum estimates for the total benthic fluxes of DIC and DOC.

3. RESULTS

3.1. Biogeochemical Characterization of the Study Area

3.1.1. Organic matter content and distribution

POC content of the homogenized surface sediment varied from less than 2 wt % to greater than 4 wt %, with the three Bay stations and Shelf-2 having relatively higher values (Table 2.3). The OC of the sediments from stations Riv-2, Bay-1 and Bay-2 was nearly inseparable from the high-density phase, indicating that it existed predominantly in the sorbed form (Table 2.3). In contrast, 10 to 40 % of the total OC in samples from the

remaining stations could be separated into a low-density phase (Table 2.3). Compared to the high-density fractions, the low-density fractions were enriched in both OC and total nitrogen (TN; Table 2.3). Large particles in the low-density material tended to be fibrous, but otherwise morphologically unrecognizable by the naked eye. Wood fragments were abundant within the sediment from Riv-1.

OC to TN ratio of the bulk sediment and high-density fractions (expressed as atomic ratios) were similar across stations (between 10 and 16), but with slightly higher values at stations Riv-1 and Riv-2 (Fig. 2.3). In contrast, the OC to TN ratio of the low-density fraction varied by a factor of 3 across stations, and was notably enriched in C compared to the high-density fraction (13-42; Fig. 2.3). Particulate inorganic carbon content was less than 1 wt% in all samples, and inorganic N (sorbed ammonia) may have been lost in the density separation process.

3.1.2. Specific mineral surface area and OC content

High-density POC and specific mineral surface area (SA) of surface sediment correlated strongly (Fig. 2.4). However, a decrease in OC:SA was observed in a downcore profile of high-density phase POC and SA at station Bay-3 (the only station analyzed for these parameters downcore) (Fig. 2.5). In agreement with the work of Mayer (1994b), these OC:SA ratios appeared to approach with depth the levels commonly reported for riverine particles and continental margin sediments (0.5 to 1.1 mg OC m⁻²; Keil et al., 1994b, 1997; Mayer, 1994a,b; Fig. 2.5). These results indicate that OC-mineral associations established by the time particles settle to become surface

sediments are still subject to dissociation, either by microbial degradation and/or by desorption.

3.1.3. Estimates for benthic fluxes of dissolved carbon

Pore-water profiles from all stations revealed elevated concentrations of DIC, NH_4 and DOC compared to overlying water, indicating that the sediments of the Hudson River-Lower New York Bay and the Inner New York Bight should support a net efflux of such species into the water column (Fig. 2.6). Oxygen microelectrode profiles obtained *in situ* at the Bay stations (Reimers, unpublished data) as well as those measured in the cores recovered from the freshwater stations (Komada, unpublished data) show penetration depths of 5 mm or less. Therefore, suboxic to anoxic processes can be assumed to have dominated the OC remineralization in the analyzed-surface and deeper sediments from the sampled sites.

Calculated diffusive fluxes of DOC varied from < 0.5 to about $3 \text{ mmol m}^{-2} \text{ d}^{-1}$ (Table 2.4) and were greatest at stations with high bulk POC values (Table 2.3). At stations where pore-water DIC profiles were determined, calculated DIC fluxes ranged from about 10 to $60 \text{ mmol m}^{-2} \text{ d}^{-1}$, similar in range, and in ratio to DOC, as has been reported for other coastal sediments (e.g. Reeburgh, 1983, Alperin et al., 1999; Burdige et al., 1999).

3.2. Resuspension Experiment Results

Net conversion of POC to DOC was observed in both continuous and series extractions although losses occurred in three of the shorter term experiments involving Bay and Shelf sediments (Fig. 2.7). Net release rates during continuous and series extractions were similar, and ranged from about -1 to 6 $\mu\text{mol OC g dry sediment}^{-1}$ (Fig. 2.7) which is equivalent to approximately 0.3 % or less of the bulk POC (Table 2.3). During continuous extraction, the amount of OC released tended to increase with extraction time, but appeared to level off after the first 1 hour (Fig. 2.7a). Series extraction results also show that DOC concentration in the supernatant quickly approached values similar to those found in the bottom water control tubes (Fig. 2.8). Based on these observations, we conclude that the majority of the readily extractable OC pool was extracted in these experiments, and that this extractable pool is not likely to be more than 0.5 % of the bulk POC. These results also indicate that the readily extractable pool is not replenished on the time scale of minutes to hours.

OC release from Riv-2 showed a smaller dependence on extraction time, and rose to a relatively higher cumulative release in the 10-minute series extractions compared to the marine sediments (Fig. 2.7). This greater pool of readily releasable OC may be a unique characteristic of the Riv-2 sediment or an artifact of freezing and thawing (Table 2.2). The duplicate extraction series run in bay water suggests the difference in release was not because the primary extractions were run in freshwater (Fig. 2.7).

An explanation for the net losses observed in three of the 10-minute continuous extractions of marine sediments despite measurable release in the 30-second treatment

(Fig. 2.7a) is that a delayed adsorption of DOC to newly precipitated Fe hydroxides occurred on a timeframe of minutes. In all treatments, dissolved Fe and PO_4 were both abundant (on the order of 10-100 μM) in the pore-water, but were low or undetectable immediately after resuspension (data not shown). This was likely a result of Fe hydroxide formation and co-precipitation or rapid scavenging of PO_4 . Because Fe hydroxides can also sorb DOC (Tipping, 1981), it is possible that a fraction of the DOC may have been removed from solution by adsorption to Fe hydroxides.

During the continuous extractions using marine sediments, NH_4 concentrations did not increase as a function of extraction time, but they did rise to a level higher than that predictable from conservative mixing (Fig. 2.9). This result is assumed to be a consequence of rapid desorption similar to observations of Simon (1989) and Morin and Morse (1999). NO_3 , on the other hand, mixed conservatively throughout the experiments (Fig. 2.9). The lack of any significant change in NO_3 or NH_4 with prolonged extraction time suggests that oxidation reactions involving organic or inorganic N did not occur to any significant extent. Thus, we assume any oxidation of OC was also minor during the resuspension experiments.

4. DISCUSSION

4.1. Sources for the OC released during resuspension

Any sediment is comprised of a complex mixture of particles and associations of particles with different sources, physicochemical characteristics, and diagenetic histories

(Thompson and Eglinton, 1978; Prahl and Carpenter, 1983; Keil et al., 1998). Because all of these particles are subject to resuspension, the source of OC released during resuspension is a question. Our density fractionation results showed the presence of both mineral-associated as well as low-density organic particles at all stations (Table 2.3). The observed OC to TN ratios of the density fractionates (Fig. 2.3) as well as the morphological characteristics (section 3.1.1.) are consistent with enrichment of vascular plant remains in the low-density fraction, and a more diagenetically altered, soil-like material in the mineral-bound fraction (Oades, 1972; Turchenek and Oades, 1979; Prahl and Carpenter, 1983; Keil et al., 1998).

In order to determine the sources for the released OC, the measured release rates were regressed against the amount of POC present in the bulk, high- and low-density fractions (calculated as the total mass of POC in each fraction normalized to dry bulk sediment mass). For this purpose (and due to data availability), the 1-hr continuous extraction results (Table 2.4) were adopted as the representative values. Results of the regression analysis show that the level of OC released was best predicted by the amount of POC found in the high-density fraction phase (Fig. 2.10; Table 2.5). Bulk POC content was a weaker predictor for OC release, and POC in the low-density fraction exhibited a non-significant relationship with release despite this fraction's greater tendency to remain in solution and its high OC content (Table 2.3). These results therefore are interpreted to indicate that OC released during resuspension is likely to originate from the mineral-bound OC pool rather than from discrete organic particles. The data also imply that in various sedimentary environments having different levels and

sources of POC, a small but fairly uniform fraction of the sorbed OC may exist in a readily extractable form (Fig. 2.10, Table 2.4).

4.2. Geochemical significance of resuspension-induced OC release

The results of our experiments indicate that resuspension alters the partitioning of OC between the mineral-sorbed fraction of a sediment and solution, resulting in a net release of OC to solution. The amount of OC released however is small and much less than what has been considered desorbable based on harsher extraction procedures (Keil et al., 1994a). In order to assess the geochemical significance of organic matter desorption during resuspension, we extrapolate the laboratory results to field conditions and ask the following questions. (1) Could resuspension-induced release of OC ever be a quantitatively significant source of DOC to the water column? (2) Is there a link between the readily extractable and the more strongly sorbed pools of OC? In other words, does resuspension-induced release of OC to solution have the potential to impact the OC content/composition of the particulate phase prior to burial?

4.2.1. Bottom resuspension as a source of DOC to the water column

Several factors must be kept in mind when extrapolating laboratory resuspension-experiment results to *in situ* conditions. First, whether or not resuspension-induced OC release is a significant source of DOC to the water column must depend on the extent of resuspension within the system of interest. This in turn is a function of the intensity and duration of resuspension events, the frequency of occurrence, and the cause (e.g., by

currents, dredging, fishing activities or bioturbation). Second, resuspension experiments in this study were conducted in a sealed tube at a solid concentration of 100 g L^{-1} which is much greater than levels usually observed in the water column of coastal environments (order of 10 mg L^{-1}). If the conversion of POC to DOC is driven by desorption, then our results are likely to underestimate the rates due to the accumulation of DOC in the solution phase; i.e. greater particle dilution under natural conditions is expected to induce greater release. Third, our experiments only document partitioning behavior during a short period of suspension (≤ 2 hours). They do not provide information on whether or not the released OC remains in solution, is oxidized, or re-sorbed onto particulate phases over time. However, if OC release is driven by desorption of loosely sorbed material, then re-adsorption onto similar particles in suspension seems unlikely, considering the lower DOC concentration in the water column relative to that in the pore-water. Keeping in mind these limitations, we present first order estimates for rates of OC release occurring *in situ* in the Hudson River-Bay, river-ocean transition zone (Table 2.6).

Release rates were computed using published sediment resuspension rate estimates for the brackish portion of the Hudson (Achman et al., 1996). For the freshwater reaches of the Hudson and the Bay complex, resuspension rates were estimated from observed turbidity ranges and inferred particle-settling rates (Duedall et al., 1979; Bokuniewicz and Arnold, 1984). Note that this approach assumes all suspended solids originate from the bottom, which is a reasonable assumption at least for the freshwater reaches of the Hudson (Findlay et al., 1991a). All three regions exhibit a range in POC content (Table 2.6), and hence according to our results (Fig. 2.10), are expected to release a range of OC per mass of sediment. However, for simplicity, we

adopted a modest estimate for the extractable pool size of $1 \mu\text{mol g}^{-1}$ for all regions. We further assumed that the extractable pool is regenerated daily.

Calculated resuspension-induced OC release rates (expressed as fluxes per unit area of estuarine floor) range by four orders of magnitude, being highest in the turbid, brackish portion of the Hudson River, and lowest in the Bay (Table 2.6). The release rates obtained for the Bay complex are about 3 orders of magnitude smaller than the diffusive DOC fluxes calculated in this study (Table 2.4). These values are further dwarfed against the estimated DOC loading from the Hudson River ($40 \text{ mmol d}^{-1} \text{ per m}^2$ of bay bottom; calculated from the average annual discharge at the Battery reported by Abood et al. (1992), and assuming a riverine DOC concentration of $250 \mu\text{M}$). It therefore appears unlikely that resuspension-induced release of OC is a significant source of DOC to the water column of the Bay complex.

Similar conclusions can be drawn for the freshwater portion of the Hudson River Estuary. The calculated release rates (Table 2.6) amount to less than 1 % of allochthonous inputs of total OC (dominant sources for reduced C to the estuary; Howarth et al., 1996), and therefore are not likely to be a quantitatively important source for OC to the water column. Nevertheless, resuspension-induced release rates are of the same order of magnitude as the calculated diffusive fluxes of DOC at stations Riv-1 and Riv-2 (Table 2.4).

In contrast, resuspension-induced fluxes may be significant sources for DOC to the turbid, brackish portion of the Hudson River Estuary. The calculated release rate (Table 2.6) is equivalent to approximately 8 % of the total OC loading from the freshwater reaches of the estuary (Howarth et al., 1996). It is also comparable to the

highest rates of benthic DOC fluxes reported for marine sediments (Alperin et al., 1999; Burdige et al., 1999).

Resuspension-induced release rates can also be estimated for shelf sediments. Based on ^{210}Pb data, Bacon et al. (1994) obtained a resuspension rate of $0.08 \text{ g m}^{-2} \text{ d}^{-1}$ for fine particulates trapped in the sandy shelf sediments of the Middle Atlantic Bight (MAB). The POC content of these fine particulates (0.5 to 5.3 %; Bacon et al., 1994) is comparable to those encountered at stations Shelf-1 and 2 (Table 2.3). If we extrapolate our results to the MAB by making the same assumptions as stated earlier, we obtain a resuspension-induced release rate of $8 \times 10^{-5} \text{ mmol m}^{-2} \text{ d}^{-1}$. This is roughly three orders of magnitude smaller than the benthic DOC fluxes reported for the MAB and other continental margins (Alperin et al., 1999; Burdige et al., 1999), and hence appears quantitatively insignificant. In contrast to our estimate, Guo and Santschi (2000) suggest that DOC is produced within the benthic nepheloid layer of the MAB by desorption from resuspended bottom sediments, and that the lateral export of this DOC may be a quantitatively important source to the open ocean. They further argue that the ^{14}C age of released OC is significantly older than the ^{14}C ages of the resuspended POC (Guo and Santschi, 2000). This debate suggests that additional work is needed to rigorously quantify the role of bottom resuspension in the benthic exchange of DOC in energetic continental margin environments.

4.2.2. Resuspension-induced release as a mechanism for altering the content and composition of OC in the particulate phase

The positive correlation of OC preserved in marine sediments with available mineral surface area has been interpreted to indicate that sorbed OC is not readily available for microbial breakdown (Mayer, 1994a,b; Hedges and Keil, 1995). If we assume that the POC that could not be extracted in our experiments was held in a strongly sorbed pool, then this pool comprises over 99.5 % of the mineral-associated POC (section 3.2., Table 2.4). Conversely, existing data show that the ratio of OC to SA as well as chemical composition of the sorbed OC vary significantly across different oceanic environments (Hedges and Keil, 1995; Keil et al., 1997; Hedges et al., 1999; Keil and Fogel, 2001), and with depth in sediment (Fig. 2.5; Mayer, 1994b). These findings indicate that even the more strongly sorbed components of POC are ultimately subject to removal.

Our study shows that, in addition to diagenetic processes that degrade OC within the sediment column (Fig. 2.5), sediment resuspension can induce net loss of sedimentary POC by releasing OC that is loosely bound to the mineral surface. The results also show that the size of the extractable fraction is equal to a small but roughly constant fraction of the mineral-associated POC (Fig. 2.10, Table 2.4). Whether or not the dynamics of this loosely-sorbed pool has the potential to impact the abundance and chemical composition of the much greater reservoir of the more strongly sorbed pool hinges on the nature and origin of this extractable fraction. Under the assumption that most of the loosely-sorbed fraction is released into solution during each resuspension event, this pool must be repeatedly regenerated during the particle's residence in the sediment column. If it is re-

supplied solely from the DOC pool, then release of loosely-sorbed material into solution has no net effect on the content/composition of bulk POC. However, if some degree of exchange takes place between the tightly- and loosely-sorbed fractions, then a periodic loss of loosely-sorbed material to solution could potentially impact the bulk POC content/composition over repeated resuspension-deposition cycles (Fig. 2.11).

Although ad/desorption have been identified as important processes that take place between the loosely-sorbed POC and DOC (Thimsen and Keil, 1998), conversions between the tightly- and loosely-sorbed fractions are less well understood (Collins et al., 1995; Henrichs, 1995). We expect processes that contribute to the net loss of the tightly-sorbed fraction (either by direct oxidation or transformation into the loosely-sorbed pool) to be primarily microbial, because strong adsorption predicts little desorption. Bottom resuspension and turbulence have been found to enhance microbial activity (Wainright, 1987; Findlay et al., 1990). Fluctuations in redox potential, as well as increased mixing with fresher detritus in the water column – both of which likely accompany resuspension events - have also been found to enhance degradation of organic matter (Graf, 1987; Aller, 1994). Therefore, the loss of the tightly-sorbed POC fraction, and possibly transformation into the loosely-sorbed pool, may be enhanced by bottom resuspension. Further supporting evidence comes from appreciable levels of dissolved lignin phenols found in the benthic nepheloid layer of shelf and slope waters, most likely due to desorption from resuspended bottom particles of terrigenous origin (Bianchi et al., 1997; Mitra et al., 2000). These findings are consistent with the idea that the tightly-sorbed fraction is gradually lost to solution. Further work is needed to determine the conversion processes between the tightly- and loosely-sorbed fractions of POC.

Table 2.1. Summary of station locations and bottom characteristics.

Station	Lat (N) Long (W)	Depth (m)	Bottom T (°C)	Sand (%)	Silt (%)	Clay (%)	Salinity	Date of Sampling
Riv-1 ¹	41.918 -73.965	3	17	89	10	0.7	Tidal Freshwater	Oct 1997
Riv-2	41.868 -73.933	2	17	50	47	3.6	Tidal Freshwater	Oct 1997
Bay-1	40.596 -74.002	5	21	83	16	0.5	24	Jun 1998
Bay-2 ²	40.549 -74.064	8	19	28	67	4.3	27	Jun 1998
Bay-3	40.458 -74.074	6	20	72	26	2.7	23	Jun 1998
Shelf-1	40.389 -73.832	24	13 ³	86	13	1.0	31	Sep 1998
Shelf-2	40.282 -73.787	58	12 ³	88	11	1.3	32	Sep 1998

1. Sediment from station Riv-1 was analyzed for biogeochemical characterization only.
Resuspension experiment results are not reported for this site.
2. Located in an area that was previously dredged for sand (operations terminated in 1973)
(Kastens et al., 1978).
3. In situ temperatures are not available for these stations. Listed data are from Bowman and
Wunderlich (1977).

Table 2.2. Summary of resuspension experiment conditions.

Sediment Source	Water Source ¹	Sediment Storage ²	Duration of Continuous Extraction (hr)	Species Monitored
Riv-2	bw	Frozen	30 sec, 10 min, 1 hr	DOC
Riv-2	Bay-3	Frozen	30 sec, 10 min, 1 hr	DOC
Bay-1	bw	Incubated	1 hr only ³	DOC, NH ₄ , NO ₃ , PO ₄ , Fe ⁴
Bay-2	bw	Incubated	30 sec, 10min, 1 hr, 2 hr	DOC, NH ₄ , NO ₃ , PO ₄ , Fe
Bay-3	bw	Incubated	30 sec, 10min, 1 hr, 2 hr	DOC, NH ₄ , NO ₃ , PO ₄ , Fe
Shelf-1	bw	Incubated	30 sec, 10min, 1 hr, 2 hr	DOC, NH ₄ , NO ₃ , PO ₄ , Fe
Shelf-2	bw	Incubated	30 sec, 10min, 1 hr, 2 hr	DOC, NH ₄ , NO ₃ , PO ₄ , Fe

1. bw denotes bottom water collected from the corresponding station. Sediment from station Riv-2 was resuspended in water from the bay as well as in Hudson River water.
2. Frozen cores were stored up to 6 months prior to running the experiment. Incubated cores were processed within 16 days of collection.
3. Data from other extractions were lost due to container leakage.
4. Total dissolved Fe.

Table 2.3. Particulate organic carbon (POC) and total nitrogen (TN) content and specific mineral surface area (SA) of homogenized surficial sediments

Station	Bulk (wt%) ¹		High Density (wt%) ¹		Low Density (wt%) ¹		Fraction Sorbed ²		SA (m ² g ⁻¹)
	POC	TN	POC	TN	POC	TN	POC	TN	
Riv-1	1.85	0.13	1.20	0.09	36.2	1.02	0.6	0.7	6.3
Riv-2	2.30	0.21	2.59	0.21	37.8	1.19	>0.9	1.0	12.4
Bay-1	3.73	0.44	3.76	0.40	38.1	3.41	>0.9	0.9	12.3
Bay-2	4.02	0.48	4.26	0.46	36.0	1.99	>0.9	1.0	21.7
Bay-3	3.28	0.34	2.89	0.28	35.8	1.72	0.9	0.8	17.0
Shelf-1	2.45	0.23	1.88	0.16	42.7	1.67	0.8	0.7	11.5
Shelf-2	4.44	0.53	3.71	0.42	30.7	1.80	0.8	0.8	18.5

1. Percent weight within each fraction.
2. Calculated as: $[(\text{wt}\% \text{ POC}_{\text{HD}}) * (\text{g dry sediment}_{\text{HD}})] / [(\text{wt}\% \text{ POC}_{\text{BK}}) * (\text{g dry sediment}_{\text{BK}})]$, where subscripts HD and BK are high-density and bulk, respectively.

Table 2.4. Calculated molecular diffusive fluxes by sediment diagenesis and measured net DOC releases during sediment resuspension experiments.

Station	Calculated Diffusive Fluxes ¹			OC Released During 1hr Continuous Extraction	
	DIC (mmol m ⁻² d ⁻¹) (<i>n</i>)	DOC (mmol m ⁻² d ⁻¹) (<i>n</i>)	NH ₄ (mmol m ⁻² d ⁻¹) (<i>n</i>)	(μmol g ⁻¹) ²	(%POC _{HD}) ³
Riv-1	13±1 (2)	0.2±0.1 (4)	3.2±0.3 (2)	-	-
Riv-2	26 (1)	0.29±0.03 (2)	3.0 (1)	2.03±0.05	0.09
Bay-1	57 (1)	2.0±0.1 (2)	8.4 (1)	2.6	0.08
Bay-2	88 (0)	3.4±0.4 (2)	13.3 (1)	3.7±0.5	0.10
Bay-3	9±5 (2)	0.3±0.4 (2)	0.92±0.07 (2)	0.7±0.3	0.03
Shelf-1	- (0)	- (0)	8.9 (1)	1.1±0.4	0.07
Shelf-2	- (0)	2.7 (1)	10.5 (1)	3.84±0.04	0.12

1. Fluxes were calculated from measured pore-water profiles (Fig. 2.6) and as described in Section 2.5. Uncertainties are standard deviations of replicate determinations from multiple profiles (*n* = number of profiles).
2. Uncertainties are ±1 standard deviation of duplicate determinations, except for station Bay-1 where only one value is available.
3. Amount of OC released expressed as percent of POC found in the high-density fraction.

Table 2.5. Linear regression coefficient R^2 and P value (in parentheses) among various environmental parameters. Those significant at the 95% level are indicated in bold.

	Calculated DIC flux	Low- dens ² POC	High- dens ² POC	Bulk POC	SA ³
Release ¹	+0.61 (0.068)	-0.027 (0.75)	+0.65 (0.052)	+0.54 (0.095)	+0.34 (0.22)
Calculated DIC flux		-0.24 (0.26)	+0.45 (0.098)	+0.46 (0.094)	+0.35 (0.16)
Low-dens POC			-0.58 (0.046)	-0.67 (0.025)	-0.71 (0.018)
High-dens POC				+0.84 (<0.01)	+0.71 (0.017)
Bulk POC					+0.69 (0.020)

1. Amount of OC released per unit gram of dry sediment during 1-hr continuous extraction as given in Table 2.4.
2. Mass of POC found in the low-or high-density fraction normalized to bulk dry sediment mass (wt %).
3. Specific mineral surface area as given in Table 2.3.

Table 2.6. Derivation of estimated sediment resuspension rates and associated release of OC into Lower New York-Raritan Bay complex and the Hudson River Estuary (HRE). Underlined values were derived from published parameters listed in the upper portion of the column. Values in brackets are for illustrative purposes only and not used directly in the derivation of fluxes.

	Bay Complex	HRE Tidal Fresh	HRE Brackish
Bulk Sediment POC Content (wt %)	1.7-4 ⁽¹⁾	~2 ⁽²⁾	3.8 ± 1.4 ⁽³⁾
Water Volume (L)	2 x 10 ⁹ ⁽¹⁾	1 x 10 ¹² ⁽⁴⁾	-
Surface Area (m ²)	318 x 10 ⁶ ⁽¹⁾	114 x 10 ⁶ ⁽⁴⁾	[108 x 10 ⁶ ⁽³⁾]
Suspended Solids (mg L ⁻¹)	9-30 ⁽⁵⁾	13-41 ⁽⁶⁾	[0-800 ⁽⁷⁾]
Estimated Particle Settling Time (d)	0.17 ⁽⁸⁾	0.3 ⁽⁹⁾	-
Estimated Sediment Resuspension Rate (g m ⁻² d ⁻¹)	<u>0.3-1.1</u>	<u>380-1199</u>	7800 ⁽³⁾
Resuspension-Induced OC Release (mmol m ⁻² d ⁻¹)	<u>0.3-1.1 x 10⁻³</u>	<u>0.4-1.2</u>	<u>8</u>

Sources: (1) Adams et al. (1998) and this study; (2) this study; (3) Achman et al. (1996); (4) Metzger et al. (1992); (5) Duedall et al. (1979); (6) from Bokuniewicz and Arnold (1984) assuming that 20 % of suspended matter is discrete organic debris; (7) Geyer (1995); (8) calculated by assigning an average depth in the Bay of 5.9 m, and a particle settling rate of 4×10^{-2} cm sec⁻¹ as reported by Bokuniewicz and Arnold (1984); (9) Bokuniewicz and Arnold (1984).

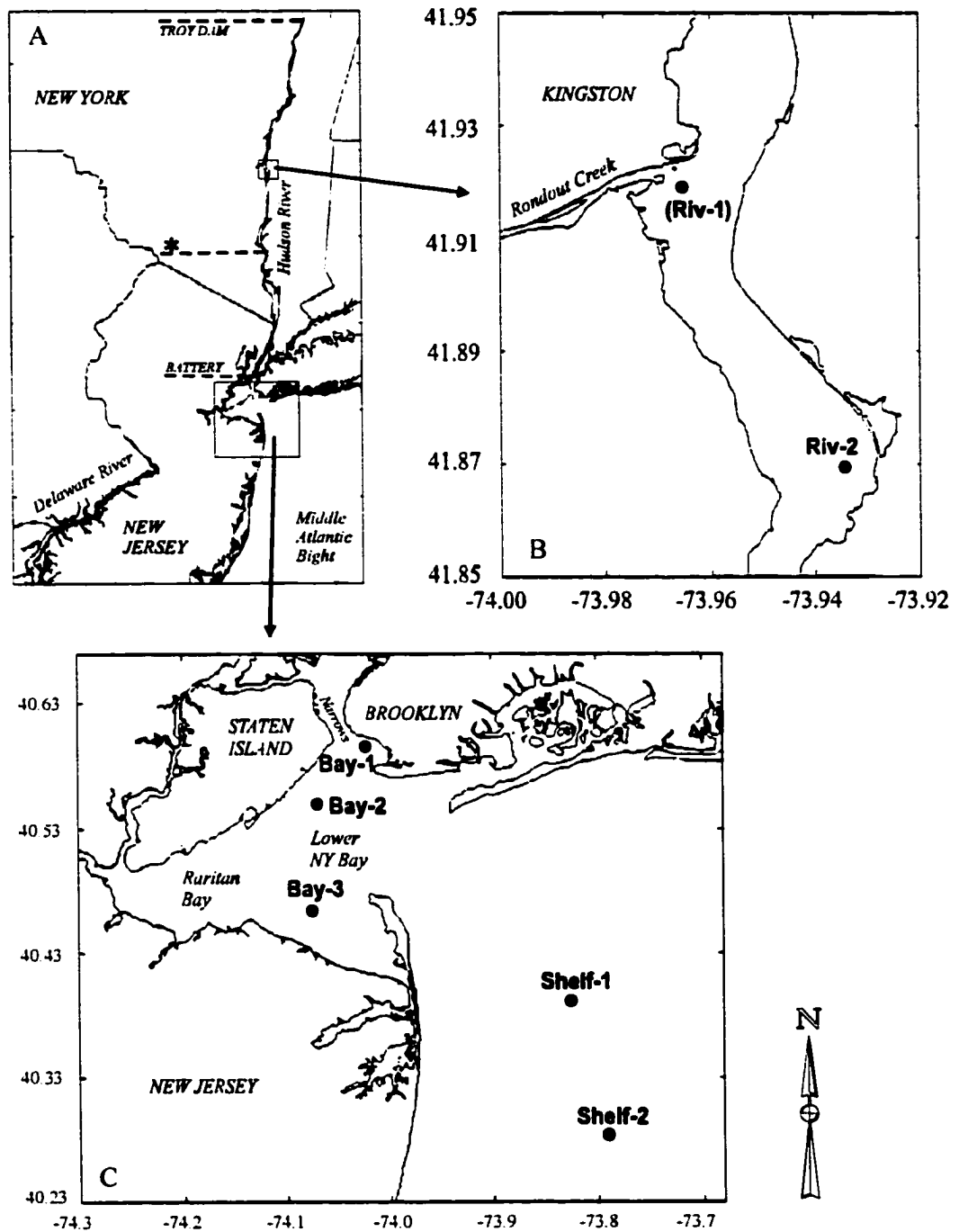


Figure 2.1. Sampling region (a) and station locations (b), (c). The asterisk in panel (a) indicates the approximate northern limit of the salinity intrusion in the Hudson River (Limburg et al., 1986), which is tidal as far north as the Troy Dam (a). Sediment from station Riv-1 (b) was analyzed only for biogeochemical characterization; resuspension experiment results are not available for this site.

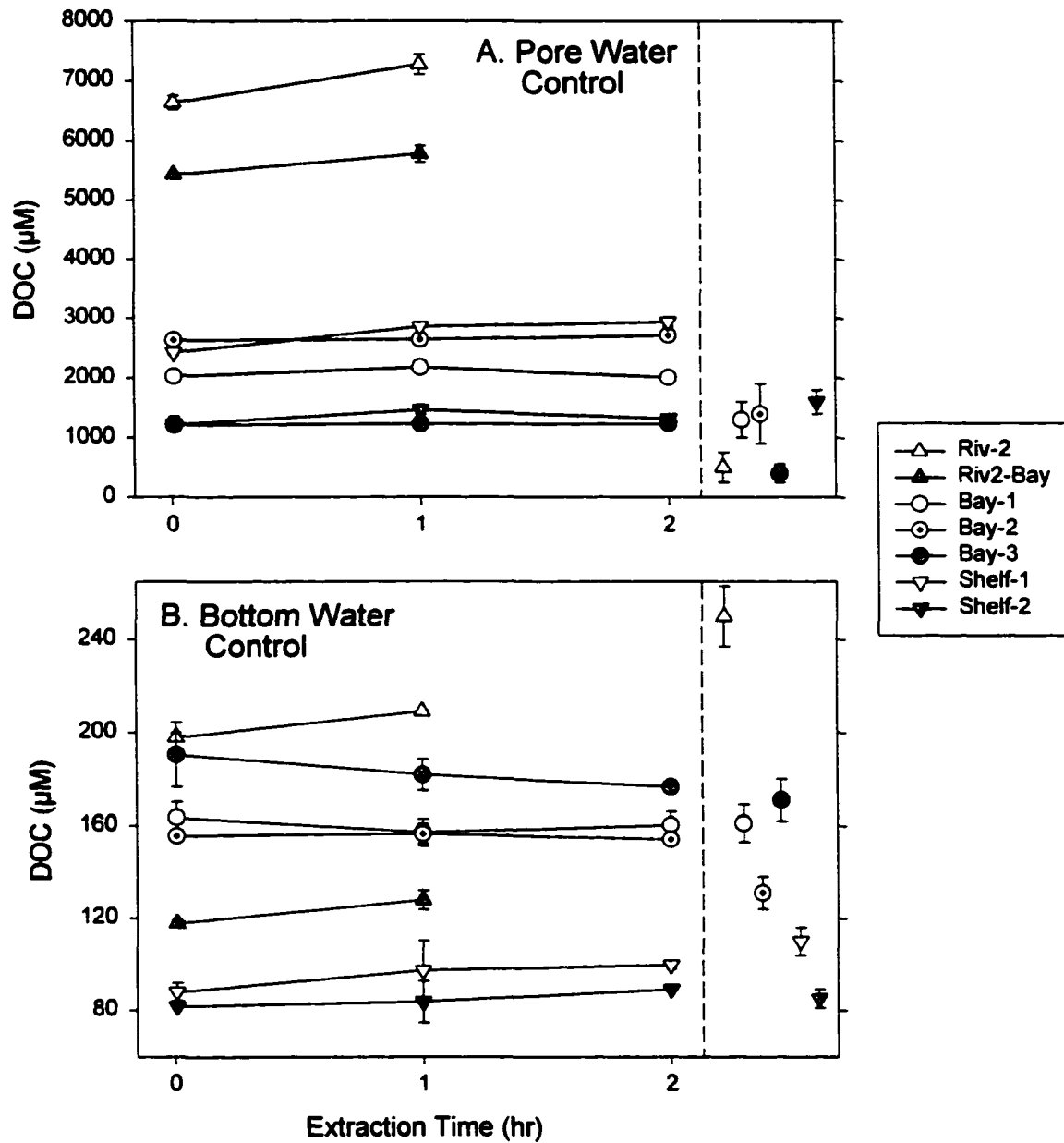


Figure 2.2. DOC concentrations observed in (a) pore water and (b) bottom water control tubes. Error bars are standard deviations of two determinations. The expected ranges in pore-water and bottom water under field conditions are shown to the right of the dashed lines (pore-water values are derived from core sectioning (Fig.2.6), and bottom water by analysis of freshly collected sample).

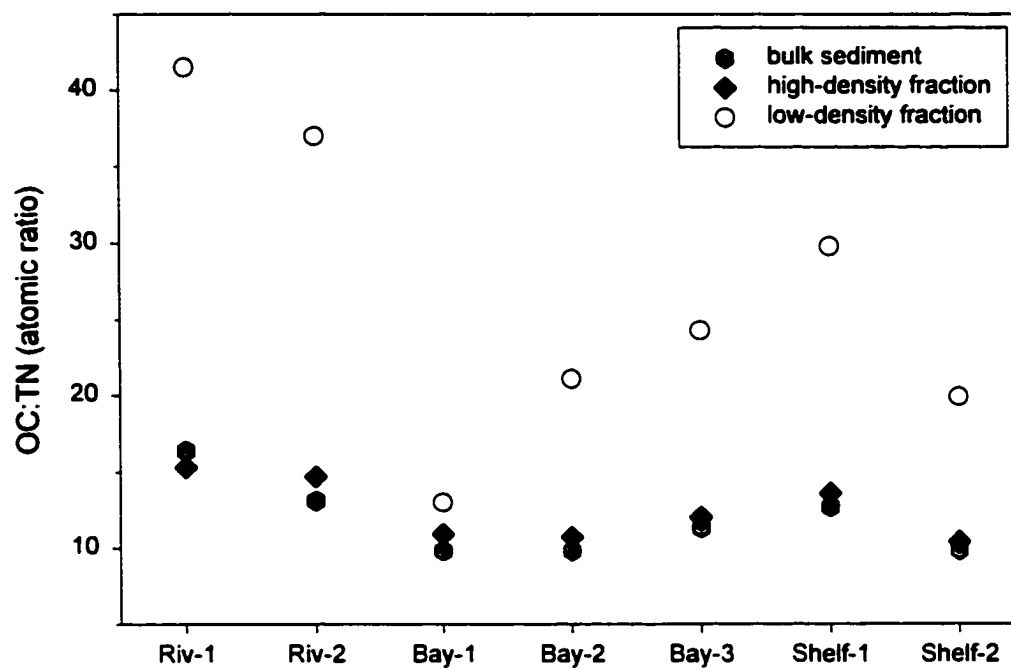


Figure 2.3. Organic carbon (OC) to total nitrogen (TN) ratios (expressed as atomic ratios) of the different density fractionates of surface sediments. Error bars are smaller than the symbols.

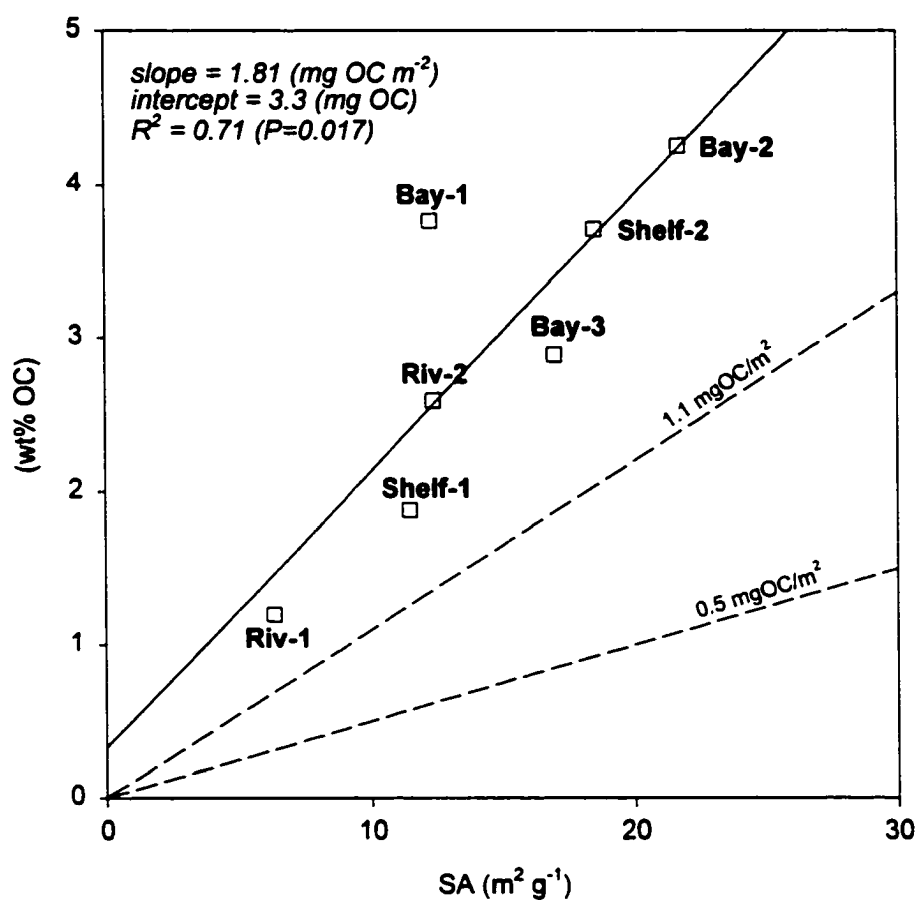


Figure 2.4. Plot of POC content in the high-density fraction (note that the result is essentially the same using bulk POC content) against corresponding specific mineral surface area (SA) of surface sediments. Linear regression result is shown with a solid line. Dashed lines show the boundaries of commonly observed OC:SA relationships in coastal sediments and soils (Mayer 1994a,b; Keil et al. 1994b, 1997).

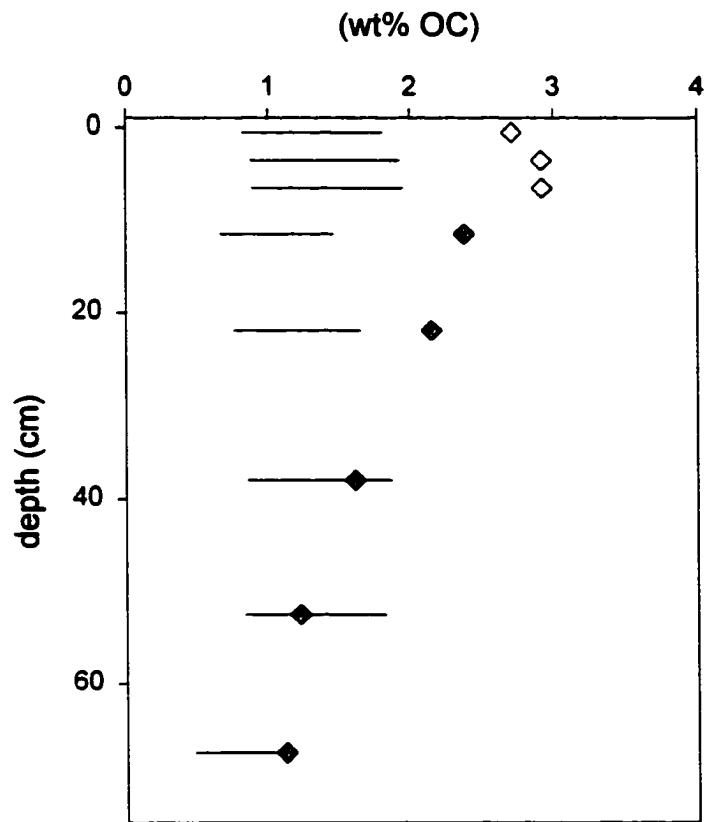


Figure 2.5. Depth profiles of measured and expected high-density phase POC for station Bay-3. Diamonds are measured values from two different cores (shown in white and gray). Horizontal bars show the expected range of POC based on the existing SA at each depth and the common OC:SA proportionality given by Mayer (1994a,b) and Keil et al. (1994b, 1997) (0.5 to 1.1 mgOC m^{-2}).

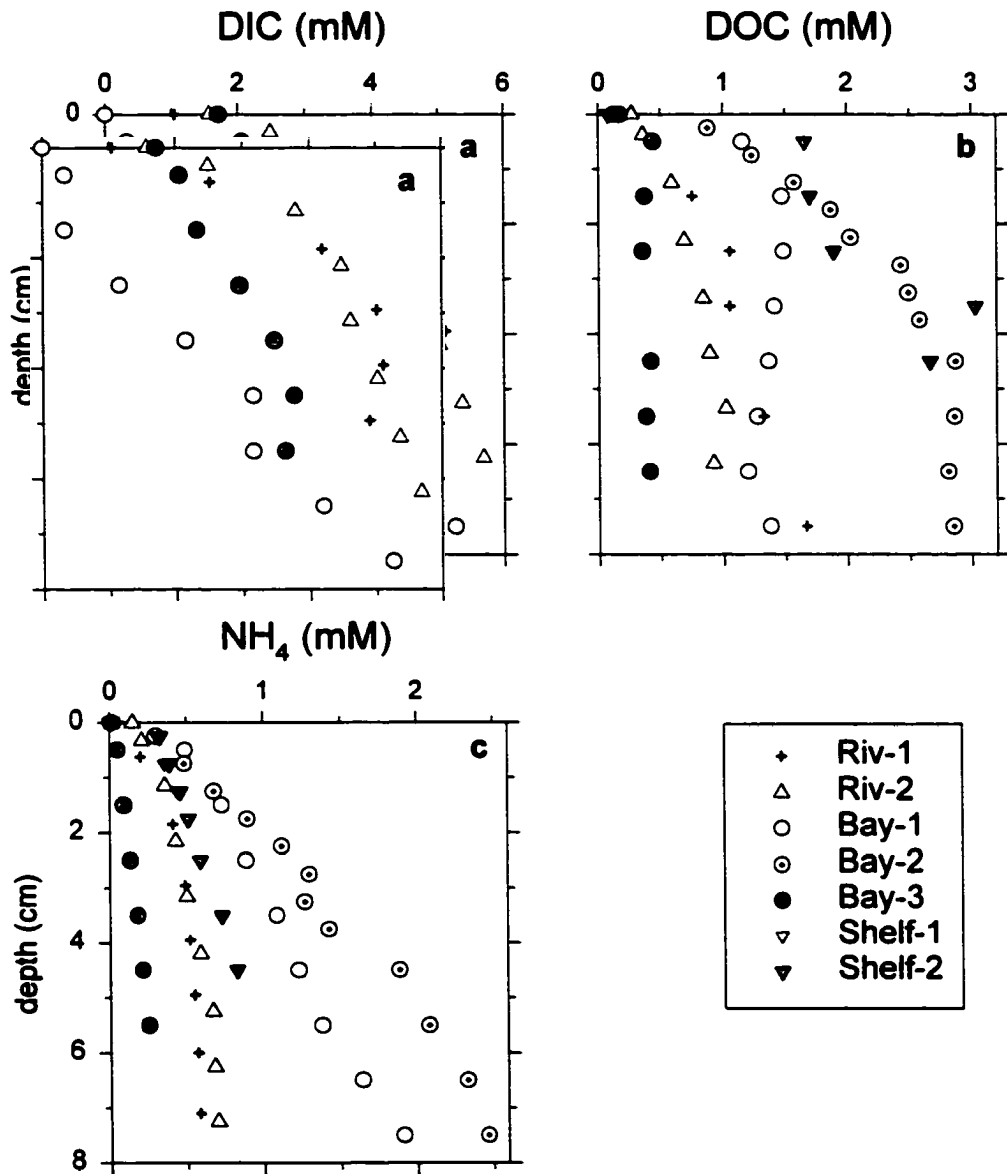


Figure 2.6. Pore-water profiles of dissolved inorganic carbon (DIC) (a), DOC (b), and NH_4^+ (c). Data points at depth of 0 cm indicate bottom-water concentrations.

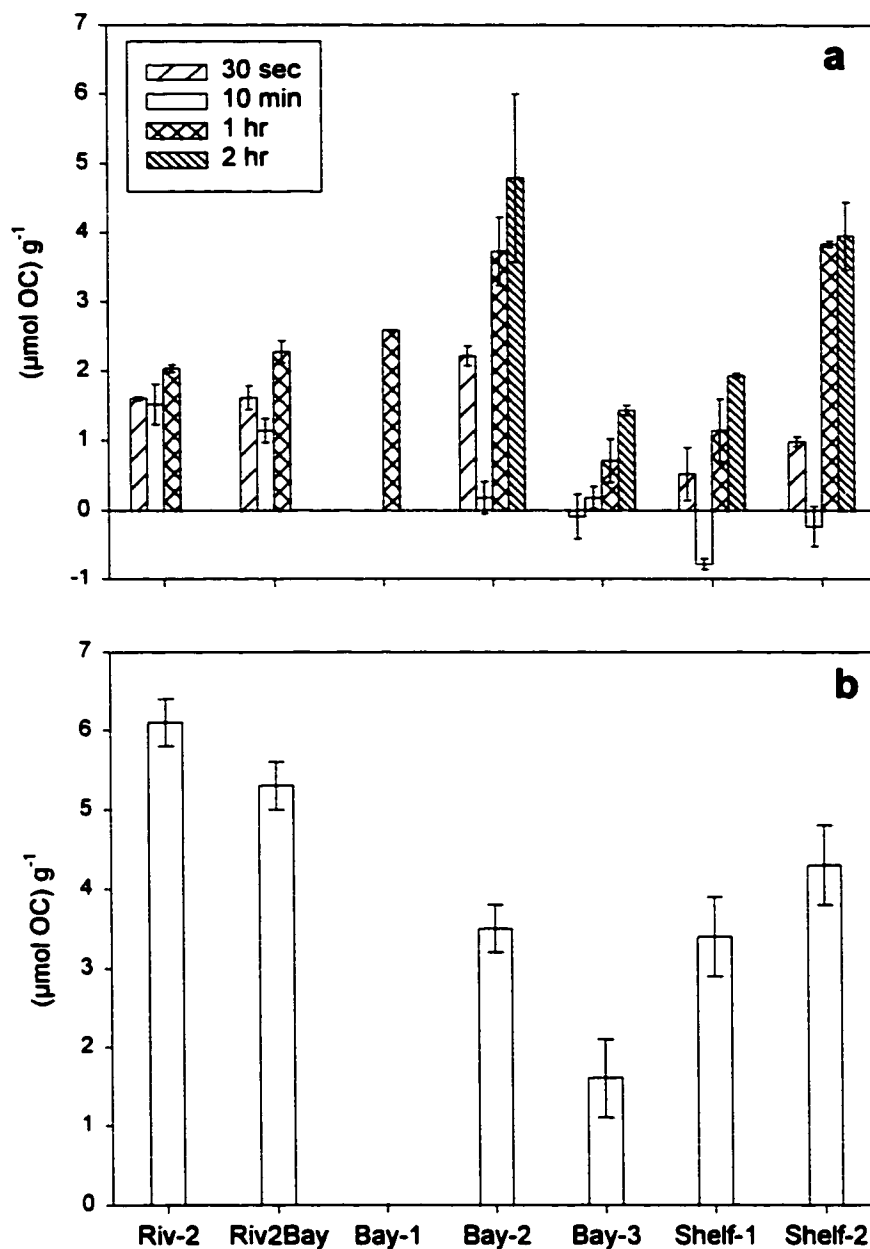


Figure 2.7. Net amount of OC released over the course of each extraction period (normalized to dry sediment mass) in (a) continuous and (b) series extractions. Series extraction results in panel b are given as the sum of four consecutive 10-minute extractions. Results for station Riv-2 resuspended in Bay-3 water are given as Riv2Bay. Only the 1-hr continuous extraction datum is available for station Bay-1 (no duplicate). For the remaining stations, error bars represent ± 1 standard deviation of duplicate determinations.

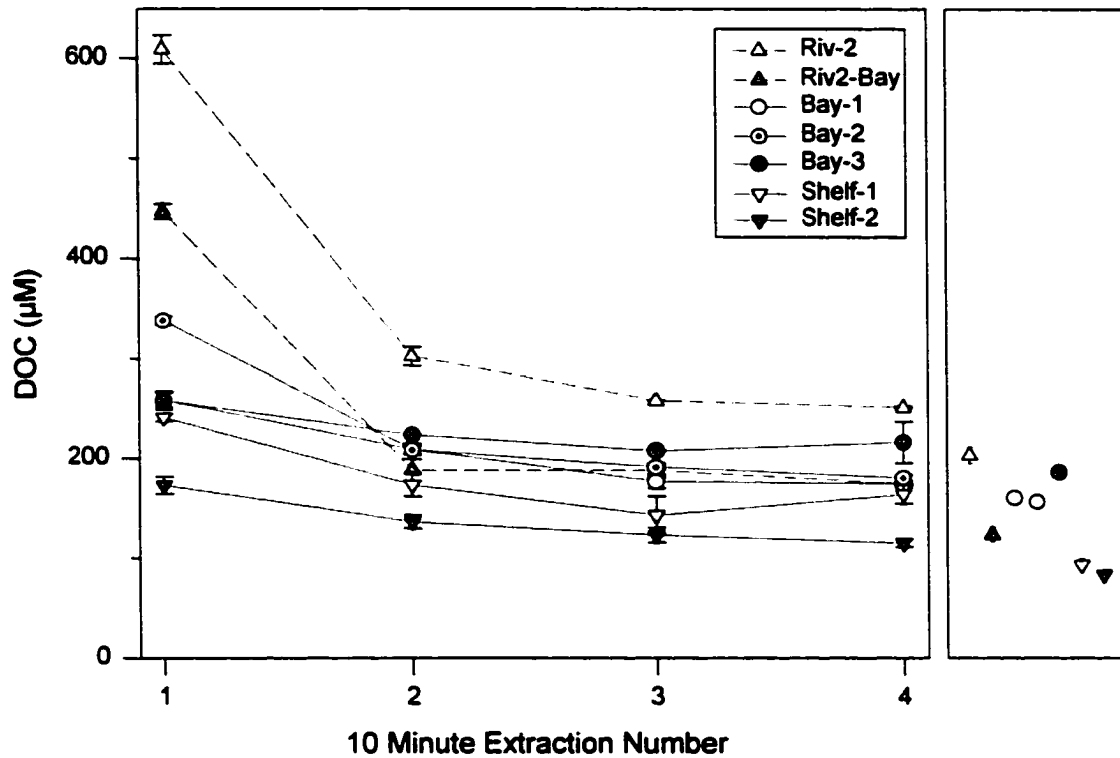


Figure 2.8. DOC concentration in the supernatant during 10-minute series extractions. Error bars are ± 1 standard deviation of duplicate determinations. The average (± 1 standard deviation) DOC concentrations in the bottom-water control tubes are shown for comparison in the right panel.

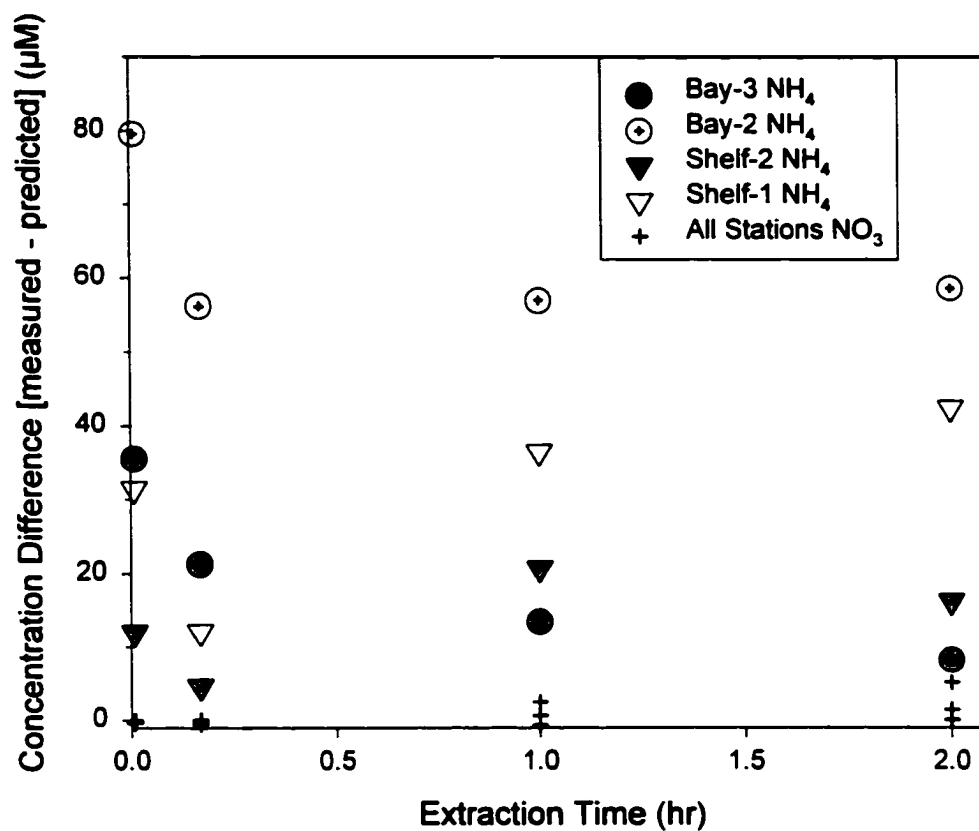


Figure 2.9. Differences between the observed and predicted concentrations of NH_4^+ and NO_3^- in the supernatant during continuous extractions. The NO_3^- results for all stations overlapped near zero (i.e., near-conservative), and are collectively presented with one symbol.

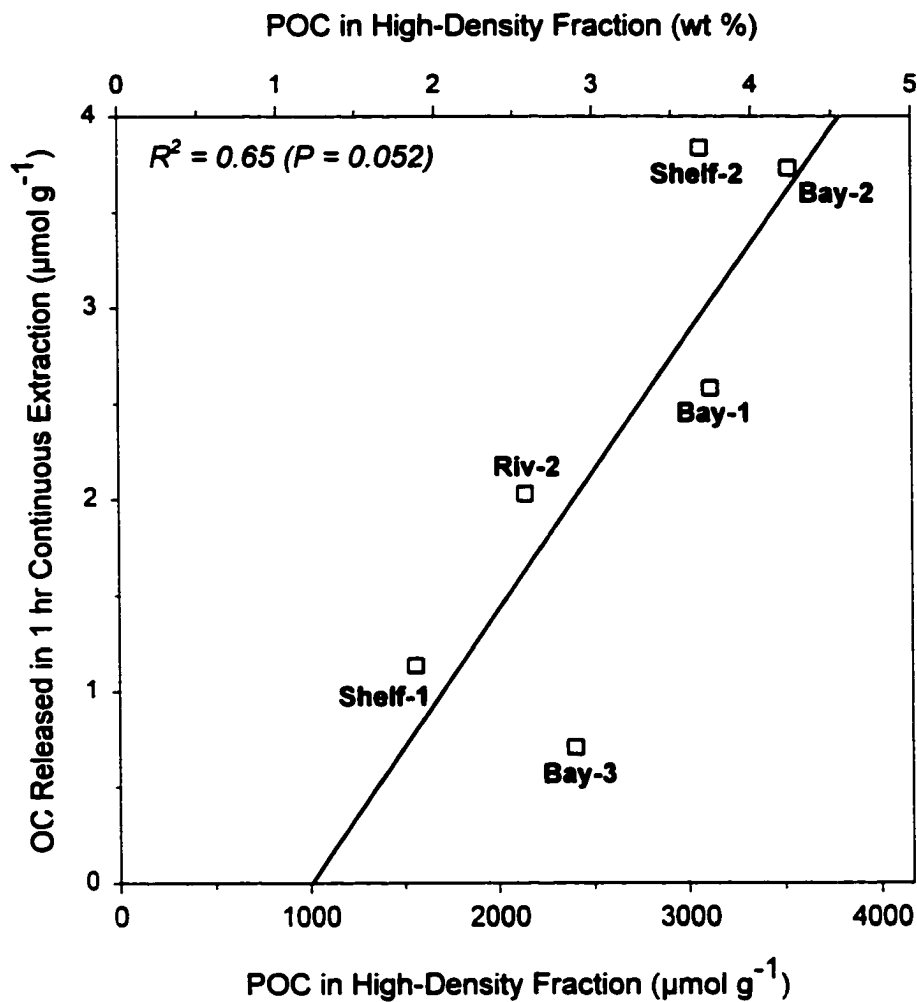


Figure 2.10. Correlation between OC released during 1-hr continuous extractions (Table 2.4) and POC present in the high-density fraction (normalized to dry bulk sediment mass).

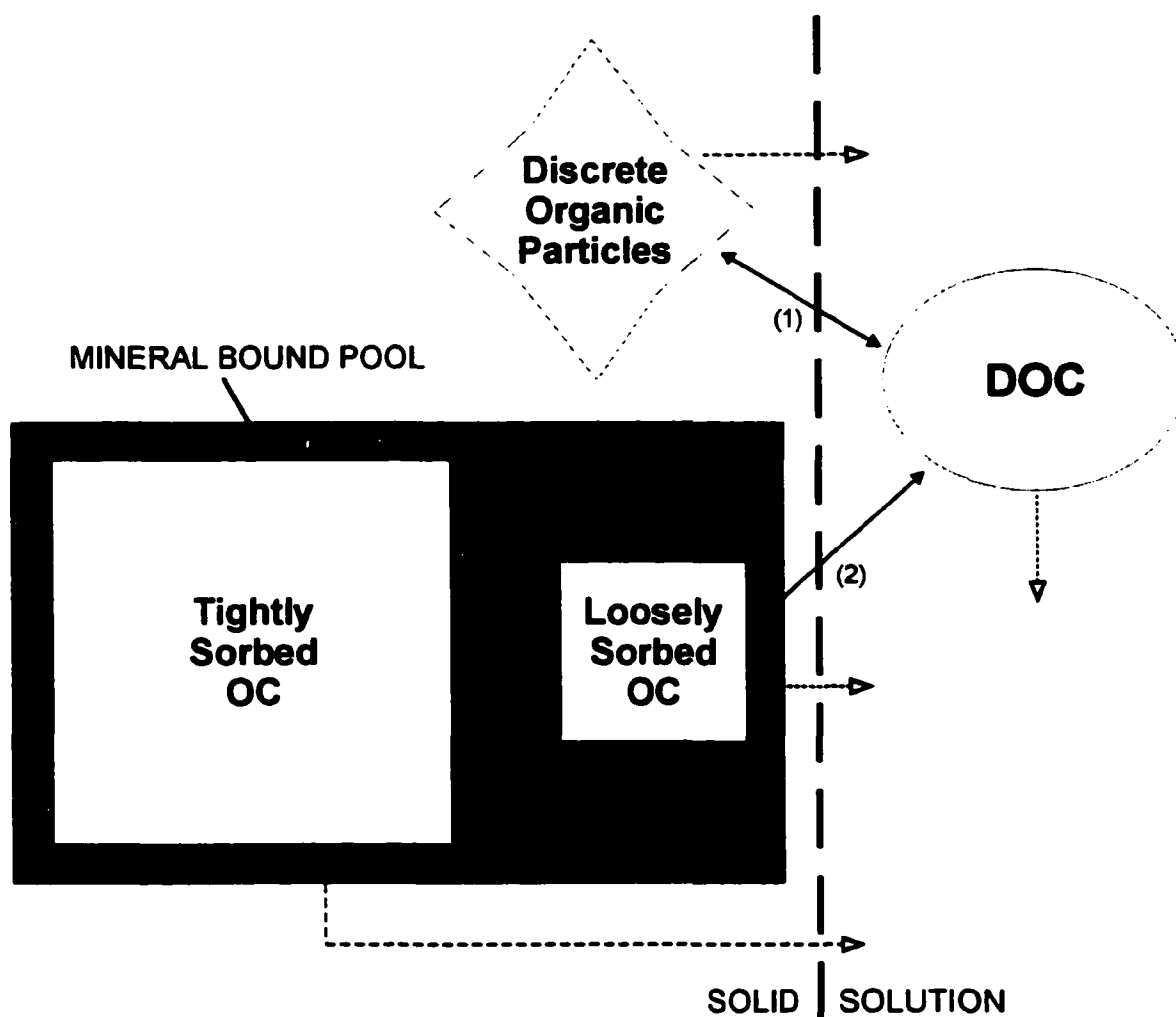


Figure 2.11. A proposed model of the interrelationships among different reservoirs of dissolved and particulate C (separated by dashed vertical line), applicable to both the sediment and water column. Discrete organic particles include both live and dead. The DOC pool represents either DOC in the bottom water or pore water of sediments. Solid arrows represent transfer processes among organic C pools including (1, 2) ad/desorption (Thimsen and Keil, 1998), aggregation/precipitation (Chin et al., 1998), hydrolysis, exudation, dissolution, uptake (Valiela, 1995); (3) microbial degradation, condensation, increase in number of attachments between polymer and mineral surface (Collins et al., 1995; Henrichs, 1995). All dashed arrows indicate loss by oxidation to DIC.

CHAPTER 3: FLUORESCENCE CHARACTERISTICS OF ORGANIC MATTER RELEASED FROM COASTAL SEDIMENTS DURING RESUSPENSION¹

ABSTRACT

Excitation-emission matrix (EEM) fluorescence spectroscopy was employed to study the chemical nature of organic matter readily released into solution from sediment particles during episodes of resuspension. Surface sediment samples collected from five locations within the Hudson River Estuary and the Inner New York Bight were resuspended in their respective bottom waters for periods ranging from 30 s to 2 h. In most cases, fluorescence characteristics of the sample after resuspension differed from those predicted by conservative mixing of bottom and pore waters. Examination of excitation-emission matrices (EEMs) revealed that resuspension resulted in: (1) more intense humic-like fluorescence (Ex/Em 310/420 nm), and (2) proportionally greater fluorescence in the longer wavelength region of the spectrum (Ex/Em 360/460 nm) relative to the predicted values. Trends in the positions of excitation-emission maxima reported in the literature strongly suggest that fluorophores emitting at longer wavelengths are increasingly degraded. Thus, the data imply that resuspension of estuarine and coastal marine surface sediments causes net release of degraded, mineral-bound organic matter from the sediment matrix to the surrounding bottom waters.

¹ To be submitted to *Marine Chemistry*

1. INTRODUCTION

Organic matter of aquatic and terrigenous origin is subject to extensive alteration and destruction through biological and physicochemical processes as it passes through the hydrosphere. In coastal waters, these changes are especially dynamic and comprise an important component of the marine C cycle (Smith and Hollibagh, 1993; Hedges, 1992; Hedges et al., 1997). Previous investigations of organic matter cycling in estuaries and in continental margins have highlighted the multiple sources and fates of particulate and dissolved organic matter (e.g., Mannino and Harvey, 1999, 2000a,b; Benner and Opsahl, 2001; Raymond and Bauer, 2001a), re-distribution of organic matter between solid and solution phases through flocculation (Sholkovitz, 1976; Sholkovitz et al., 1978; Fox, 1983), and the possible importance of adsorption/desorption (Bianchi et al., 1997; Mannino and Harvey, 1999; Guo and Santschi, 2000; Mannino and Harvey, 2000a; Mitra et al., 2000). In the present study, the chemical nature of organic matter released as a consequence of resuspension-induced desorption is examined.

In a preceding study (Komada and Reimers, 2001), the effects of resuspension on organic carbon (OC) partitioning between surface sediments from estuarine and coastal marine environments and their respective bottom waters were evaluated under laboratory conditions. The results showed that a small ($\leq 0.3\%$) but reasonably constant fraction of the mineral-bound particulate organic carbon (POC) is readily available for release upon resuspension, whereas the remainder appeared strongly sorbed over time scales of minutes to hours. While the small size of the loosely-sorbed POC pool indicates that the impact of a single resuspension event on OC dynamics is minimal, it was speculated that

over repeated resuspension-deposition cycles, OC release may become geochemically significant. This is particularly true if the strongly-sorbed fraction of the POC re-supplies OC to the loosely-sorbed pool as a consequence of microbial degradation or transformation (Komada and Reimers, 2001). Such a partitioning scheme also seems consistent with geochemical evidence showing losses and alteration of mineral-sorbed OC across various environments (Keil et al., 1997; Hedges et al., 1999; Keil and Fogel, 2001). In this study, this model is tested further by characterizing the chemical nature of the OC released from the solid phases using excitation-emission matrix (EEM) fluorescence spectroscopy.

EEM fluorescence spectroscopy has been applied to various aquatic environments as a means to investigate the humic-like component of dissolved organic matter (e.g., Coble et al., 1990; Coble, 1996; Matthews et al., 1996; Moran et al., 2000). Humic-like compounds dominate dissolved OC (DOC) fluorescence and typically represent 30-50 % of the total DOC of natural waters (Thurman, 1985). The molecular structure of the humic-like organic matter is not fully understood (Hedges et al., 2000), therefore, the mechanism responsible for fluorescence is currently unknown. However, unlike single excitation scans, construction of an EEM allows the detection of the position of maximum emission at maximum excitation (Ex/Em-max). This unique information has been used to distinguish and track water masses (Coble et al., 1998; Del Castillo et al., 1999), infer the source character of the fluorescent matter (Coble, 1996; Coble et al., 1998; McKnight et al., 2000), and to investigate the impact of degradative processes on the fluorescent component of dissolved organic matter (Moran et al., 2000; Partlanti et al., 2000).

Based on the results of greater than 60 freshwater and marine, as well as sediment pore-water samples, Coble (1996) reported the Ex/Em-max of the humic-like peaks that are stimulated by visible light (visible humic-like peaks) to vary significantly across different environments (Table 3.1). A variety of samples, ranging from riverine to open ocean deep waters fluoresce in the spectral region Ex/Em 320-360/420-460 nm (region C), while those that fluoresce in the shorter wavelength region Ex/Em 290-310/370-410 nm (region M) appear to be limited to surface marine waters harboring moderate to high phytoplankton production (Coble, 1996; Coble et al., 1998). Based on these observations, the relationship between peak position and organic matter source (i.e., terrestrial or marine) appears equivocal. However, in the present study, an alternative interpretation linking peak position and the degree of organic matter degradation and humification is proposed based on additional literature data.

The following questions were addressed. (1) What are the fluorescence characteristics of the OC released from the solid phases during resuspension? (2) How do they differ from the fluorescence characteristics of bottom waters and pore waters that the particles are immersed in? (3) Based on evidence from the literature, what can be said about the chemical nature of the released OC and its ultimate source? Based on the findings, the role of resuspension-induced OC partitioning in the marine C cycle is further evaluated.

2. MATERIALS AND METHODS

2.1. Sample collection

Sediment cores and bottom water samples were collected from five locations along an estuarine gradient: station Riv-2 in the tidal freshwater reaches of the Hudson River, stations Bay-2 and Bay-3 in the Raritan-Lower New York Bay complex, and stations Shelf-1 and Shelf-2 in the Inner New York Bight. Site description and details of the sampling procedures are given in Komada and Reimers (2001). Briefly, sediment cores for resuspension experiments were collected by subcoring from Peterson grabs, transported back to the laboratory in New Brunswick, NJ, and incubated in the dark at ambient temperatures prior to further processing (section 2.3.). The only exceptions were cores collected from station Riv-2 which were frozen. Sediment cores used to determine pore-water profiles of DOC and fluorescence (section 2.2.) were collected using a push corer, gravity corer, or a Peterson grab sampler, and ranged in length from <10 cm to 70 cm. These cores were processed under a N₂ atmosphere within 12 hours of retrieval. Bottom water was collected by a Niskin bottle and filtered (0.45 μm). Samples intended for DOC and fluorescence analyses (section 2.2.) were frozen immediately. Additional bottom water samples for resuspension experiments were refrigerated in the dark in glass jugs.

2.2. Analyses

Fluorescence measurements were made on bottom and pore waters from the study region, and samples collected during the resuspension experiments (section 2.3.) using an AMINCO-Bowman Series 2 Luminescence Spectrometer equipped with a continuous wave 150W xenon lamp. In order to make the results comparable to those collected from different instruments in other laboratories, both excitation and emission spectra were fully corrected for distortions that arise from wavelength-dependent efficiencies of the instrument (Parker, 1968; Miller, 1981). Excitation correction factors were obtained from excitation spectra (Ex 200-600 nm; Em at 625 nm) of 5 g L⁻¹ rhodamine B (Fluka, fluorescence grade) in ethylene glycol (Fluka, 99.9 % purity) placed in a triangular quartz cuvette. Emission correction factors were provided by the manufacturer. Emission spectra of quinine sulfate dihydrate (NIST) in 0.105 M HClO₄ agreed to generally within 3 % of values given by NIST (Velapoldi and Mielenz, 1980).

Immediately prior to conducting the fluorescence measurements, optical density of the sample was measured using a spectrophotometer. To avoid inner filter effects, samples exhibiting high absorbances were diluted with distilled de-ionized water so that absorption at 260 nm was reduced to 0.02 (Parker, 1968). To construct excitation-emission matrices (EEMs), 40 emission spectra were obtained following the method of Coble et al. (1993). Scan rate was 4 nm sec⁻¹, integration time was 0.5 sec, and excitation and emission bandpasses were both 4 nm. All measurements were made in ratio mode, and at a fixed photomultiplier voltage. The sample cell compartment was maintained at 25 °C.

In order to remove Raman scatter peaks, an emission spectrum of either distilled de-ionized water (in the case for non-experimental bottom and pore waters), or experimental blanks (in the case for experiment samples; section 2.3.) was subtracted from each sample spectrum. In most cases, remnant peaks (both positive and negative) centered about the Raman line maximum were visible after subtraction. The presence of these peaks did not interfere with the fluorescence associated with the humic-like component of the organic matter, therefore, they are present in the final EEMs. Following the method of Coble et al. (1993), the peak intensity of the Raman line of distilled de-ionized water (at Ex/Em 275/303 nm) was monitored daily to account for small day-to-day changes in the overall signal intensity. All fluorescence intensities are expressed in units of ppbQSE, where 1 ppbQSE is equivalent to the fluorescence intensity of a solution of 1 ppb quinine bisulfate in 0.05 M H₂SO₄ at Ex/Em 348/449 nm.

At excitation wavelengths of 310 and 370 nm, peak positions of 5 replicate emission spectra agreed to within 4 nm (bandpasses), and the intensities generally within 2 %. In contrast, reproducibility at shorter excitation wavelengths was poor due to the lowered lamp intensity in this region of the spectrum. For this reason, quantitative discussions are limited only to the region of Ex >290 nm and the visible humic-like peak (Table 3.1). Peak positions in the EEMs (Ex/Em-max) could generally be determined to within ± 10 nm Ex/Em. Effects of salinity on fluorescence intensities were not tested in this study. However, previous work by Mobed et al. (1996) indicate minimal impact of varying ionic strength (between 0-1 M KCl) on the EEM of humic substances.

DOC was determined by high-temperature catalytic oxidation (Sugimura and Suzuki, 1988) using a Shimadzu 5000A TOC Analyzer following recommendations by

Sharp et al. (1993). Precision was typically within 5 %. DOC values of reference materials prepared by the laboratory of Dr. J. H. Sharp generally agreed to given values (Komada and Reimers, 2001).

2.3. Resuspension experiments

Details of the experiments mimicking resuspension are given in Komada and Reimers (2001). Briefly, the uppermost 2 cm of the sediment core was homogenized under an N₂ atmosphere, and mixed with air-saturated, filtered bottom water from the same site (to make slurries having solid concentrations of approximately 100 g L⁻¹) for 30 seconds, 10 minutes, 1 hour, or 2 hours (continuous extractions). At the end of each extraction period, samples were centrifuged and the supernatant analyzed for DOC concentration and fluorescence (section 2.2.). The 10-minute treatments were further subjected to series extractions, where additional bottom water was added to the sediment pellet after centrifugation, and the same cycle was repeated 3 times. An additional set of experiments identical to the above was conducted using sediment collected from station Riv-2, but with water collected from station Bay-3 instead of Riv-2. This experiment is referred to as Riv-2Bay.

Control samples containing only sediment or bottom water were also prepared and processed in parallel with the experimental samples. The DOC concentration and fluorescence intensities of the supernatant of the extraction samples were compared to those that can be predicted from linear combinations of the corresponding values of the bottom- and pore-water controls assuming conservative mixing. Similar to what was

observed previously for DOC (Komada and Reimers, 2001), fluorescence intensity at Ex/Em-max changed little in the control tubes with time, but the fluorescence intensities of pore-water controls were in several cases greater than values observed in newly collected cores (Fig. 3.1).

In addition to controls, blanks containing distilled deionized water were also processed in duplicate for a given set of experiments. DOC concentrations at the end of the run were less than 14 μM and generally exhibited EEMs that were indistinguishable from those of unprocessed distilled deionized water. Control blank values were subtracted from all experimental sample data.

Establishment of sediment and solution mass balance during these experiments has been verified previously (Komada and Reimers, 2001). To determine if mass balance is also attained for fluorescence intensity, a test experiment was conducted where bottom and pore waters from stations Riv-2 and Shelf-2 were mixed (for 30 seconds and 2 hours) under conditions identical to those encountered during the resuspension experiments, but in the absence of sediment. EEM of the resultant mixtures were compared to those predicted from the linear combinations of the parent pore- and bottom-water EEMs. Subtraction of the predicted EEMs from the measured EEMs of the mixtures are flat and featureless for Ex > 300 nm (Fig. 3.2), demonstrating good agreement (within about 2 ppbQSE) between measured and predicted EEMs, and conservative mixing of fluorophores.

3. RESULTS

3.1. Fluorescence characteristics of non-experimental bottom and pore waters

All bottom and pore waters collected from the study area exhibited similar EEMs with a broad peak spanning the two visible humic-like regions C and M, as well as the UV humic-like region (Table 3.1., Fig. 3.3). Protein-like peaks were also observed in many pore-water samples, as well as in some bottom waters (Fig. 3.3). However, as stated earlier (section 2.2.), the remainder of this paper will focus primarily on the peaks found in the vicinity of the visible humic-like regions, for they were common to all samples and could be detected with greater precision.

The humic-like peak (from here on, the word “visible” will be dropped) of the bottom and pore waters generally clustered near Ex/Em 310/420 nm, in between regions C and M (Fig. 3.4, Table 3.1). The clustering of the peaks suggests that similar fluorophores were present along the salinity gradient as well as within bottom and pore waters (as deep as 68 cm in sediment) of this region. The humic-like peaks of the pore- and bottom-water controls employed in the experiments also fell in the same region (Fig. 3.4), showing that the experimental handling alone had little or no impact on the Ex/Em-max of the humic-like fluorescence of the bottom and pore waters.

Fluorescence intensities of both the bottom and pore waters correlated positively and linearly with DOC concentration with a slope of approximately $0.2 \text{ ppbQSE } \mu\text{M DOC}^{-1}$ (Fig. 3.5). Linear relationships between DOC and fluorescence have been reported previously for estuarine to continental margin waters (e.g., Laane and Koole,

1982; Vodacek et al., 1995; Chen, 1999), and sediment pore waters (Chen et al., 1993; Chen and Bada, 1994). The results presented in Fig. 3.5 indicate that carbon-normalized fluorescence intensity did not vary significantly between pore and bottom waters, or across the estuarine gradient of this region. Carbon-normalized fluorescence intensities of most experimental controls overlapped with those of the non-experimental water samples (Fig. 3.5), again indicating little alteration of humic-like fluorescence during the experiments.

Clear departures from the above trend were observed for pore-water controls from stations Riv-2 and Shelf-1 which exhibited attenuated carbon-normalized fluorescence intensities (data points enclosed in ellipses in Fig. 3.5(b)). These samples exhibited strong protein-like fluorescence (ratio of protein-like peak to humic-like peak = 4-10) compared to their corresponding counterparts that fell along the main regression line (ratio of protein-like peak to humic-like peak = 1-2; data not shown). This suggests that these samples were contaminated by protein-like organic matter most likely introduced by the lysis of living biomass. For station Riv-2, freezing and thawing the sediment prior to the experiment may have led to this deviation. For station Shelf-1, it appears that centrifugation may have been the cause. While a pore-water sample collected from the upper 2 cm of the sediment column using a sipper fell along the main regression line, pore water collected from the same sediment aliquot by centrifugation exhibited lower C-normalized fluorescence intensity similar to the control samples (Fig. 3.5(b)). Shelf-1 is also the only station where DOC concentrations of pore-water samples collected by the two devices do not agree (Komada, unpublished data). These data further emphasize the

importance of minimizing sediment disturbance when collecting DOC samples (Martin and McCorkle, 1993; Alperin et al., 1999).

3.2. Fluorescence characteristics of organic matter released from the solid phase

3.2.1. Humic-like peak intensity

During the resuspension experiments, there was a net release of OC into solution during both continuous and series extractions (Fig. 3.6, 3.7; Komada and Reimers, 2001). Near-conservative mixing and net losses of OC were also observed in the Bay and Shelf stations during 30-second and the first cycle of the 10-minute treatments. Otherwise, the amount of OC released tended to increase with extraction time (Fig. 3.6), and either decreased or changed little with each cycle of the series extractions (Fig. 3.7). Overall, the amount of readily releasable OC from a given sediment was best predicted by the OC content of the high-density fraction of the sediment matrix, implying that OC was released from the mineral-bound POC (Komada and Reimers, 2001).

The EEM of the supernatant after extraction was similar to the predicted value (calculated from EEMs of pore- and bottom-water controls; section 2.3.), but with different humic-like peak intensities (Fig. 3.8(a),(b),(d),(e)). To determine the net change in humic-like fluorescence during the extractions, the difference between the humic-like peak intensities of measured (Fig. 3.8(a),(d)) and predicted (Fig. 3.8(d),(e)) EEMs were determined and normalized to the sediment mass in each tube. In the Bay and Shelf stations, humic-like fluorescence tended to intensify whenever OC was released into solution (Fig. 3.6, 3.7). However, in experiments involving the River sediment, there was

a clear de-coupling of OC and fluorescence, where net losses of fluorescence intensity accompanied net releases of OC into solution (Fig. 3.6, 3.7). The reason for this is currently unclear. Excluding the cases where OC and fluorescence were de-coupled, increase in fluorescence intensity correlated, albeit weakly, with OC release for both continuous and series experiment results (Fig. 3.9(a)). This suggests that the released OC included fluorophores similar to those found in the bottom and pore waters. Meanwhile, the slope of this relationship was about a factor of 7 smaller than those observed for the bottom and pore waters (Fig. 3.5), indicating that although the released OC may have included similar fluorophores, its bulk characteristics were distinct.

3.2.2. Long-wavelength peak intensity

To determine if the released OC was composed of identical sets of fluorophores as those encountered in the bottom and pore waters, an emission intensity ratio, R , was computed for each pair of measured and predicted EEMs (Fig. 3.8) for a given sample supernatant:

$$R = r_{\text{meas}}/r_{\text{pred}}$$

where

$$r = (\text{maximum emission intensity at Ex 360 nm})/(\text{maximum emission intensity at Ex 310 nm})$$

and subscripts *meas* and *pred* represent measured and predicted EEMs, respectively. Ex 310 was selected as the average position of the humic-like peak, whereas Ex 360 is the red-most boundary of the peak C region (Fig. 3.4; Table 3.1). If the released OC included an identical set of fluorophores as those in the bottom and pore waters, then $R =$

1; otherwise, $R \neq 1$. The value of R for replicate EEMs of an identical sample, as well as measured and predicted EEMs determined in the test experiment to verify fluorophore mass-balance (section 2.3.) averaged 1.03 ± 0.06 ($n=6$; $P=0.05$).

In both continuous and series experiments, R was in many cases greater than 1 (Fig. 3.10), indicating that briefly dispersing the sediment in bottom water tended to result in a proportionally stronger fluorescence signal in the longer wavelength region of the EEM. For the few cases where net losses in the humic-like signal were observed (Fig. 3.6, 3.7), increases in R could also be driven by the weakening of the signal at Ex 310 nm. In cases where $R > 1.1$, subtraction of the predicted EEM from the measured EEM resulted in the appearance of a distinct peak near Ex/Em 360/460 nm (Fig. 3.8c,f), approximately 50/40 nm (Ex/Em) red-shifted from the visible humic-like peak cluster (Fig. 3.4). The intensity of this long-wavelength peak became stronger with increasing release of OC into solution (Fig. 3.9(b)), demonstrating that in addition to the humic-like fluorophore (Ex/Em-max 310/420 nm), released OC included additional fluorophores with distinct, red-shifted Ex/Em-max.

Further examination of Fig. 3.10 shows that the R values tended to be greater for the Shelf than the Bay and River sediments; in both continuous and series experiments, the two Shelf stations exhibited the highest values ($R=1.1$ to 1.3), while the Bay and River stations gave moderate to low values ($R=1.0$ to 1.15). It is also interesting to note that in the series experiments, Riv-2Bay exhibited much higher values ($R \geq 1.1$) than Riv-2 ($R \approx 1$) (Fig. 3.10(b)). This apparent dependence of R on region or salinity is in contrast to trends in bulk OC release (Fig. 3.6, 3.7), which is driven more by the abundance of POC associated with the mineral phase (Komada and Reimers, 2001).

4. DISCUSSION

4.1. Nature of the long-wavelength peak fluorophore

The above results show that released OC included fluorescent matter, part of which was most likely structurally similar to the compounds responsible for the humic-like fluorescence observed in bottom and pore waters (Fig. 3.8, 3.9(a)). Relative to bottom- and pore water DOC, released OC was also proportionally enriched in fluorescent compounds that emit in the long-wavelength region (Ex/Em 360/460 nm; Fig. 3.8, 3.9(b), 3.10). These findings, along with the lowered carbon-normalized fluorescence intensity of the released OC (Fig. 3.5, 3.9), are evidence for the unique compositional character of the OC released from the solid phase relative to the DOC pools in the bottom and pore waters.

As a means to investigate the chemical nature of the fluorophore responsible for the long-wavelength peak, positions of Ex/Em-max observed in this study were compared to those previously published for various organic matter samples of aquatic and soil origin. In contrast to the humic-like peak whose Ex/Em-max fell well within the range of peak positions previously reported for various aquatic samples, the long-wavelength peak appeared within and to longer wavelengths of the peak C region (Fig. 3.4). To the best of my knowledge, these are one of the few peak positions (derived from fully-corrected spectra) reported in the literature that lies further towards the red than the C region (Table 3.2). The true nature of the fluorophores responsible for the humic-like fluorescence is unknown, although products of oxidative crosslinking of polyunsaturated fatty acids

(Harvey, 1984) and an imine-enamine (Laane, 1984) have been proposed. Without knowing the structure of the fluorophores, it is impossible to understand the meaning of the relative peak positions at the molecular level. Nevertheless, some useful and important insight at the bulk OC level can be drawn.

While many riverine and coastal waters have been found to fluoresce in the C region (e.g. Coble, 1996; Moran et al., 2000), open ocean waters fluoresce in both M and C regions: surface waters supporting high primary productivity commonly exhibit peaks in the M region, and deeper waters fluoresce increasingly more into the C region (Coble, 1996; Coble et al., 1998). Therefore, for marine dissolved organic matter, progression of the peak position from region M to C has been proposed to be the result of increased aging and degradation (Coble et al., 1998). Similar conclusions have been drawn by Partlanti et al. (2000) who observed a red-shift in the humic-like peak position (from region M to C) during 2-month long degradation experiments of macro-algae. Furthermore, this trend does not appear to be limited to marine organic matter. For example, Zsolnay et al. (1999) compared the position of the emission maximum of three different extracts of a soil sample: (1) fulvic acid; (2) CaCl₂ extract; and (3) CaCl₂ extract after fumigation with CHCl₃ to induce cell lysis. Their results show that the position of the emission maximum shifted to longer wavelengths with increasing level of humification: fumigated-CaCl₂ < CaCl₂ < fulvic acid. Senesi et al. (1991) compared excitation and emission spectra of humic acid extracts of various soils, sludge and compost, and soil fungi, and found their Ex/Em-max to differ from one another across a range of 80/80 nm. The peak position shifted increasingly to longer wavelengths in the order: fungi, compost and sludge < various soils and peat < paleosol.

All of the above literature data suggest that increased degradation of the organic matter results in a progressive red-shift of the position of the Ex/Em-max. A possible explanation for this phenomenon is increased conjugation and condensation that may take place during the process of humification (Stevenson, 1994). Compared to soils, condensation may not be an important process in the marine environment (Hedges et al., 2000), but concentration of the more polymeric and increasingly crosslinked components during the course of degradation is possible (Hatcher et al., 1983; Tegelaar et al., 1989; Hedges et al., 2000). A well-documented phenomenon for aromatic compounds is that with increased linear conjugation - which de-localizes the π -electron systems and hence reduces the energy separation between the ground and excited states - absorption and fluorescence shift to longer wavelengths (Berlman, 1965). Furthermore, compared to a free molecule, polymerization of multiple fluorophores enhances the probabilities for bimolecular processes such as radiative energy transfer and excimer/exciple formations that also increase the wavelength of emission (Phillips, 1985). The red-shift may also be the result of the addition or increased relative abundance of certain functional groups during the humification/degradation process. For example, addition of carboxyl, nitro, and hydroxyl groups to aromatic compounds have been shown to shift fluorescence to longer wavelengths (Berlman, 1965; Guilbault, 1973; Seitz, 1981).

Based on the above, it is concluded that released OC was proportionally enriched in an increasingly degraded form of organic matter compared to bottom- and pore-water DOC.

4.2. Possible source for the long-wavelength peak fluorophore

As discussed by Komada and Reimers (2001), the amount of readily-releasable OC is a very small ($\leq 0.3\%$) fraction of the total POC content of the sediment; the majority of the POC is tightly associated with the mineral phases, and hence not readily available for release. Despite the limited size of the loosely-sorbed pool, resuspension-induced OC release has the potential to be a geochemically significant process when one takes into consideration the fact that resuspension-deposition cycles (triggered by forces such as tidal motion, storms, and dredging) tend to be repetitive. Upon re-deposition, if the readily-releasable pool of the sediment particle is solely replenished by re-adsorption of DOC, then the observed release of OC has zero net impact on either the dissolved or the solid OC reservoirs. If, on the other hand, some OC mass-transfer takes place between the loosely-sorbed and the more tightly-sorbed fractions (perhaps through microbial hydrolytic activity), then repeated OC release over multiple resuspension-deposition cycles has the potential to impact the bulk OC content/composition of the particulate phase prior to permanent burial and diagenesis (Komada and Reimers, 2001).

The results of this study show that relative to the bottom and pore waters which exhibited similar fluorescence characteristics, the loosely-sorbed fraction of the POC is enriched in what appears to be increasingly degraded fluorescent organic matter. In a recent study, Raymond and Bauer (2001b) presented radiocarbon signatures of DOC and suspended POC of North Atlantic rivers showing POC to be in general older than DOC of the same site. In the freshwater reaches of the Hudson River, suspended POC had an average radiocarbon age of greater than 4500 years BP, more than 3000 years older than

corresponding DOC. Raymond and Bauer (2001b) argued that the old radiocarbon age of POC is in part due to the presence of refractory organic matter that aged within the soil horizons, whereas the more recent age of DOC reflects greater contribution from younger and hydrolyzable soil/litter leachates. Therefore, considering the coastal setting of the study sites, the relatively degraded fluorescent organic matter detected in the loosely-sorbed fraction of the sediment POC likely originated from a relatively old fraction of the POC that is tightly associated with the mineral surface than from bottom-water DOC (via adsorption). The data presented in this study are then consistent with the idea that at least a part of the readily-releasable POC is re-supplied from the older and more degraded OC reservoir that is strongly associated with the mineral phase.

4.3. Geochemical implications

Correlations between available mineral surface area and OC in marine sediments and soils suggest that OC is adsorbed strongly to mineral surfaces, and that it is not readily available for microbial degradation (Mayer, 1994a,b; Hedges and Keil, 1995, Henrichs, 1995). Meanwhile, large variations have been documented in the OC loading per unit mineral surface area, as well as the chemical composition of the sorbed OC across different oceanic environments (Hedges and Keil, 1995; Keil et al., 1997; Hedges et al., 1999; Keil and Fogel, 2001). The corollary is that organic-mineral associations are rarely permanent, and that even strong associations are eventually subject to destruction.

If, as the results of this study suggest, there is indeed transfer of OC from the strongly-sorbed to the loosely-sorbed pool, then the loosely-sorbed fraction – despite its small size within the total POC pool (Komada and Reimers, 2001) – may function as a

dynamic link between the bulk of the sediment POC and the surrounding environment. One implication of this hypothesis is that resuspension-induced OC releases over repeated resuspension-deposition cycles can potentially impact the content/composition of the strongly-sorbed OC pool prior to permanent burial of the particle (and subsequent diagenesis) in the sediment column. Additionally, net transfer of OC from the strongly-sorbed pool to the water column via the loosely-sorbed pool may enhance overall OC remineralization by increasing the likelihood of photochemically-mediated losses (Miller and Zepp, 1995; Amon and Benner, 1996; Miller and Moran, 1997), and perhaps microbial degradation (Gordon and Millero, 1985; Henrichs and Sugai, 1993; Keil et al., 1994).

Resuspension-induced release may be particularly important in estuaries and the coastal ocean where microbial activities, as well as OC loading per unit mineral surface area are high (Mayer, 1994a,b), and strong physical forcings (tides, bottom currents) are commonplace. Further studies of resuspension-induced partitioning of OC and its consequences may prove fruitful in increasing our understanding of the role of estuaries and the coastal ocean in the marine C cycle.

Table 3.1. Fluorescence peak types and corresponding ranges in Ex/Em-max as reported by Coble et al. (1998).

Type of Peak	Ex-max (nm)	Em-max (nm)
UV Humic-like	260	400-460
Visible Humic-like; M ¹	290-310	370-410
Visible Humic-like; C ¹	320-360	420-460
protein-like ²	275	305, 340

1. Collectively referred to as “visible humic-like” or “humic-like” peak in the text.
2. Attributed to tyrosine- (Em 305 nm) and tryptophan- (340 nm) like fluorescence.

Table 3.2. Fluorescence peak positions that lie to the red of the visible humic-like region C.

Sample Description	Ex-max (nm)	Em-max (nm)	Reference
Melanoidin (made from 1:1 mixture of glycine and lysine)	363	458	Coble, (1996)
humic acid extract from corals, solid corals, untreated seawater (collected near coral reef), Aldrich and Fluka humic acid	390	490	Matthews et al., (1996)
Aldrich and Fluka humic acid	460	540	Matthews et al., (1996)
Readily-releasable OC of surficial coastal sediments	340-380	445-470	this study

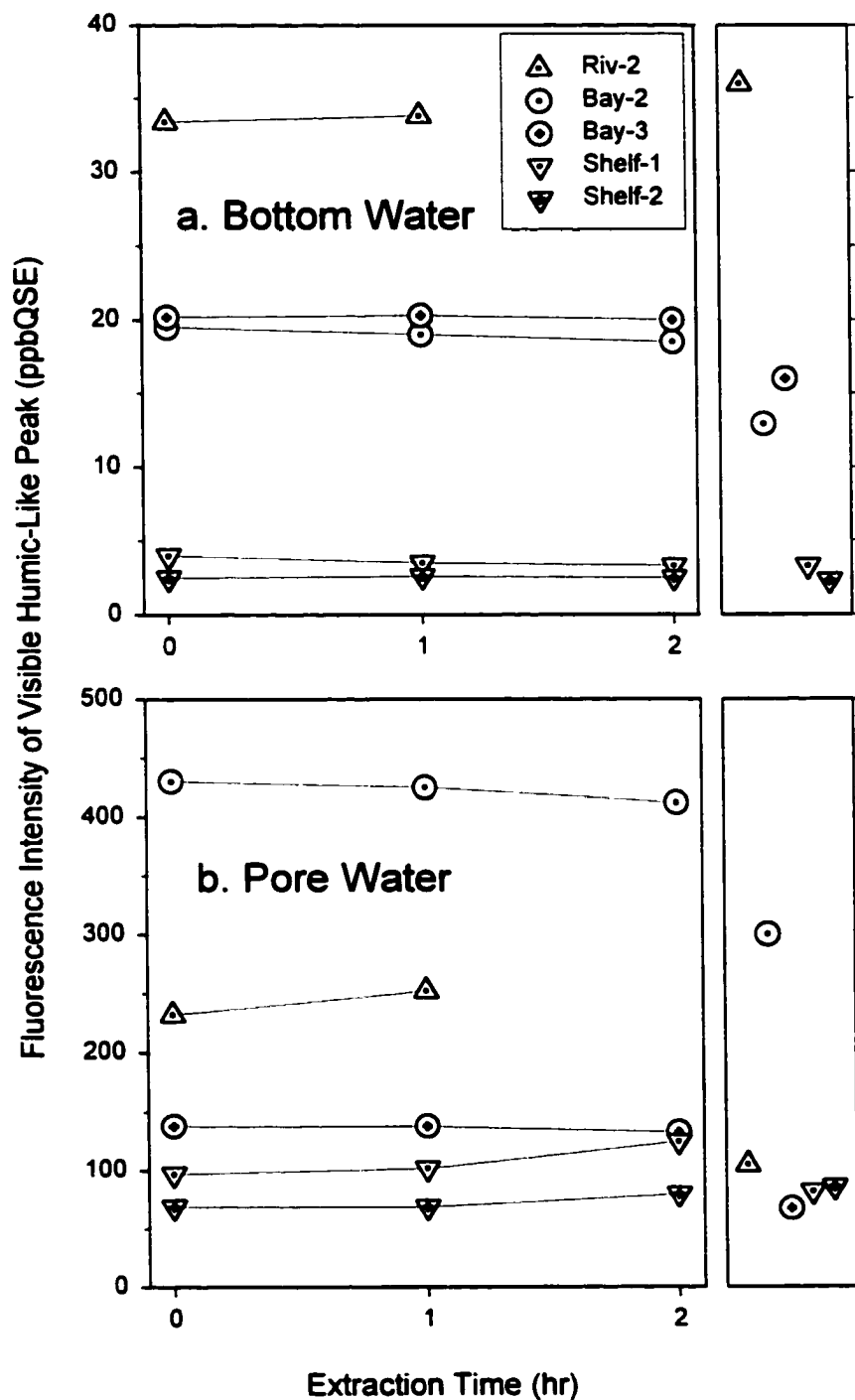


Figure 3.1. Visible humic-like peak intensities observed in (a) bottom-water and (b) pore-water control tubes (left panels). The expected ranges in pore water and bottom water under field conditions are shown on the right (pore-water values are derived from core sectioning, and those of bottom water by analysis of freshly collected sample).

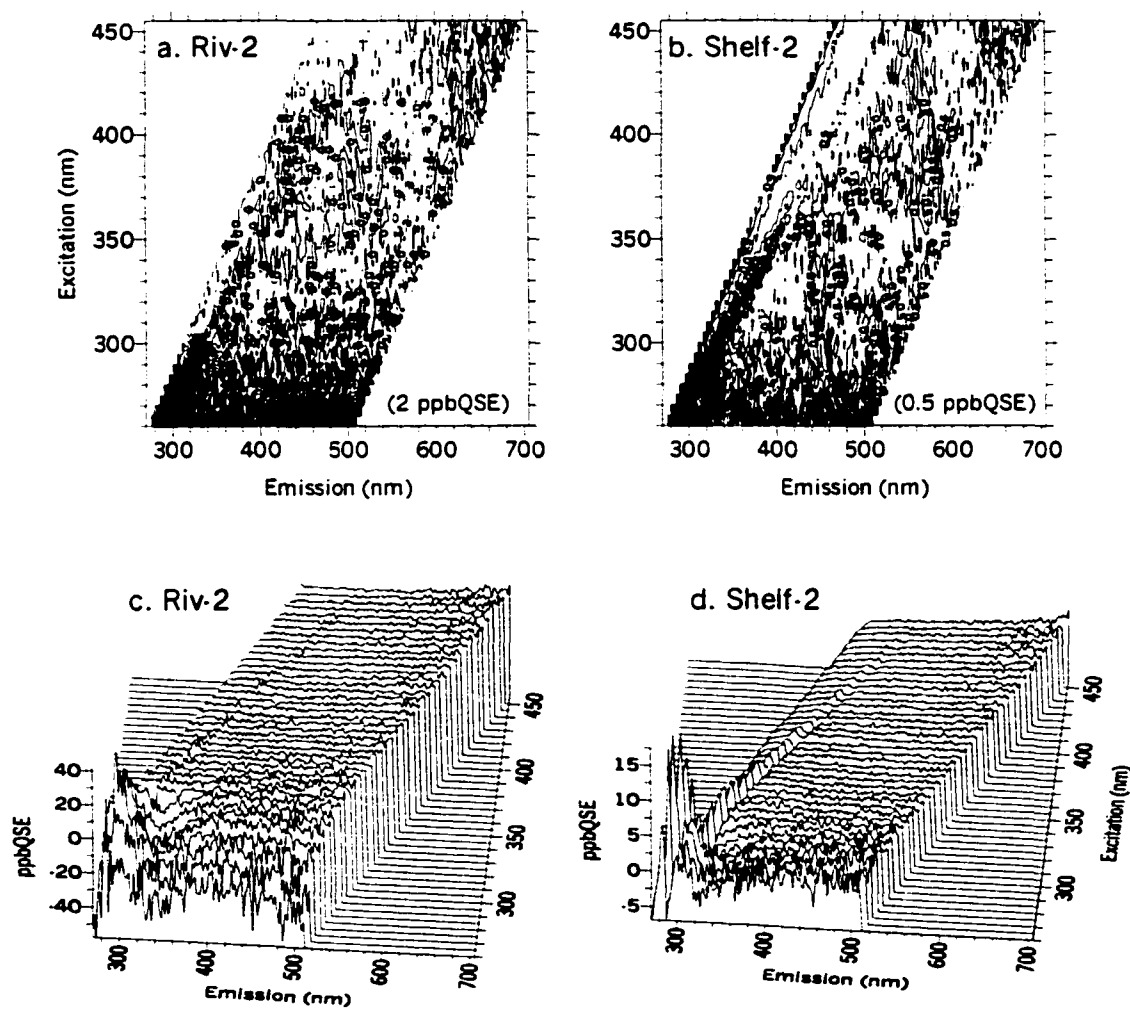


Figure 3.2. EEMs of 2-hour test experiment samples after subtraction of predicted EEMs (calculated from known EEMs of the parent pore and bottom waters; see text) for station Riv-2 (a,c) and Shelf-2 (b,d). Panels c and d are surface plot representations of contour plots shown in panels a and b (contour intervals are given in parentheses). Similar results were obtained for samples that were shaken for 30 seconds.

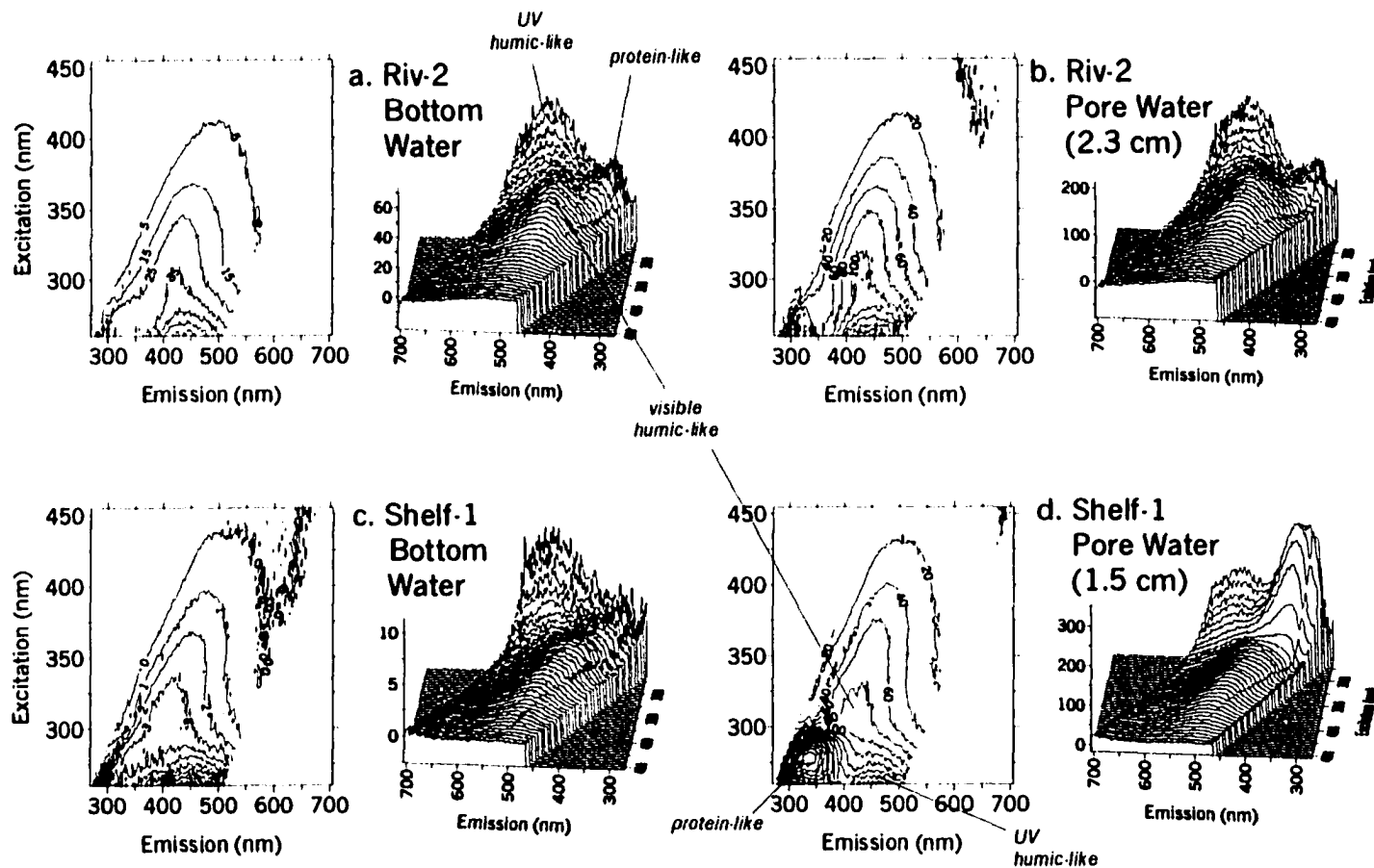


Figure 3.3. Contour and surface representations of EEMs of bottom- and pore-water samples from stations Riv-2 (a, b) and Shelf-1 (c, d) that were collected and analyzed independently of the extraction experiments. Note that surface plots are rotated 180° in order to make all peaks visible. All fluorescence intensities are given in units of ppbQSE (contour-line labels in contour plots, and z-axes in surface plots). The same set of peaks, but with different intensities were observed at other locations in the study area, as well as at different depths (as deep as 68 cm) in the sediment. See Table 3.1 for peak identification.

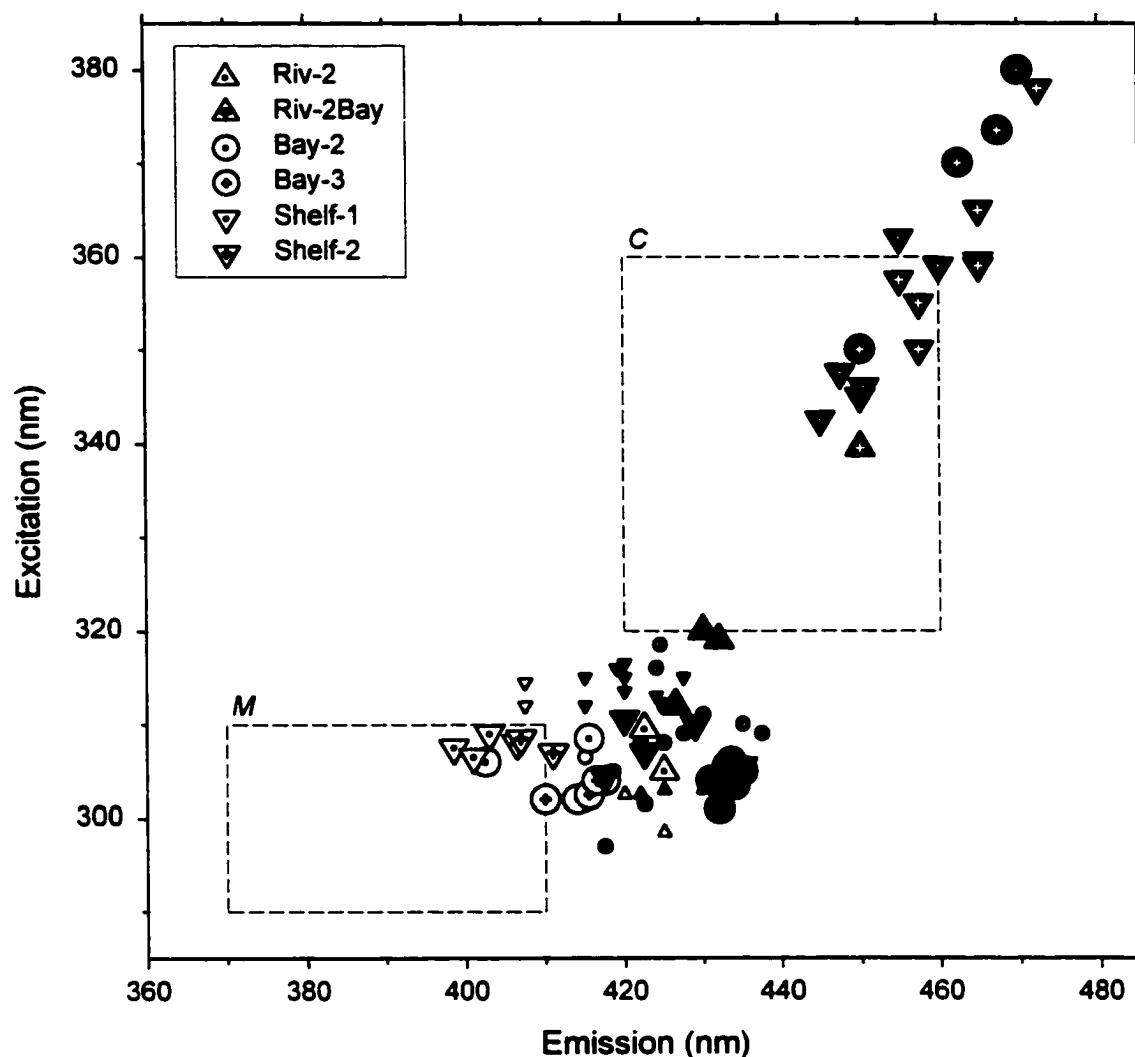


Figure 3.4. Peak positions (Ex/Em-max) observed in various EEMs. Data points clustered around Ex/Em 310/420 nm are bottom- (white) and pore-water (gray) EEMs of experimental controls (larger symbols that are dotted or crosshatched; see legend) and those collected and analyzed independently of the experiments (smaller symbols; upwards triangle = river; circle = bay; downwards triangle = shelf). Black symbols spanning Ex 340 to 380 nm are long-wavelength peaks observed in the extraction supernatants after subtraction of predicted EEMs. Dashed square regions are peak M and C areas as given by Coble et al. (1998) (Table 3.1).

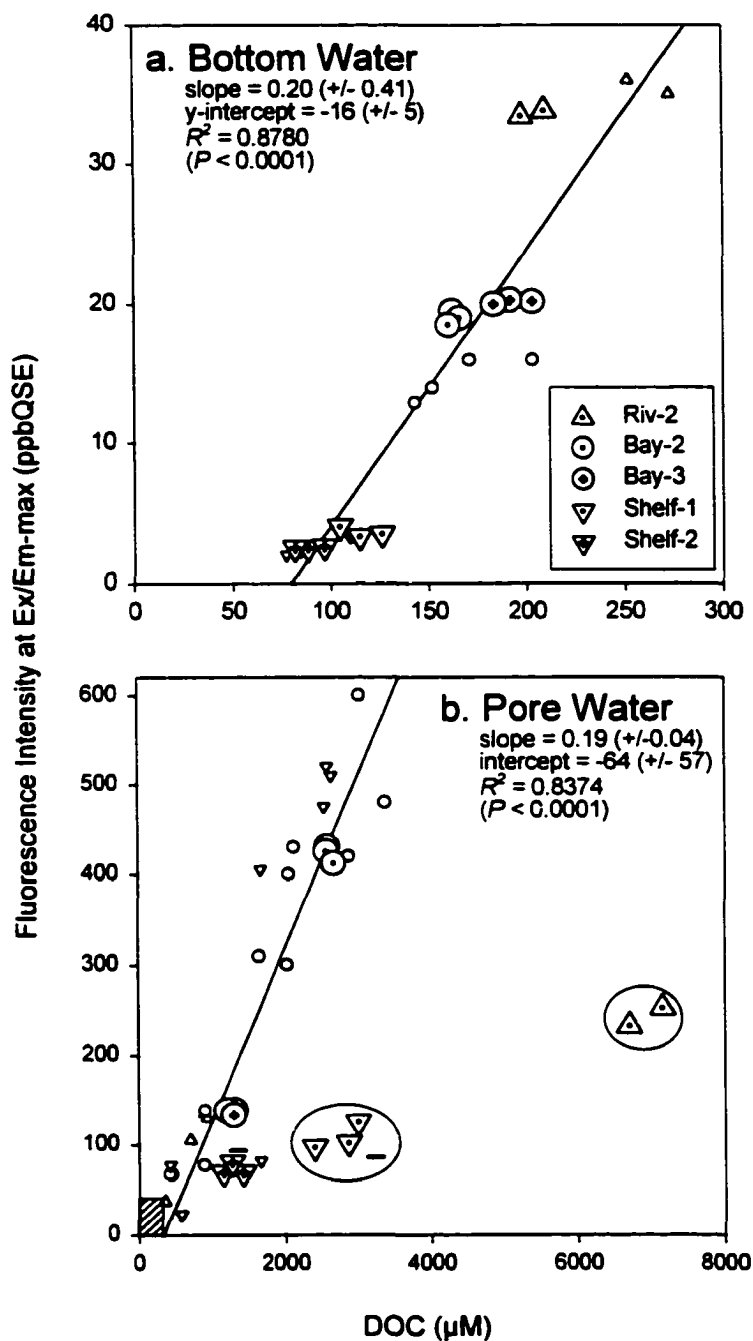


Figure 3.5. Fluorescence intensity of the visible humic-like peak plotted against DOC concentration of (a) bottom and (b) pore waters. Note differences in scale in both axes (the shaded box in (b) indicates the data-range of (a)). Larger symbols (corsshaired or dotted) are experimental controls (see legend). Smaller symbols are samples collected and analyzed independently of the experiments (upwards triangle = river; circle = bay; downwards triangle = shelf). Regression analyses include all data points except in (b) where those enclosed in ellipses were excluded (see text). In (b), the two horizontal bars near 100 ppbQSE represent data for centrifuged (in ellipse) and sipped (along main regression line) pore water from a core collected from station Shelf-1 (see text).

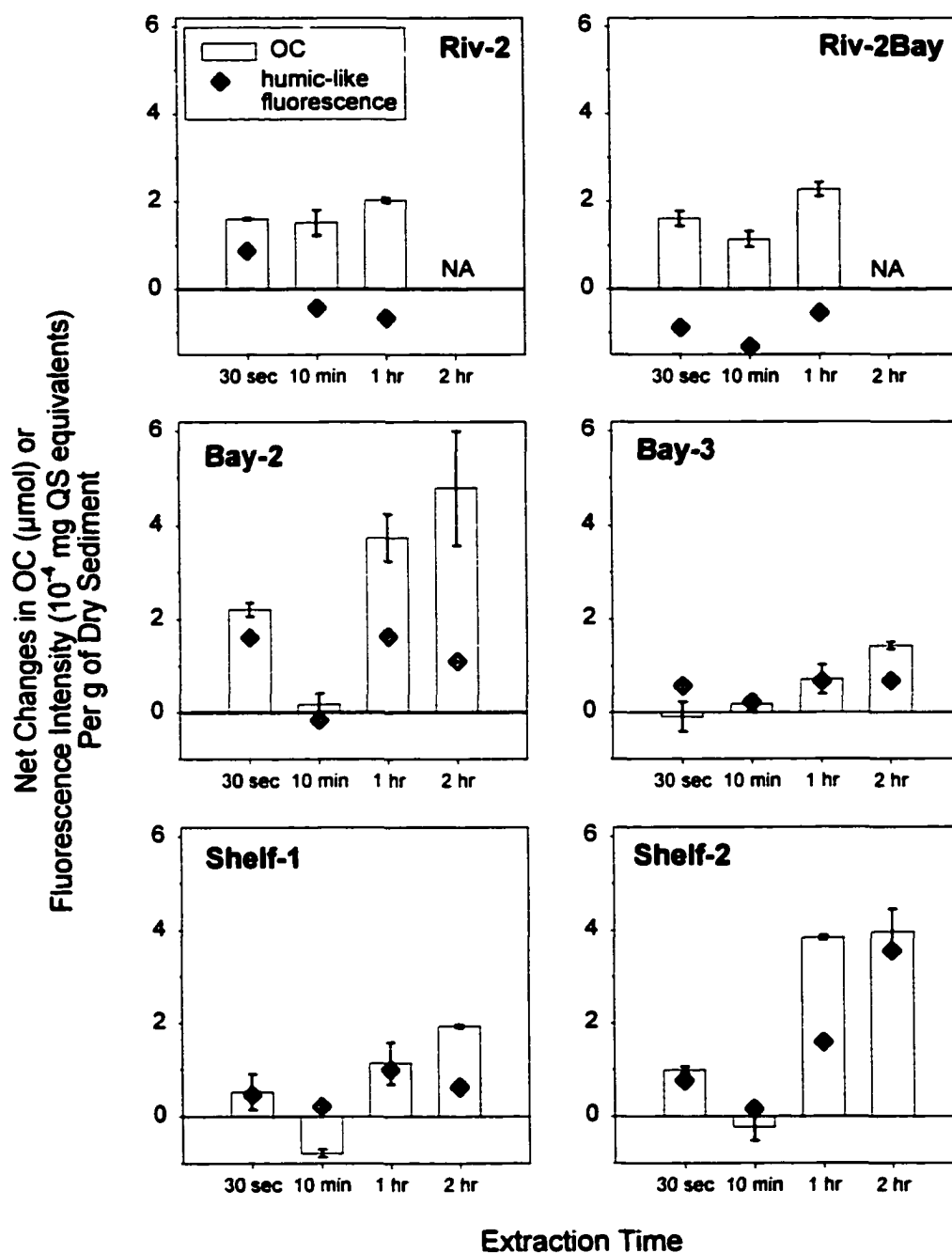


Figure 3.6. Net changes (positive is net increase) in DOC concentration and humic-like peak intensity (Ex/Em near 310/420 nm) in the sample supernatant during continuous extraction experiments. Results have been normalized to the mass of dry sediment that was present in each sample tube. OC data are from Komada and Reimers (2001) and are averages (± 1 S.D.) of two replicate runs. Fluorescence intensities are single determinations. 2-hour extraction results are not available for experiments Riv-2 and Riv-2Bay (Riv-2 sediment resuspended in Bay-3 water).

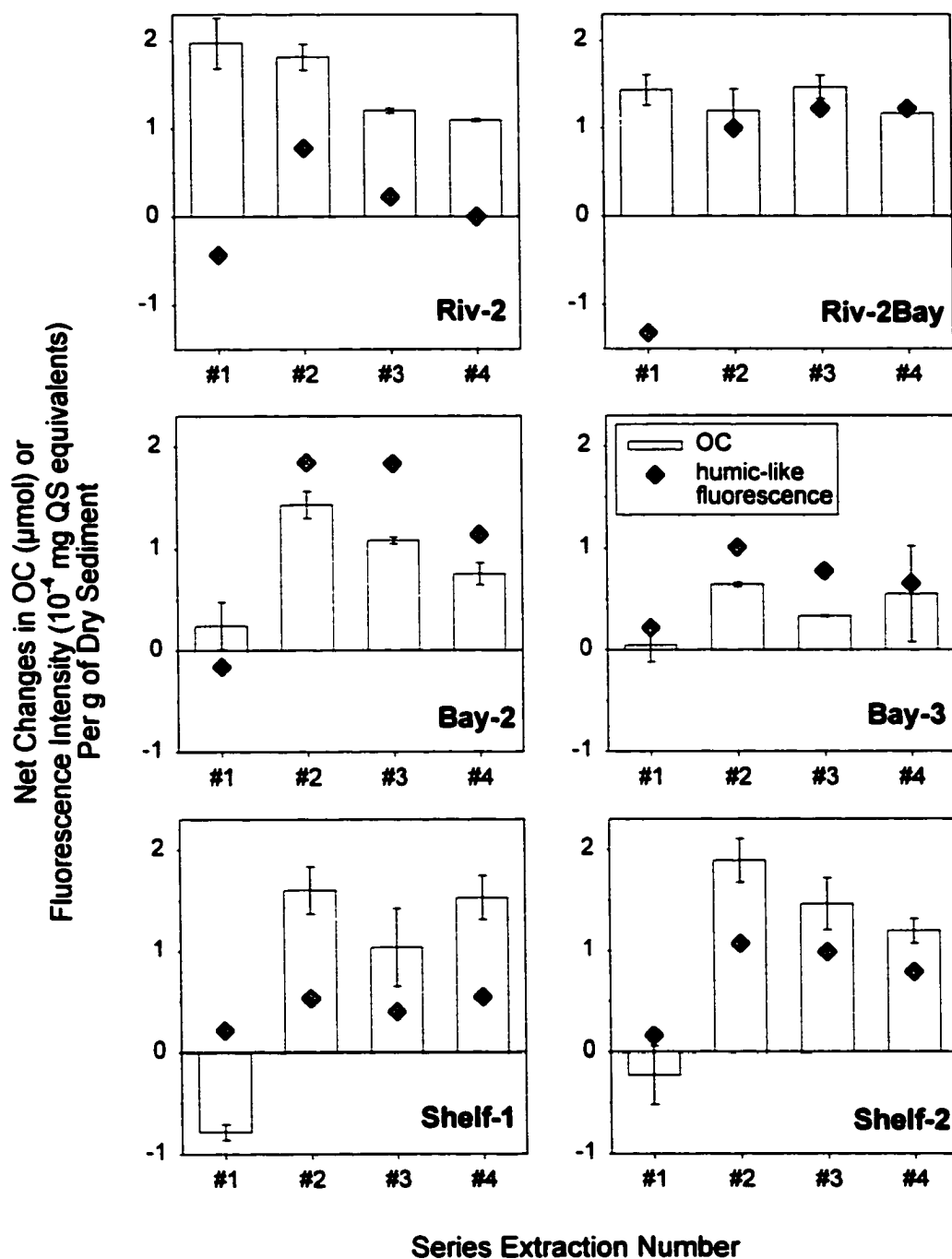


Figure 3.7. Net changes (positive is net increase) in DOC concentration and humic-like peak intensity (Ex/Em near 310/420 nm) in the sample supernatant during series extraction experiments. Results have been normalized to the mass of dry sediment that was present in each sample tube. OC data are from Komada and Reimers (2001) and are averages (± 1 S.D.) of two replicate runs. Fluorescence intensities are single determinations.

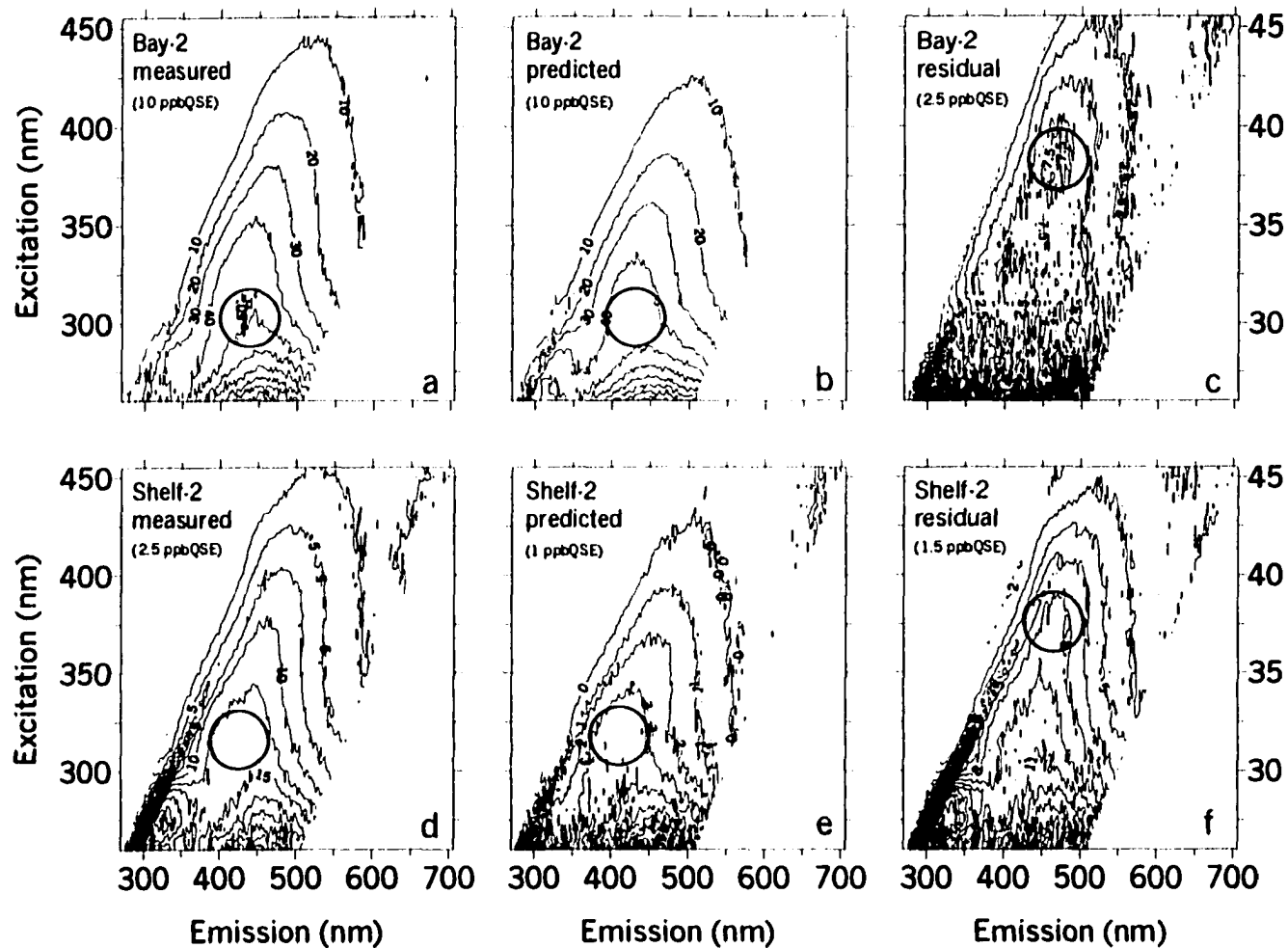


Figure 3.8. Measured, predicted and residual EEMs of 2-hour extraction samples from stations Bay-2 (a-c) and Shelf-2 (d-f). Predicted EEMs were calculated from known EEMs of pore and bottom water controls (section 2.3.). Residual EEMs were obtained by subtracting the predicted EEMs from the measured EEMs. Approximate peak positions are indicated with circles. Contour lines are labeled with fluorescence intensities in units of ppbQSE, and contour intervals are given in parentheses. Similar results were obtained for other treatments and stations.

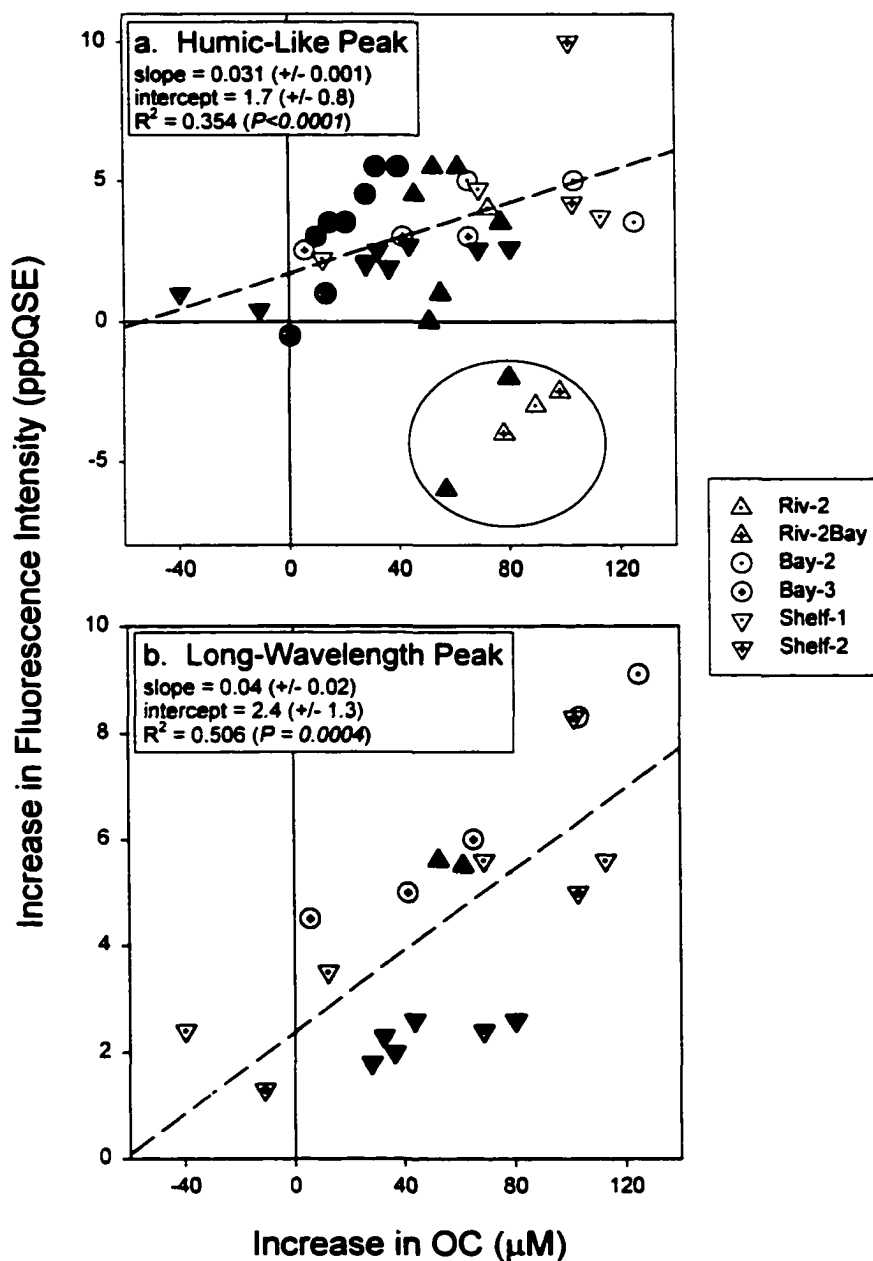


Figure 3.9. Increases in fluorescence intensities of the humic-like peak (Ex/Em near 310/420 nm; (a)) and the long-wavelength peak (Ex/Em near 360/460 nm; (b)) against increases in DOC in the sample supernatant. Continuous experiment results are shown with white symbols, whereas series experiment results are shown in gray. Regression analyses include all data points except those involving River sediment (enclosed in an ellipse in (a); see text).

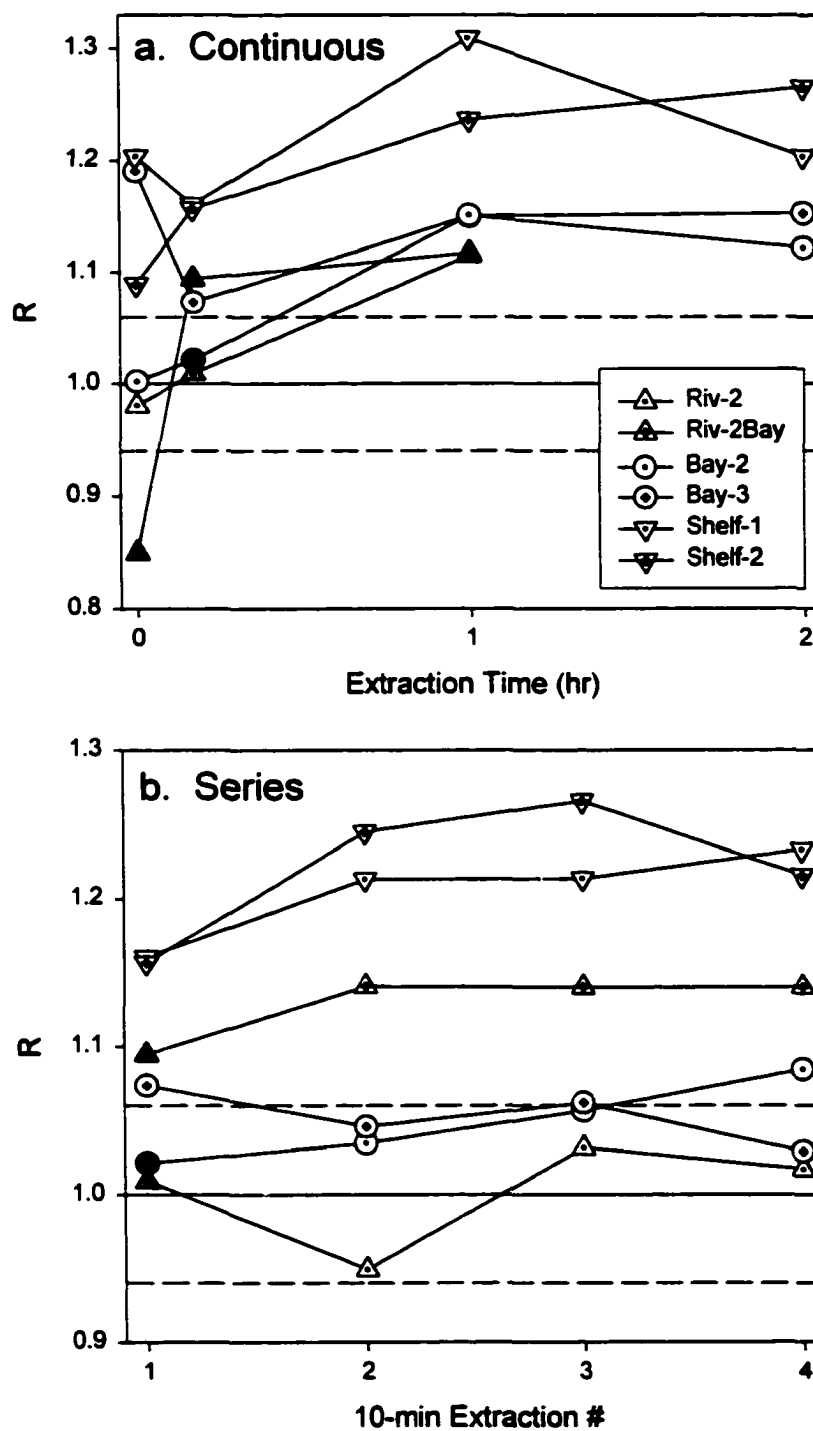


Figure 3.10. Variations in emission ratio, R , with extraction time in continuous experiments (a) and with extraction number in series experiments (b). Filled symbols represent data points that accompanied net decreases in the visible humic-like peak intensity (Figs 3.6, 3.7). Dashed lines indicate 95 % confidence limits as determined from replicate EEM analyses and fluorescence mass-balance test experiment results (section 2.3.).

CHAPTER 4: FACTORS AFFECTING DISSOLVED ORGANIC MATTER DYNAMICS IN SUBOXIC TO ANOXIC COASTAL SEDIMENTS

ABSTRACT

Suboxic to anoxic marine sediments from the Raritan – New York Bay complex and the Inner New York Bight of the eastern U.S. were studied to investigate the factors controlling the vertical accumulation patterns of pore water dissolved organic carbon (DOC). DOC concentrations increased with depth at each of six study sites, but the rate of accumulation was generally lower in the oxic/suboxic relative to anoxic sediment zones. The slope of a correlation between humic-like fluorescence intensity of the pore solutions and DOC concentration also differed between oxic/suboxic and anoxic zones of the sediment ($P = 0.05$), such that anoxic pore solutions were relatively enriched in fluorescent, humic-like compounds.

A modified version of a pore water DOC model developed by Burdige (in press) was applied to aide in the explanation of these geochemical patterns. Model results for a heavily irrigated, and a non-bioturbated site are both consistent with the idea that accumulation of DOC in pore waters is suppressed in the oxic/suboxic compared to the anoxic zones of the sediment due to enhanced oxidation and/or lowered production. An assessment of sorptive behavior of DOC in the surface sediments of the study area further confirms that redox-dependent microbial processes and sediment mixing most often dominate DOC cycling within the benthos. DOC fluorescence appears to match model

distributions of the less labile component of the total DOC pool that accumulates as a function of sediment depth because of low oxidative reactivity and little adsorption.

1. INTRODUCTION

Dissolved organic carbon (DOC) in the pore waters of marine sediments represents a small but dynamic fraction of the total sedimentary organic carbon (OC) pool. DOC is also typically found at concentrations higher than that in the overlying bottom water (e.g., Starikova, 1970; Krom and Sholkovitz, 1977; Martin and McCorkle, 1993; Alperin et al., 1994), indicating net production of DOC within the sediment column. Understanding the reaction and transport processes that produce observed distributions of DOC in sediment pore waters is important, considering the fact that DOC is an intermediate in the overall remineralization of sedimentary OC (Henrichs, 1992). Additionally, because DOC produced in the sediments can be transported into the overlying water (e.g., Burdige et al., 1992; Alperin et al., 1999; Holcombe et al., 2001), understanding pore water DOC cycling will also help better assess the role of sedimentary OC dynamics in the oceanic C cycle.

DOC in pore waters is a heterogeneous pool comprised of various types of compounds (e.g., Henrichs and Farrington, 1979; Barcelona, 1980; Saliot et al., 1988; Burdige et al., 2000) exhibiting a range of molecular weights (Chin and Gschwend, 1991; Burdige and Gardner, 1998) and reactivities (e.g., Sansone, 1986; Burdige and Martens, 1990; Alperin et al., 1994; Arnosti and Holmer, 1999). The accumulation of pore-water DOC is therefore the integrated and complex result of reaction and transport processes

influencing each of these DOC components. Despite this complexity, Burdige (in press) recently demonstrated that a first order understanding of the factors that influence DOC distribution and cycling in sediments may be gained by modeling total DOC as a mixture of high-molecular-weight (HMW) DOC (labile component), and polymeric low-molecular-weight (pLMW) DOC (less reactive component). In this model, the labile pool of HMW-DOC is initially produced from sediment POC by microbial hydrolytic activity. Of the HMW-DOC thus produced, a large fraction (~0.9) is rapidly oxidized to dissolved inorganic carbon (DIC) via monomeric, low-molecular-weight (mLMW) DOC. Meanwhile, the remaining fraction of the HMW-DOC is converted into pLMW-DOC which subsequently accumulates in the pore waters due to its limited reactivity.

One important prediction of this model is that the majority of the DOC accumulating in sediment pore waters consists of relatively non-reactive pLMW-DOC, while the more labile HMW-DOC is quantitatively significant only near the sediment surface where the remineralization rate is usually at a maximum (Burdige, in press). Based on biogeochemical data from two locations within the Chesapeake Bay, Burdige (2001) further reasoned that the accumulation of pLMW-DOC should be suppressed under suboxic, or oscillating redox conditions relative to anoxic conditions, due to enhanced oxidation and/or lowered production. The model output agrees with trends in general (Burdige, in press), but how it reflects reality has not yet been fully tested.

The objective of this study was to test and further advance the conceptual and numeric model of DOC cycling formulated by Burdige (in press) in order to permit comparative treatment and interpretation of data covering a range of sedimentary environments found in the Hudson River Estuary and the Inner New York Bight. This

was conducted first by modifying the model so as to explicitly predict DIC in addition to the two DOC pools, HMW-DOC and pLMW-DOC. Specific questions addressed were:

1. Can measured pore water DOC and DIC profiles be predicted with the DOC model developed by Burdige (in press)? Is there evidence that much of the DOC accumulating in sediments is refractory, and that the cycling of this relatively refractory material is significantly affected by redox conditions?
2. Adsorption and desorption were not considered in Burdige's model, but the potential of these processes to influence DOC as well as POC distribution and dynamics has been stated previously (Hedges and Keil, 1995; Thimsen and Keil, 1998). Thus, we also use Burdige's model to consider the role of adsorption and desorption in pore water DOC cycling.

2. DEVELOPMENT OF A COUPLED DOC-DIC MODEL

The original steady state, advection/reaction/diffusion model for pore water DOC developed by Burdige (in press) portrayed labile HMW-DOC as a reactive intermediate produced from sediment POC at a rate that decays exponentially with depth to a constant, positive value. Most of the HMW-DOC thus produced was then quickly remineralized via mLMW-DOC, but a small fraction ($\alpha = 0.1$) was converted into pLMW-DOC. In the current version of the model (Fig. 4.1), the separation of HMW-DOC into two pools is maintained, but the reactivity patterns of OC are modified so that the production of HMW-DOC from sediment POC is assumed to decrease exponentially with depth towards zero (process (a) in Fig. 4.1). In response, the consumption rate of pLMW-DOC

decreases exponentially with depth as well (process (f) in Fig. 4.1; see Table 4.1 for explanation of symbols). Under these conditions, pore water DOC and DIC concentrations settle to asymptotic values as both production and consumption approach zero with depth.¹

Adopting these modifications and further adding the effects of linear equilibrium adsorption of DOC to the model, one-dimensional diagenetic equations assuming steady state, no compaction, and constant porosity can be written for HMW-DOC (H), pLMW-DOC (P) and DIC (C) as (Berner, 1980):

$$\frac{d}{dx} \left[[(1+K)D_B + D_S] \frac{dH}{dx} \right] - (1+K)\omega \frac{dH}{dx} - \alpha(H - H^0) + R^x - k_H H = 0 \quad (1)$$

$$\frac{d}{dx} \left[[(1+K)D_B + D_S] \frac{dP}{dx} \right] - (1+K)\omega \frac{dP}{dx} - \alpha(P - P^0) + ak_H H - k_p^x P = 0 \quad (2)$$

$$\frac{d}{dx} \left[(D_B + D_S) \frac{dC}{dx} \right] - \omega \frac{dC}{dx} - \alpha(C - C^0) + (1-a)k_H H + k_p^x P = 0 \quad (3)$$

where x is the depth below the sediment-water interface, D_B and D_S are biodiffusion and whole sediment diffusion coefficients, K is the non-dimensional linear adsorption constant for both forms of DOC (see section 3.3.), ω is the sedimentation rate, α is the bioirrigation constant (Emerson et al., 1984), R^x is the net sediment POC reaction rate, a is the fraction of H converted to P, k_H and k_p^x are rate constants for the degradation of H and P, and the superscript 0 represent values at the sediment-water interface (Table 4.1).

The parameters k_p^x and R^x are both defined to decrease exponentially with depth with an attenuation constant λ :

¹ In our study area, the near-Redfield ratio of calculated DIC to NH_4 flux ratio (see section 3.2. and Fig. 7) suggests that processes that may consume DIC (carbonate precipitation and

$$k_p^x = k_p^0 \exp(-\lambda x) \quad (4)$$

$$R^x = R^0 \exp(-\lambda x) \quad (5)$$

where R^0 and k_p^0 are values at the sediment-water interface (Table 4.1). In addition, a and k_p^x are allowed to differ above and below a depth horizon (L) that marks the onset of permanently anoxic conditions (Fig. 4.2) in order to account for the redox dependence of consumption and production rates of pLMW-DOC. Above L , a is reduced by a factor a_r , and the *average* k_p^x above horizon L is enhanced by a factor k_{pr} (see Appendix-1 for handling depth-dependence of k_p^x). For the coastal sites examined here, L is defined as extending to 3 cm below the depth horizon where dissolved Fe disappears and free sulfide begins to accumulate. The reason for this definition is that it is assumed that critical microbial communities that are responsible for organic matter cycling are established by seasonally oscillating redox conditions (Aller, 1994). In which case, not only the redox condition at a particular time but how it has varied in the past few months will also affect reactivity patterns. It is fully expected that the suboxic-anoxic boundary at each of our stations oscillates due to factors such as spring pulses of phytodetritus and seasonal temperature changes. Therefore, since most cores were collected in summer (see Table 4.2) the observed suboxic-anoxic boundary was probably not at its deepest extent (Fig. 4.2).

Model solutions are determined numerically using the boundary conditions:

$$H = H^0, P = P^0, C = C^0 \text{ at } x = 0; \text{ and}$$

$$dH/dx = dP/dx = dC/dx = 0 \text{ as } x \rightarrow \infty.$$

methanogenesis) are insignificant. Therefore, only DIC production is predicted by the model and assumed to approach zero with depth.

The first and second order differentials are discretized using the centered-differencing scheme, and the resulting algebraic equations are solved by Gaussian elimination (Boudreau, 1997) using a step size of 0.05 cm. DOC profiles are computed by summing the calculated profiles of HMW and pLMW-DOC pools. While developing this version of the model, the numerical solution to Eq. 3. was verified against the analytical solution of its simplified form (no bioturbation, constant irrigation with depth), and the results agreed well. The numerical solution was also insensitive to variation in step size. The numerical solutions to Eq, 1 and 2 have been verified previously (Burdige, in press).

3. DATA SET

3.1. Station locations, sampling, and analyses

Sediment samples were collected from eight stations in the Raritan –New York Bay complex (stations Bay-1 to 5) and the Inner New York Bight (stations Shelf-1 to 3; Fig. 4.3) for down-core profiling (conducted at all 5 Bay stations and Shelf-3), and evaluation of DOC partition coefficients (conducted at stations Bay-1 to 3 and Shelf-1, 2; Fig. 4.3, Table 4.2). Station locations are listed in Table 4.2; additional general characteristics of this region have been given elsewhere (Komada and Reimers, 2001). In 1997, the significance of bioturbation/irrigation was assessed for cores collected from stations Bay-3 and Shelf-3. An x-radiograph image of a core from station Bay-3 showed the presence of deep (> 25 cm) burrow structures (M. Buchholtz ten Brink, personal communication). In contrast, x-radiograph images, infaunal abundance, and ^{210}Pb and

^{137}Cs profiles all indicated negligible rates of bioturbation and irrigation at station Shelf-3 (M. Buchholtz ten Brink, personal communication). The importance of bioturbation/irrigation was not directly assessed for the remaining stations (Table 4.2).

Bottom water samples were collected using a Niskin bottle; sediment coring methods and pore water extraction procedures are listed in Table 4.2. Analysis methods applied to pore waters (DIC, nutrients, DOC, total Fe and Mn, total sulfide, and humic-like fluorescence) and sediment solids (Fe oxyhydroxides and acid volatile sulfide) are summarized in Appendix-2.

3.2. Pore water and solid phase profiles

3.2.1. DIC and NH_4 accumulation and redox regime

High rates of organic matter remineralization were indicated by large pore water DIC, NH_4 and PO_4 gradients at each of the stations (Fig. 4.4-4.6). DIC and NH_4 profiles tended to co-vary, and generally increased steadily with depth (Fig. 4.4-4.6). At the Bay stations, the occasional presence of inversions in the concentration gradient within the uppermost ~10 cm of the sediment suggests that bioturbation/irrigation was occurring at these sites (Fig. 4.4-4.6). Consistent with the x-radiograph images (section 3.1.), Bay-3 (particularly 6/97 and 8/99) appeared strongly impacted by bioturbation/irrigation based on a distinct subsurface minima in the NH_4 and DIC profiles (Fig. 4.4, 4.6).

Oxygen penetration depths at the Bay stations were measured by microelectrodes in situ, and were generally 2-4 mm (Luther et al., 1999; Reimers, unpublished data).

Aerobic respiration was therefore not the major pathway of organic matter

rem mineralization in these sediments. At the Bay stations where pore water Mn and Fe concentrations were determined, these metals were present at high levels over a depth interval of several centimeters indicating the occurrence of extensive suboxic diagenesis in the upper 5-10 cm of these sediments (Fig. 4.4). The accumulation of acid volatile sulfide (AVS) at the Bay stations (Fig. 4.4, 4.6) demonstrates that sulfate reduction was also significant. However, free sulfide was not detectable at station Bay-3 (one of 2 stations where this analysis was conducted; Appendix-2) in both 7/99 (to a depth of 30 cm) and 8/99 (to a depth of 10 cm; Appendix-2). The mirror image distributions of AVS and Fe oxyhydroxides (Fig. 4.4) suggest that oxidized iron (enhanced near the surface by bioturbation) reacted rapidly with free sulfide to form AVS. In contrast, free sulfide was present at levels as high as 1.5 mM at Shelf-3 (Fig. 4.6).

In the following paragraphs, the depth where dissolved Fe disappears, or in the case for Shelf-3, the depth where free sulfide begins to accumulate, will be used as a reference for the suboxic-anoxic boundary (Fig. 4.2).

3.2.2. Depth-integrated production rates and accumulation patterns of DOC

In the deeper, anoxic regions of the sediment column, DOC concentration increased steadily in parallel to DIC and NH_4 (Fig. 4.6), similar to trends reported previously for anoxic coastal sediments (e.g., Alperin et al., 1994; Burdige and Homstead, 1994). DOC also increased steadily with depth in the suboxic zones of the sediment at station Bay-2 (Fig. 4.4). Otherwise, DOC clearly deviated from DIC and NH_4 and appeared to remain constant (at a concentration greater than that of the overlying water) throughout and several cm beyond the suboxic-anoxic boundary (Fig.

4.4-4.6). This apparent lack of accumulation with depth, which has also been observed in other suboxic marine sediments (e.g., Sholkovitz and Mann, 1984; Martin and McCorkle, 1993; Bauer et al., 1995), appears consistent with the hypothesis put forth by Burdige (2001) that suboxic (or oscillating redox conditions) result in greater consumption and/or lower production of the more refractory pLMW-DOC relative to anoxic sediments. These patterns were not observed in the apparently heavily bioturbated/irrigated cores from Bay-3 (8/99 and 6/97), where DIC, NH_4 and DOC closely paralleled each other throughout depth (Fig. 4.4, 4.6).

In spite of these departures of DOC accumulation patterns compared to DIC and NH_4 , calculated diffusive fluxes of DOC correlated positively with those of DIC and NH_4 (Fig. 4.7), and comprised approximately 3 % of the DIC flux. The ratio of DIC to NH_4 flux was ~ 7 , close to the Redfield ratio. These results are in agreement with previous findings (Alperin et al., 1999; Burdige et al., 1999) and support the notion that microbial remineralization of organic matter is an important factor affecting the net production of DOC in sediments.

3.2.3. *Fluorescence profiles*

Excitation-emission fluorescence spectroscopy was employed as a means to investigate the variations in the abundance and chemical composition of the humic-like components of the DOC pool with depth in sediment. When excited with UV light, naturally occurring organic matter commonly exhibits broad, featureless fluorescence attributed to humic-like substances in the visible region of the spectrum (e.g., Coble, 1996). Based on the tendency for humic-like fluorescence to closely parallel pore water

DOC concentrations (Chen et al., 1993; Chen and Bada, 1994), it has been suggested that pLMW-DOM and humic-like substances may be synonymous (Burdige, 2001).

Humic-like peaks were observed at all stations and depths, and were all positioned near Ex/Em 310/420 nm well within the previously reported humic-like peak positions (see Chapter 3.). The close agreement of the peak positions across samples suggests that chemically similar humic-like substances were present in these sediment pore waters. The intensity of the peaks increased with depth in the sediment, and in general co-varied with bulk DOC concentration (Fig. 4.4, 4.6), similar to what has been reported for other marine sediments (Chen et al., 1993; Chen and Bada, 1994).

However, a plot of humic-like fluorescence intensity versus total DOC concentration revealed distinct correlations between these two properties above and below the suboxic-anoxic boundary (Fig. 4.8). In agreement with a previous report (Chen and Bada, 1994), the fraction of the total DOC that is composed of fluorescent humic-like DOM was greater in the anoxic than in the oxic/suboxic zones of these sediments ($P=0.05$), suggesting that the chemical composition of pore water DOC can vary between these two zones. Furthermore, if humic-like fluorescence is indeed representative of pLMW-DOC, then these results are consistent with the model concept that pLMW-DOC is a quantitatively significant fraction of pore water DOC, and that its accumulation is suppressed in the suboxic relative to anoxic zones of the sediment column.

3.3. Partitioning of OC between pore water and sediment particles

In a related study of a subset of the sediments discussed here, we determined that approximately 0.1 % of the surface (< 2 cm deep) sediment POC was readily releasable into solution when suspended in bottom water for 1 hour (Table 4.3; Komada and Reimers, 2001). A positive correlation between the amount of OC released and the POC content of the high-density phase ($\rho > 1.9$) of the sediment matrix further suggested that OC adsorbed to the mineral particles was the major source for the released OC (Komada and Reimers, 2001).

To further interpret these results in the context of linear equilibrium adsorption, non-dimensional partition coefficients, K , were calculated as:

$$K = \rho_s \left(\frac{1 - \phi}{\phi} \right) K_{ads} \quad (6)$$

where ρ_s is the specific gravity of dry sediment (2.5), ϕ is the sediment porosity, and K_{ads} is the partition coefficient with dimensions of $L \text{ g}^{-1}$ (Berner, 1980; Table 4.3). K_{ads} was determined for the surface sediments by dividing the readily-desorbable fraction of the sedimentary POC ($\mu\text{mol OC g dry sediment}^{-1}$) by the DOC concentration of the surrounding pore solution (μM) (Table 4.3). This approach assumes that the sorptive behavior of pore water DOC can be represented with a single representative K , which is likely to be an oversimplification (Thimsen and Keil, 1998; Arnarson and Keil, 2000). Also, because these experiments were conducted in air, the results may not be fully applicable to anoxic sediments; previous sorption studies using model compounds have generally shown lower K 's under anoxic compared to oxic conditions (Wang and Lee, 1993; Montluçon and Lee, 2001). Despite these limitations, we present these results to

provide a first order estimate for equilibrium adsorption as included in our model (Eq. 1, 2) in order to predict its effect on pore water DOC distributions.

The resulting values of K were similar across stations and ranged from 0.8 to 1.3 (Table 4.3). In order to compare these results to previously published values, the adsorption coefficients reported (in $L\ g^{-1}$) by Thimsen and Keil (1998) and Arnarson and Keil (2000) (determined under oxic conditions) were converted to non-dimensional form according to Eq. 6 using reported porosities of the experimental slurries and assuming dry sediment densities of $2.5\ g\ cm^{-3}$. The resulting K of Thimsen and Keil (1998) and Arnarson and Keil (2000) are 0.04-6.4 and 0.4-0.9, respectively, and overlap with our estimates. These values of K are also similar to non-dimensional partition coefficients reported for melanoidin in oxic coastal sediments (~ 2 ; Montluçon and Lee, 2001). Together, these observations indicate a value of $K=1$ is a good estimate for our pore water DOC model.

4. MODEL APPLICATION AND DISCUSSION

Profiles of pore water DOC (Fig. 4.4-4.6) clearly show that the rate of DOC accumulation can be lower in the oxic/suboxic zone compared to the majority of the deeper, permanently anoxic portions of the sediment column. Fluorescence data further indicate differences in the chemical composition of DOC between the two zones such that anoxic pore waters tend to be relatively more enriched in the humic-like component (Fig. 4.8). Combined, these observations appear consistent with the hypothesis put forth by Burdige (2001) that the accumulation of the more refractory component of pore water

DOC is suppressed in the oxic/suboxic relative to anoxic regions of the sediment due to enhanced consumption and/or lowered production.

To further test this hypothesis, the coupled DOC-DIC model (section 2.) was applied to the DOC and DIC profiles encountered in this study. As borne out in the model equations (Eq. 1, 2), DOC profiles encountered in nature are expected to reflect the composite effects of diffusion, reaction (including any possible redox effects), burial, as well as any impacts from bioturbation/irrigation. In order to test the effects of redox potential on pLMW-DOC cycling without the added complication of bioturbation/irrigation, the model was first fit to the profiles from station Shelf-3 where macrofaunal activity has been shown to be negligible (section 3.1.).

4.1. Model fit to a non-bioturbated/irrigated site (Shelf-3)

The overall fitting procedure was to first constrain the sediment POC reaction rate, R^x (process (a) in Fig. 4.1), using the pore water DIC data. The factors affecting DOC accumulation patterns were then investigated by adjusting a , a_r , k_{Pr} , and L (Table 4.1). As a starting condition, it was assumed that the reactivity of pLMW-DOC was not redox dependent, such that $a_r = k_{Pr} = 1$, and $L = 0$ cm. Thus, the model parameters that needed to be constrained were: a , H^0 , k_H , k_P^x (through k_P^0 and λ ; Eq. 4), and R^x (through R^0 and λ ; Eq. 5) (Table 4.1). Of these parameters, best estimates for R^0 and λ (129,000 $\mu\text{M yr}^{-1}$, and 0.21 cm^{-1} , respectively) were determined by independently modeling the DIC profile (Appendix-3). The remainder, however, were unknown, therefore the values that were adopted by Burdige (in press) were also used here ($a = 0.1$, $H^0 = 5 \mu\text{M}$, $k_H =$

3650 yr⁻¹, $k_P^0 = 1.22 \text{ yr}^{-1}$). Of these, a k_H of 3650 yr⁻¹ is of similar magnitude as degradation rate constants measured for dissolved free amino acids, while k_P^0 of 1.22 yr⁻¹ lies within range of rate constants reported for POC of coastal sediments (0.02-11 yr⁻¹; Henrichs, 1992). Setting $a = 0.1$ is purely an assumption, but may be reasonable if the acid-volatile DOC pool comprises most of the mLMW-DOC pool in this model (Fig. 4.1). Alperin et al. (1994) determined that 97 % of the DOC produced annually in Cape Lookout Bight sediments was in the form of acid volatile DOC.

The DOC and DIC profiles predicted using these parameter values (Case-1; Table 4.4) are given in Fig 4.9(a,b). Under these conditions, the model slightly underestimated DIC concentration and clearly overestimated DOC. Prior to fine-tuning the model to fit the DOC profile, R^0 was increased to 141,000 $\mu\text{M yr}^{-1}$ to produce an improved fit for the DIC data (Case-2; Table 4.4, Fig 4.9(a)). This approach is justified, because DIC profiles are more sensitive to variations in R^0 and λ than to variations in a , k_H and k_P^0 (data not shown). The resulting ~10 % increase in R^0 from the value obtained by independently modeling the DIC profile (Appendix-3) makes logical sense when one considers the fact that a fraction of the DOC escapes oxidation to DIC through diffusion to the bottom water and burial (Fig. 4.1).

Under this new setting, the model reproduced the interfacial gradient and the depth-attenuation of DOC concentration reasonably well (Case-2; Fig. 4.9(b)), but the overall predicted DOC concentrations were still too high by at least 1 mM. The model also failed to reproduce the break in the DOC profile within the upper 6 cm of the sediment. Increasing k_P^0 and decreasing a both had the effect of lowering the overall

DOC concentration without impacting the DIC profile; however, it was impossible to explain the break in the DOC curve by adjusting these parameters alone (data not shown).

In order to test if the break in the DOC profile can be explained as being the result of enhanced consumption and/or lowered production of pLMW-DOC induced by suboxic or oscillating redox conditions, α and k_p^x were allowed to vary across a depth horizon L (section 2., Fig. 4.2). L was set to 6 cm, 3 cm below the depth at which free sulfide appeared (Fig. 4.6). a_r was then arbitrarily set to 0.1 while k_{pr} was maintained at 1 (Case-3; Table 4.4). Doing so decreased the overall DOC concentration, but did not reproduce the break in the profile (Fig. 4.9(b)). The result was similar when k_{pr} was arbitrarily set to 10 while $a_r = 1$ (Case-4), although in this case, a small break in the curve appeared near 6 cm depth (Fig. 4.9(b)). Overall, because $a_r < 1$ and $k_{pr} > 1$ both resulted in decreases in the DOC concentration across the sediment-water interface, it was impossible to reproduce the observed DOC profile using this model setting.

Nevertheless, it was possible to produce pLMW-DOC profiles which agreed reasonably well with the depth trends in the humic-like fluorescence intensity by setting $a_r = 0.1$ and $k_{pr} = 10$ and further adjusting α (Case-5) and also L (Case-6; Table 4.4, Fig. 4.9(d)). If humic-like fluorescence intensity is indeed proportional to the concentration of pLMW-DOC, then these results can be interpreted to mean that the coupled DOC-DIC model can predict with reasonable accuracy the depth distribution of the more refractory component of the DOC pool. These results are also consistent with the hypothesis that reduced production ($a_r < 1$) and enhanced loss ($k_{pr} > 1$) of the more refractory fraction of pore water DOC occurs in the oxic/suboxic parts of the sediment column. Furthermore, the inability of the current version of the model to fully account for the large DOC

gradient across the sediment-water interface points to the possibility that HMW-DOC is being produced at high rates (and possibly under non-steady state conditions) in the uppermost parts of the sediment column. This scenario is in accord with previous reports suggesting enhanced production of labile dissolved organic matter near the sediment-water interface (Burdige and Zheng, 1998; Burdige, 2001).

4.2. Application to an irrigated site (Bay-3)

In addition to the possible redox dependence of DOC reaction rates, DOC profiles in the Bay sediments are most certainly further complicated by advective processes due to macrofaunal activity (Fig. 4.4-4.6, section 3.1.). In order to test the significance of redox-dependent DOC cycling under such conditions, the coupled DOC-DIC model was applied to the core from Bay-3 collected in 6/97.

The broad inversion in the concentration profiles of DIC, NH_4 and DOC to approximately 20 cm depth (Fig. 4.6) indicate that this core was heavily irrigated. It is possible that this core was also bioturbated, however, because neither bioturbation nor irrigation rates are known for this site, and solute profiles are generally more sensitive to variations in the irrigation than in the biodiffusion coefficient, it was assumed that this core was impacted by irrigation only. Irrigation rates for this site were estimated by fitting a finite series of possible solutions to the DIC profile using various combinations of R^0 , α , and λ . To reproduce the inversion in the DIC profile, any choice of R^0 must be counterbalanced by an appropriate α ; larger R^0 requires larger α , and vice versa. Once a pair of R^0 and α is selected, a unique λ is easily obtained by fine-tuning the overall

attenuation. Estimates for the lower and upper limits for R^0 (and α) are set by the steepness of the interfacial gradient (increasing R^0 results in sharper gradients). The higher limit can also be set by the size of α - increasing α enhances the mid-depth concentration minima.

Setting the irrigated depth to 18 cm, three curves were fit to the DIC data with R^0 ranging from 100,000 to 180,000 $\mu\text{M yr}^{-1}$, and α between 10 and 18 yr^{-1} (Cases 7, 8, 9; Table 4.4, Fig. 4.10(a)). The corresponding DOC profiles were then calculated by setting H^0 , k_H , and k_P^0 as stated above (section 4.1.; Table 4.1), $a = 0.1$, and $a_r = k_{Pr} = 1$. The resulting DOC profiles were similar to each other and clearly overestimated the measured values (Fig. 4.10(b)), indicating that throughout the modeled sediment column, the model overestimated the production rate or underestimated the consumption rate of pLMW-DOC. Taking Case-8 as a representative first order approximation, the DOC model profile was adjusted by decreasing a to 0.04 (Case-10; Table 4.4), which resulted in a good fit below ~ 20 cm, but still overestimated the measured values near the interface (Fig. 4.10(d)). In order to reduce the production rate of pLMW-DOC in the upper part of the sediment column, L was then set to 21 cm (assuming that the irrigated depth oscillates similar to the suboxic-anoxic boundary; section 2., Fig. 4.2) and a_r to 0.6 (Case-11; Table 4.4), which improved the fit. Similar adjustments were necessary if Cases 7 and 9 were used initially; the production rate of pLMW-DOC above L had to be reduced ($a_r = 0.6$) to obtain a reasonable fit to the data (results not shown). It was also possible to reduce the overall modeled DOC concentration by increasing k_P^0 and k_{Pr} , but doing so resulted in strong concentration minima around 18 cm. Although a reasonable fit was obtained in

this case by decreasing the production rate (by adjusting a and a_r) alone; in reality, what we may be observing is a net change in both production and consumption rates within L.

The above results are again consistent with the model concept that the accumulation of DOC is suppressed within the oxic/suboxic zone of the sediment. Combined with the results for station Shelf-3 (section 4.1.), these findings demonstrate that redox-dependent production and/or consumption of pLMW-DOC is likely an important factor influencing DOC distribution and dynamics across a spectrum of heavily irrigated to non-disturbed coastal sedimentary environments. The shorter cores collected from the Bay (Fig. 4.4, 4.5) did not penetrate deep enough into the permanently anoxic zone, therefore, it was not possible to test the significance of redox-dependent reactivity using these profiles. However, the model results strongly suggest that the DOC profiles and fluorescence characteristics in the surface sediments of the Bay stations are integrated results of various combinations of redox-dependent reaction and transport processes.

4.3. Significance of adsorption/desorption on sediment DOC cycling

As seen in Eq. 1 and 2, including the equilibrium partition coefficient, K , in a steady state diagenetic equation under the conditions assumed in this study (section 2.) results in an enhancement of the rate of burial and bioturbation by a factor $(1+K)$. Consequently, as stated by Berner (1978), when rates of burial and bioturbation are low enough to be neglected, effects of sorption can also be neglected. This was the case for station Bay-3 (6/97; section 4.2.) where the reported burial rates are low (0.15 cm yr^{-1} ;

Olsen et al., 1984), and it was assumed that biological mixing was limited to irrigation. In this situation, the inclusion of $K = 1$ within each diagenetic equation has little or no impact on the calculated DOC distributions (data not shown). Instead, these distributions can be explained primarily as consequences of redox-dependent organic matter degradation and irrigation.

Conversely, at station Shelf-3 where sedimentation rates are on the order of several cm per year (Bopp et al., 1995), the inclusion of K in the model has greater impact on the calculated DOC concentration. Varying the magnitude of K between 0 and 3 for Case-5 calculated earlier for Shelf-3 (Fig. 4.9) produces asymptotic pLMW-DOC concentrations that differ by approximately 1 mM, with larger K 's resulting in lower DOC concentrations (Fig. 4.11). An accurate determination of K is therefore important in order to correctly model pore water DOC under the conditions encountered at station Shelf-3. Furthermore, if K is indeed smaller in anoxic conditions as has been reported for some model compounds (Wang and Lee, 1993; Montluçon and Lee, 2001), then K must be modeled as a depth-dependent parameter. Future studies should focus on determining the redox-dependence of K of pore water DOC.

4.4. Additional controls on pore-water DOC distribution: Potential role of Fe

So far in this study, it was assumed that pore-water DOC distribution and cycling can be largely explained by incorporating the effects of redox-dependent microbial reactions, various modes of advective transport, sorption, and diffusion into a diagenetic model. While a combination of these factors appears reasonably adequate to explain the

observed pore-water DOC distributions, additional factors are most likely at work in nature; non-steady state processes and redox-dependent sorption are two of them, as pointed out above (sections 4.1. and 4.3.).

Another process that was not incorporated in this model, but may help better explain the observed pore-water DOC accumulation patterns is complexation and subsequent precipitation of DOC with Fe above the depth horizon L. Fe dissolved in the interstitial waters of sediments can exist as organic complexes in both redox states +II and +III (Luther et al., 1996; Taillefert et al., 2000). Both Fe (II) and Fe (III) organic complexes have been found to precipitate out of pore solution under very low pH conditions (≤ 3) in marsh sediments, indicative of humic complexes (Luther et al., 1996). Fe (III) complexed to a model ligand has also been found to precipitate at circumneutral pH in synthetic seawater as the complex ages and aggregates (Taillefert et al., 2000).

Solid-state voltammetric profiles obtained at station Shelf-3 at the time our core was collected (6/97) show that relatively freshly-produced Fe (III) organic complexes were present in the uppermost 3 cm of the sediment column (Taillefert et al., 2000). Although this depth interval does not fully overlap with the estimated depth of the horizon L (approximately 6 cm; Table 4.4), it is possible that DOC loss through aggregation of Fe (III) complexes contributed to the overall lowered accumulation of DOC in the suboxic zone of this station.

5. CONCLUDING REMARKS

The data presented in this study suggest that a quantitatively important fraction of the DOC accumulating in the pore waters of coastal sediments is composed of fluorescent, humic-like compounds. The results of the modeling exercises are also consistent with the notion that most of the DOC that accumulates is of low reactivity, especially if distributed within permanently anoxic sediment zones. The inferred significance of redox conditions on the oxidation of refractory components of the DOC pool is consistent with the potential effects of redox-oscillation (Aller, 1994) and oxygen exposure time (Hartnett et al., 1998; Hedges et al., 1999) on overall sediment POC remineralization. Our results further imply that the thickness of the oxidized/suboxic layer in the sediment column may influence not only the quantity, but also the reactivity of the DOC diffusing out of the sediment into the overlying bottom water. Additional studies involving profile data from a greater number of sedimentary environments are required to further test our conclusions.

Table 4.1. List of symbols used in the coupled DOC-DIC model.

Symbol	Meaning	Values used
KNOWN PARAMETERS		
C^0	Concentration of DIC in the bottom water (μM)	Observed bottom water concentration
D_s	Whole sediment diffusion coefficient of DOC and DIC ($\text{cm}^2 \text{yr}^{-1}$)	52.5 (P and H) and 160.8 (DIC) $\text{cm}^2 \text{yr}^{-1}$
K	Equilibrium linear partition coefficient for DOC (dimensionless)	1 (section 3.3.)
ω	Sediment burial rate (cm yr^{-1})	See Table 4.4
UNKNOWN PARAMETERS		
a	Fraction of H that is converted to P	See Table 4.4
a_r	Attenuation factor for a above L	See Table 4.4
D_B	Biodiffusion coefficient within the bioturbated zone ($\text{cm}^2 \text{yr}^{-1}$)	0 $\text{cm}^2 \text{yr}^{-1}$
H^0	Concentration of HMW-DOC in the bottom water (μM)	5 μM (Burdige, in press)
k_H	Degradation rate constant for H (yr^{-1})	3650 yr^{-1} (Burdige, in press)
k_P^0	Degradation rate constant for P at the sediment-water interface (yr^{-1})	1.22 yr^{-1} (Burdige, in press)
k_{Pr}	Enhancement factor for k_P^x above L (see Appendix-1)	See Table 4.4
L	Depth horizon below which sediment is permanently anoxic (cm); above L, $k_r \geq 1$ and/or $a_r \leq 1$	Suboxic-anoxic boundary plus 3 cm (section 2., Fig. 4.2)
p^0	Concentration of pLMW-DOC in the bottom water (μM)	Observed DOC concentration minus concentration of H^0
R^0	Net reaction rate of sediment POC at the sediment-water interface ($\mu\text{M yr}^{-1}$)	See Table 4.4
α	Bioirrigation constant within the bioturbated zone (yr^{-1})	See Table 4.4
λ	Depth attenuation constant for R^x and k_P^x (cm^{-1})	See Table 4.4
VARIABLES		
C	Concentration of DIC (μM)	
H	Concentration of HMW-DOC (μM)	
P	Concentration of pLMW-DOC (μM)	
x	Depth below the sediment-water interface (cm)	

Table 4.2. Summary of station locations and general characteristics.

Station	Lat (N) Lon (W)	Depth (m)	Date of Sampling	Salinity	Bottom T. (°C)	Coring Method ¹	PW sampling method ²	Bioturbation/ Bioirrigation rates ³	Determination of K ⁴
Bay-1	40.596 -74.002	5	6/26/98	24	21	Grab	Slice	n.a.	+
Bay-2	40.549 -74.064	8	6/28/98	27	19	Push core	Slice	n.a.	+
Bay-3	40.458 -74.074	6	6/27/97	27	20	HGC	Squeeze	High	+
			6/25/98	23	20	Grab	Slice	n.a.	
			7/22/99	28	n.a.	Gravity	Slice	n.a.	
			8/3/99	28	n.a.	Grab	Slice	n.a.	
Bay-4	40.451 -74.066	6	6/28/98	23	20	Grab	Slice	n.a.	-
Bay-5	40.486 -74.186	7	6/29/98	23	21	Push core	Slice	n.a.	-
Shelf-1	40.389 -73.832	24	10/12/98	31	13 ⁵	Grab	n.d.	n.a.	+
Shelf-2	40.282 -73.787	58	10/12/98	32	12 ⁵	Grab	n.d.	n.a.	+
Shelf-3	40.317 -73.791	50	6/26/97	32	9	HGC	Squeeze	Negligible	-

1. Grab = Peterson grab sampler; Push core = a push core mounted on an ROV; HGC = hydrostatically-damped gravity corer built by the U.S Geological Survey; Gravity = conventional gravity corer.
2. Sliced cores were processed in a N₂ atmosphere as described in Komada and Reimers (2001). Squeezed cores were processed on deck using a squeezer similar to that reported by Jahnke (1988). n.d. = not determined.
3. Rates are based on x-radiograph images, ²¹⁰Pb, ¹³⁷Cs profiles, and infaunal abundance (section 3.1.).
4. Plus and minus signs indicate that the analysis was or was not conducted, respectively.
5. In situ temperatures are not available from these stations. Listed are data from Bowman and Wunderlich (1977).
n.a.= not available.

Table 4.3. Estimated equilibrium partition coefficients of DOC in surficial (uppermost 2 cm) sediments.

Station	Experimental Data ⁽¹⁾			Core Sectioning Data (uppermost 2cm)		K_{ads} (10^4 L m^{-2})	$K^{(3)}$
	HD- POC ⁽²⁾ (wt%)	Mass- normalized OC release ($\mu\text{mol g}^{-1}$)	Fraction of HD-POC released (%)	Av. pore water DOC (μM)	Av. porosity		
Bay-1	3.76	2.58	0.08	1310	0.84	1.6	0.9
Bay-2	4.26	3.73	0.11	1443	0.84	1.2	1.2
Bay-3	2.89	0.71	0.03	405	0.77	1.0	1.3
Shelf-1	1.88	1.14	0.07	1164	0.69	0.9	1.1
Shelf-2	3.71	3.84	0.12	1678	0.88	1.2	0.8

1. Data from Komada and Reimers (2001)
2. POC content in the high-density ($\rho > 1.9$) phase of the sediment matrix
3. Non-dimensional partition coefficient derived using Eq. 6.

Table 4.4. Parameter values used to calculate DOC-DIC model outputs for stations Shelf-3 and Bay-3 (6/97).

Case No.	Model fit to:	a	a_r	D_B ($\text{cm}^2 \text{yr}^{-1}$)	k_{Pr}	L (cm)	MLD ⁽¹⁾ (cm)	R^0 ($\mu\text{M yr}^{-1}$)	α (yr^{-1})	λ (cm^{-1})	$\omega^{(2)}$ (cm yr^{-1})
1	Shelf-3	0.1	1	0	1	0	0	129,000	0	0.21	2
2	Shelf-3	0.1	1	0	1	0	0	141,000	0	0.21	2
3	Shelf-3	0.1	0.1	0	1	6	0	141,000	0	0.21	2
4	Shelf-3	0.1	1	0	10	6	0	141,000	0	0.21	2
5	Shelf-3	0.14	0.1	0	10	6	0	141,000	0	0.21	2
6	Shelf-3	0.16	0.1	0	10	7	0	145,000	0	0.21	2
7	Bay-3 (6/97)	0.1	1	0	1	0	18	100,000	10	0.11	0.15
8	Bay-3 (6/97)	0.1	1	0	1	0	18	150,000	15	0.119	0.15
9	Bay-3 (6/97)	0.1	1	0	1	0	18	180,000	18	0.124	0.15
10	Bay-3 (6/97)	0.04	1	0	1	21	18	150,000	15	0.119	0.15
11	Bay-3 (6/97)	0.043	0.6	0	1	21	18	150,000	15	0.119	0.15

1. MLD = mixed layer depth (depth to which sediment is impacted by bioturbation/irrigation). All other symbols are explained in Table 1.
2. Sedimentation rates are from Bopp et al., (1995) and Olsen et al. (1984) for Shelf-3 and Bay-3, respectively.

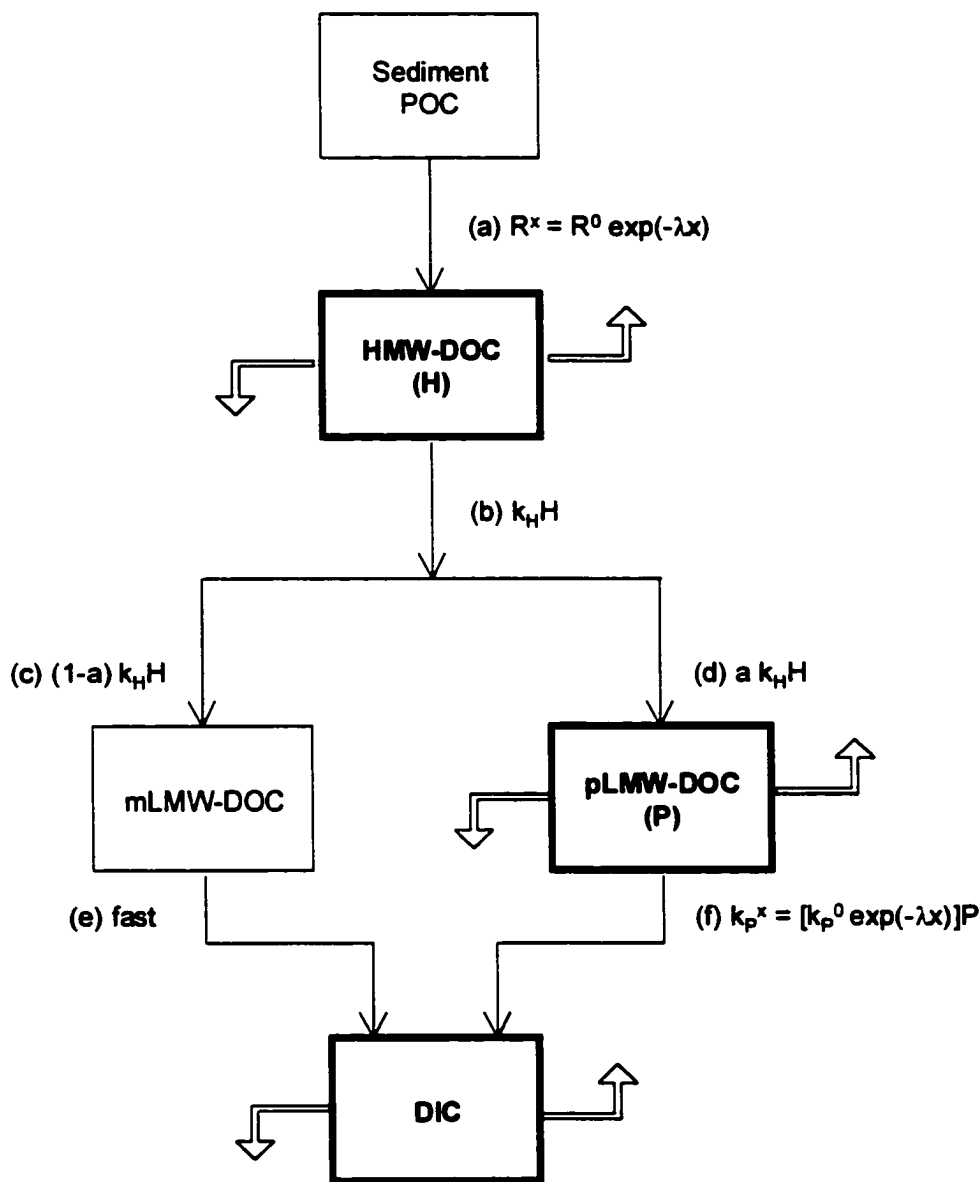


Figure 4.1. A diagrammatic representation of the coupled DOC-DIC model modified after the pore-water DOC model developed by Burdige (in press). Dissolved carbon species that were explicitly modeled are indicated in bold. Upward- and downward-facing box arrows represent losses of the dissolved species from the system by diffusion into the bottom water and pore water burial, respectively. Symbols used to describe the processes (a) to (f) are explained in Table 4.1.

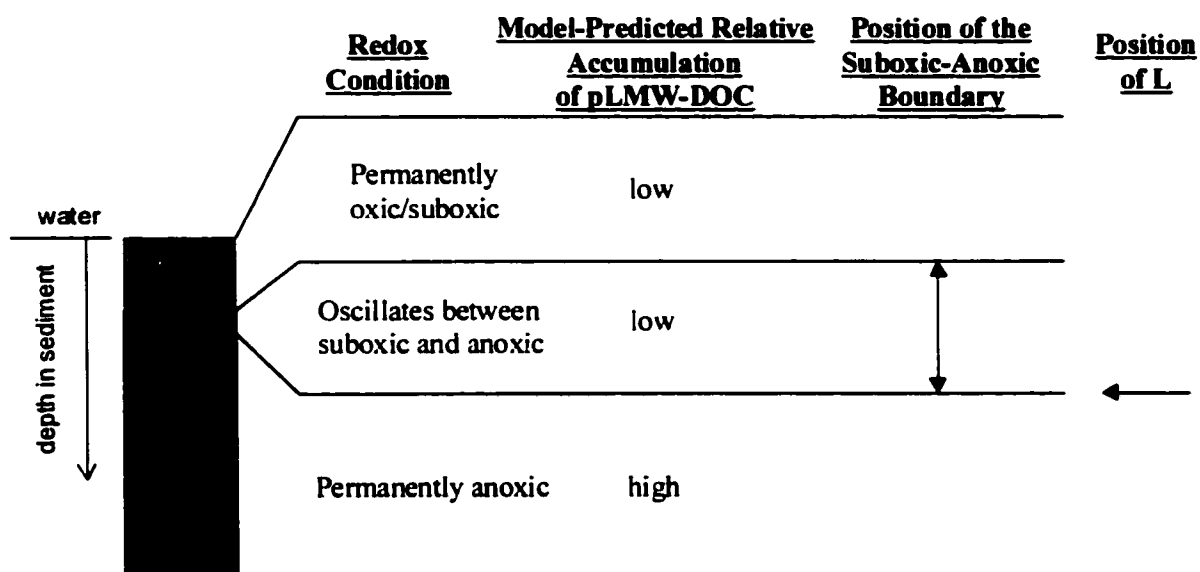


Figure 4.2. A schematic describing the relative positioning of the suboxic-anoxic boundary and L in the sediment column.

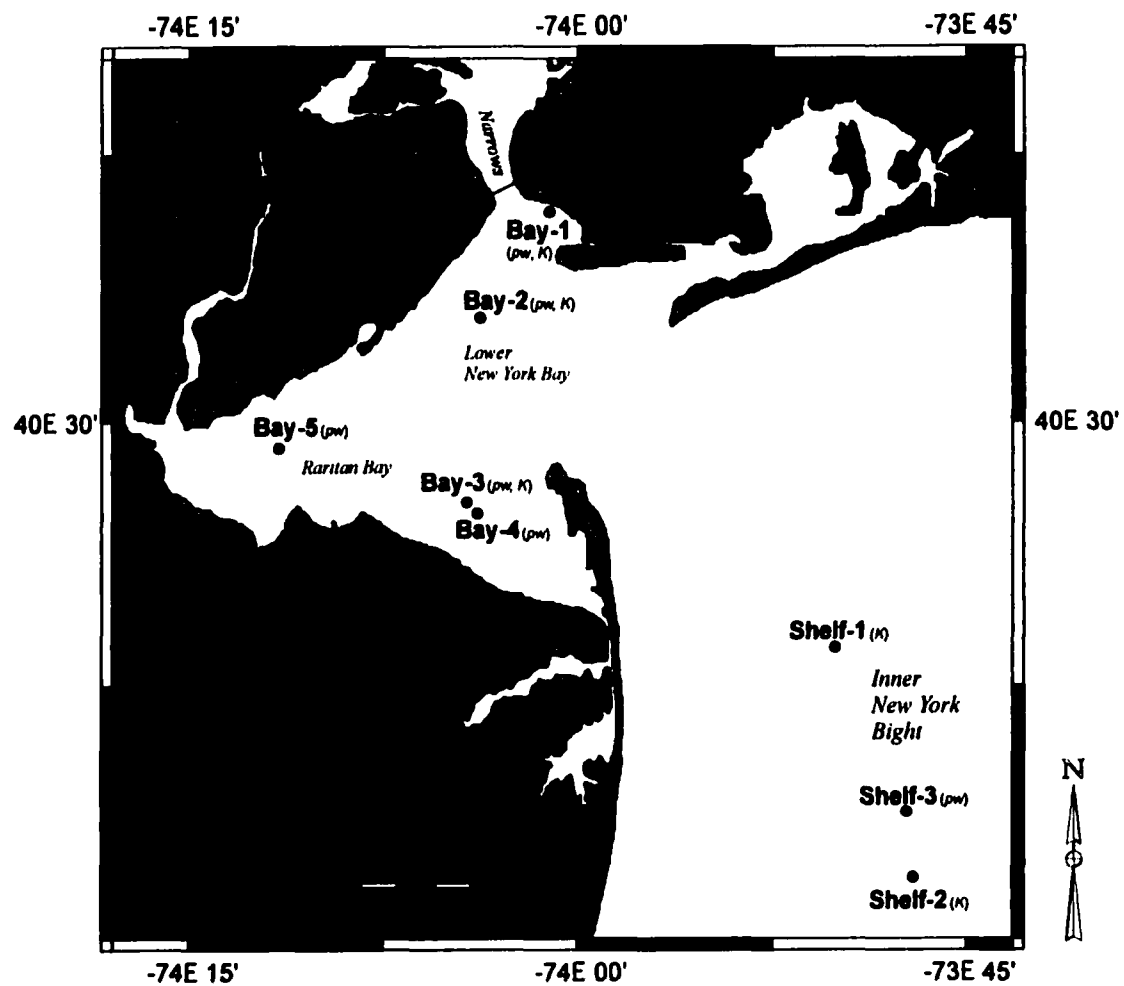


Figure 4.3. Sampling locations in the Raritan Lower New York Bay complex and the Inner New York Bight. *pw* and *K* in parentheses indicate stations where down-core profiles and DOC partition coefficients were determined, respectively.

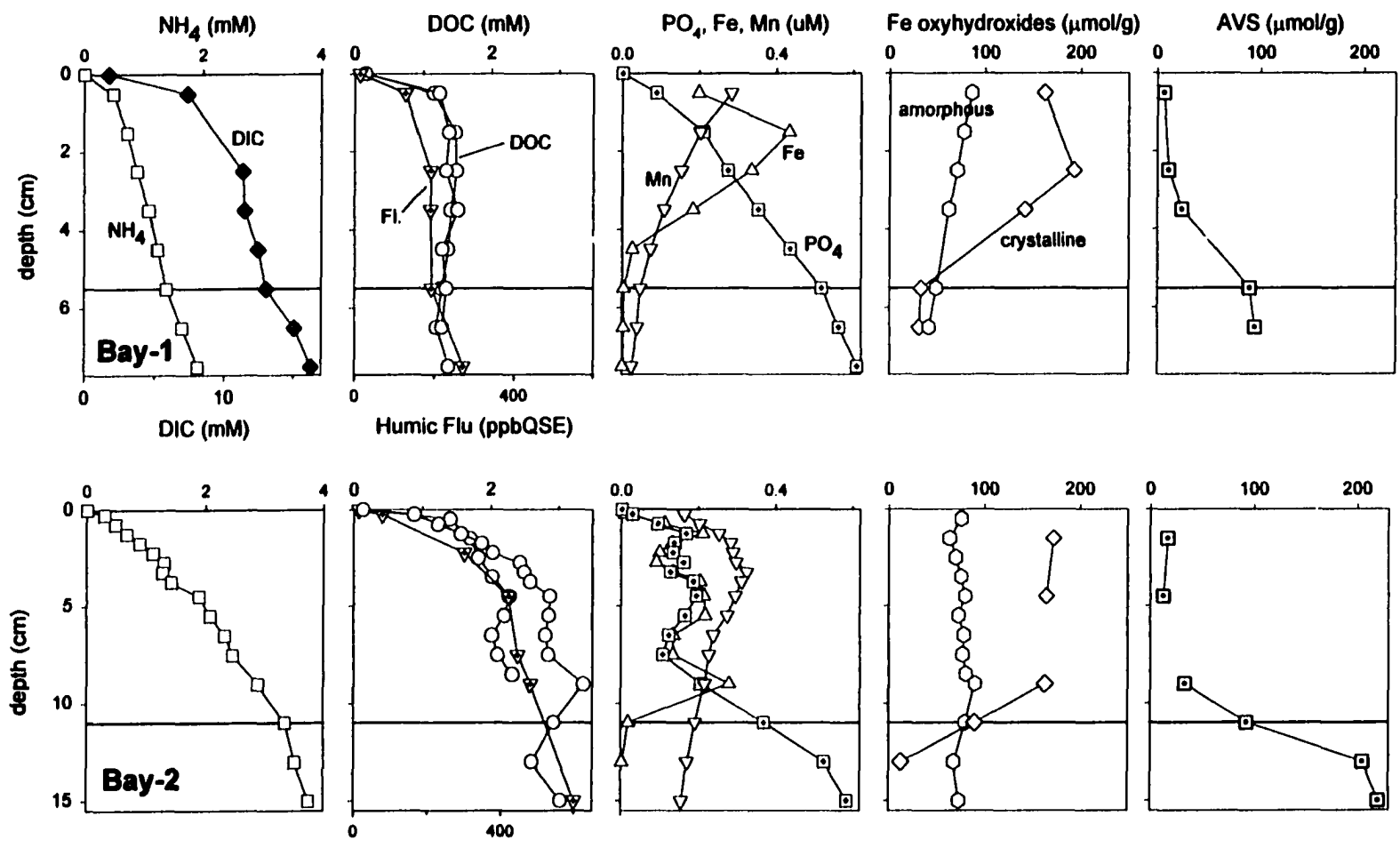


Figure 4.4 (continues on to next page). Short (<15 cm) pore-water and solid-phase profiles from stations Bay-1 and Bay-2. Note differences in the scale in the y-axes. Humic-like fluorescence is the intensity of the peak in the excitation-emission matrix (Appendix-2) positioned near Ex/Em 310/420 nm. AVS = acid volatile sulfide. The horizontal lines indicate the estimated locations of the suboxic-anoxic boundary.

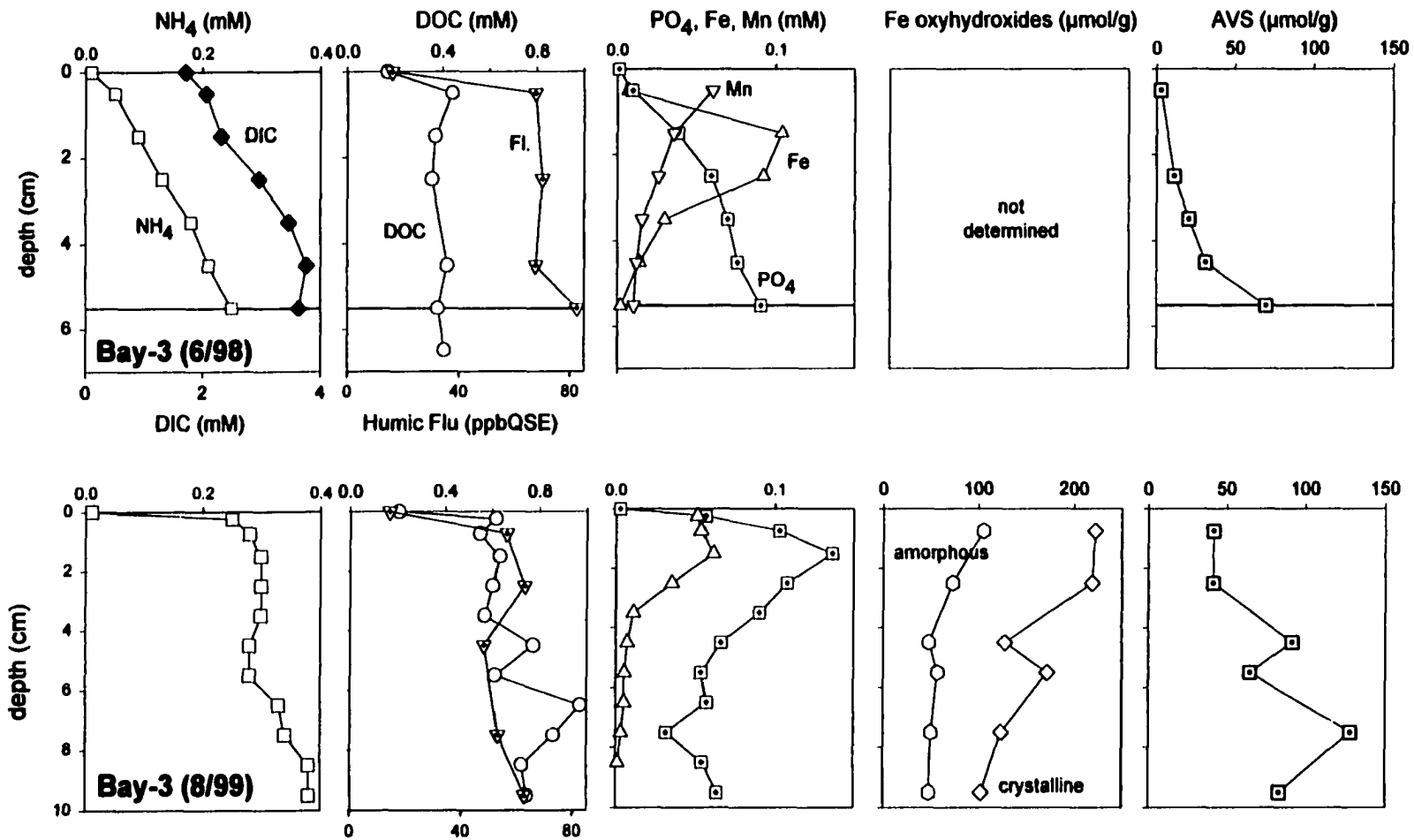


Figure 4.4 (continued). Continuation of Profiles-1, but for station Bay-3 (6/98 and 8/99) and using different scales for the x-axes. The suboxic-anoxic boundary is not indicated for the core collected in 8/99, because of the likelihood that dissolved Fe depletion is due to irrigation (oxidation) rather than due to anoxia.

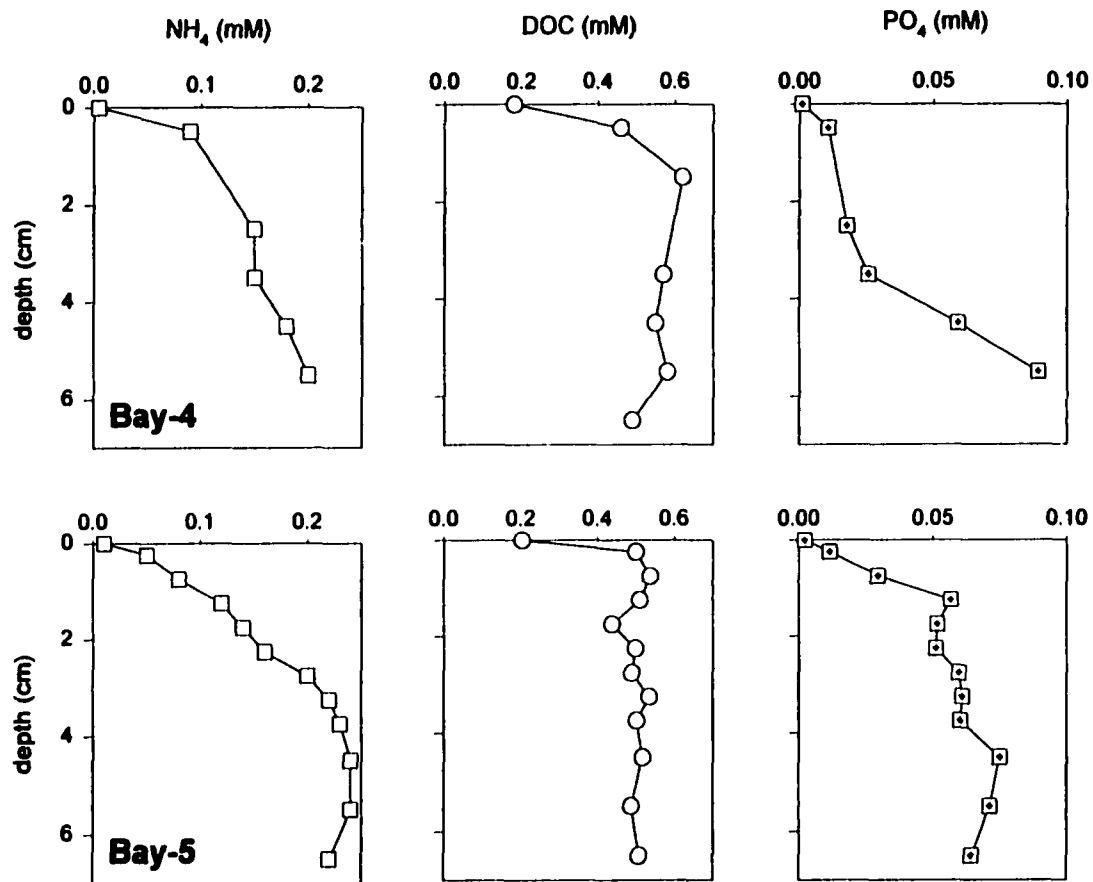


Figure 4.5. Short (<7 cm) pore-water profiles of NH_4 , DOC, and PO_4 for stations Bay-4 and Bay-5. Other dissolved species and solid phase data (Fig. 4) are not available for these stations.

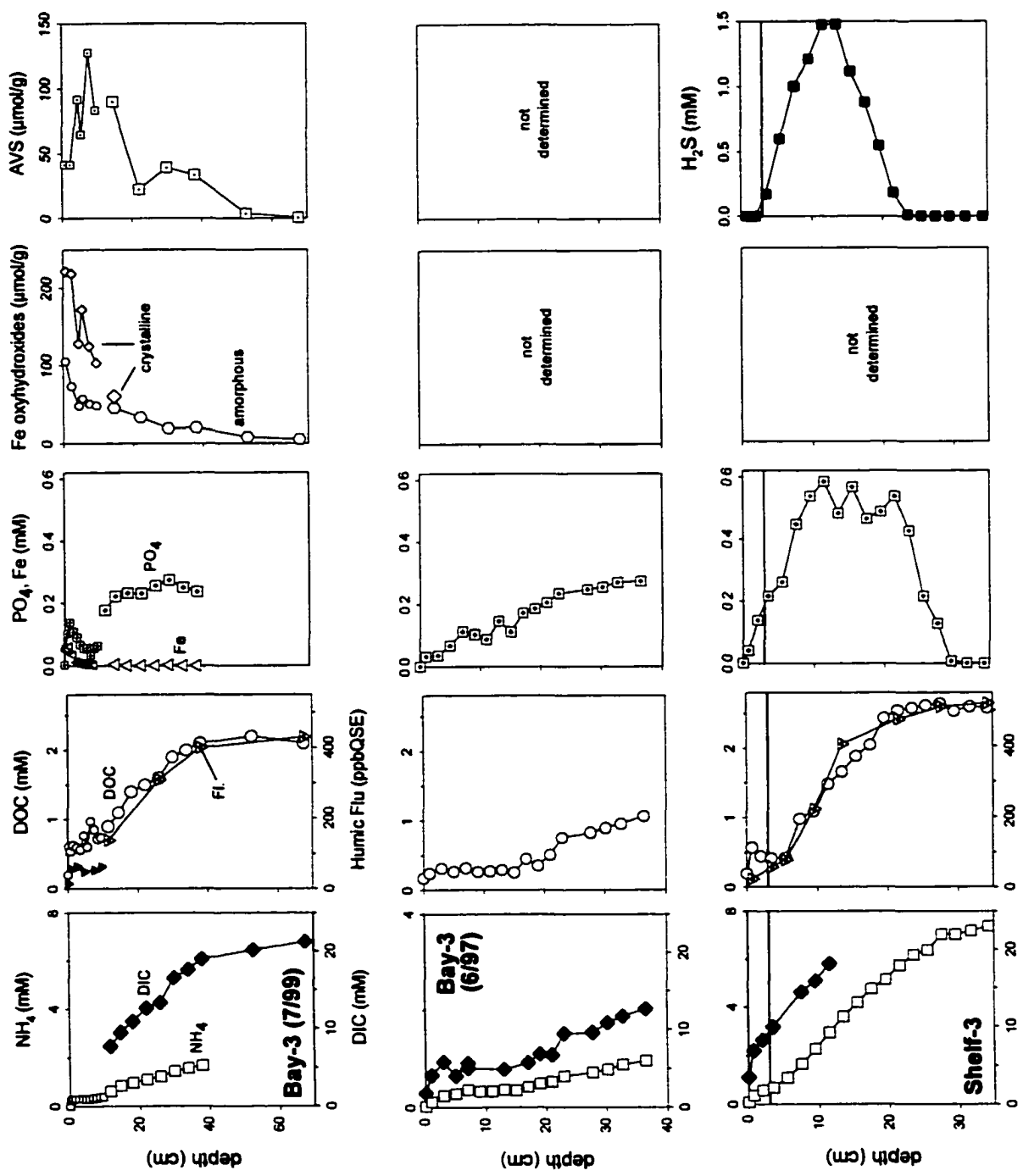


Figure 4.6 (previous page). Longer (>15 cm) pore-water and solid-phase profiles from stations Bay-3 (7/99 and 6/97) and Shelf-3. Humic-like fluorescence is the intensity of the peak in the excitation-emission matrix (Appendix-2) positioned near Ex/Em 310/420 nm. AVS = acid volatile sulfide. Note that total dissolved sulfide is shown instead of AVS in the right-most column for station Shelf-3. Dissolved sulfide was determined for Bay-3 in 7/99, but was not detectable (Appendix-2). Data from the short core collected in 8/99 are shown in smaller symbols along with the 7/99 Bay-3 data. The horizontal lines indicate the estimated locations of the suboxic-anoxic boundary.

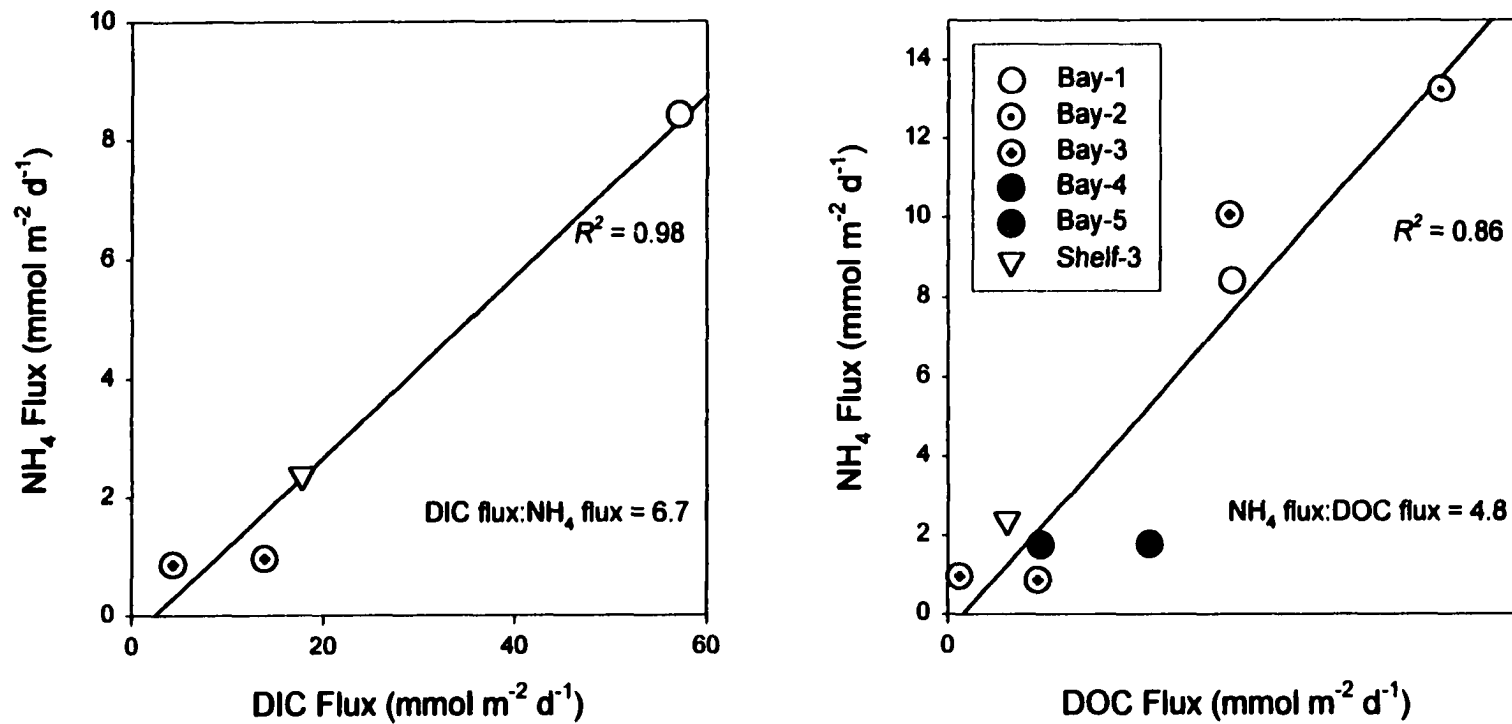


Figure 4.7. Diffusive fluxes of DIC, NH₄ and DOC calculated using the Fick's first law as described in Berner (1980) and the concentration difference between the bottom water and the uppermost pore water value. Solid lines indicate best-fit linear regressions. Due to the effects of irrigation and bioturbation (section 3.1.), these fluxes most likely underestimate total fluxes.

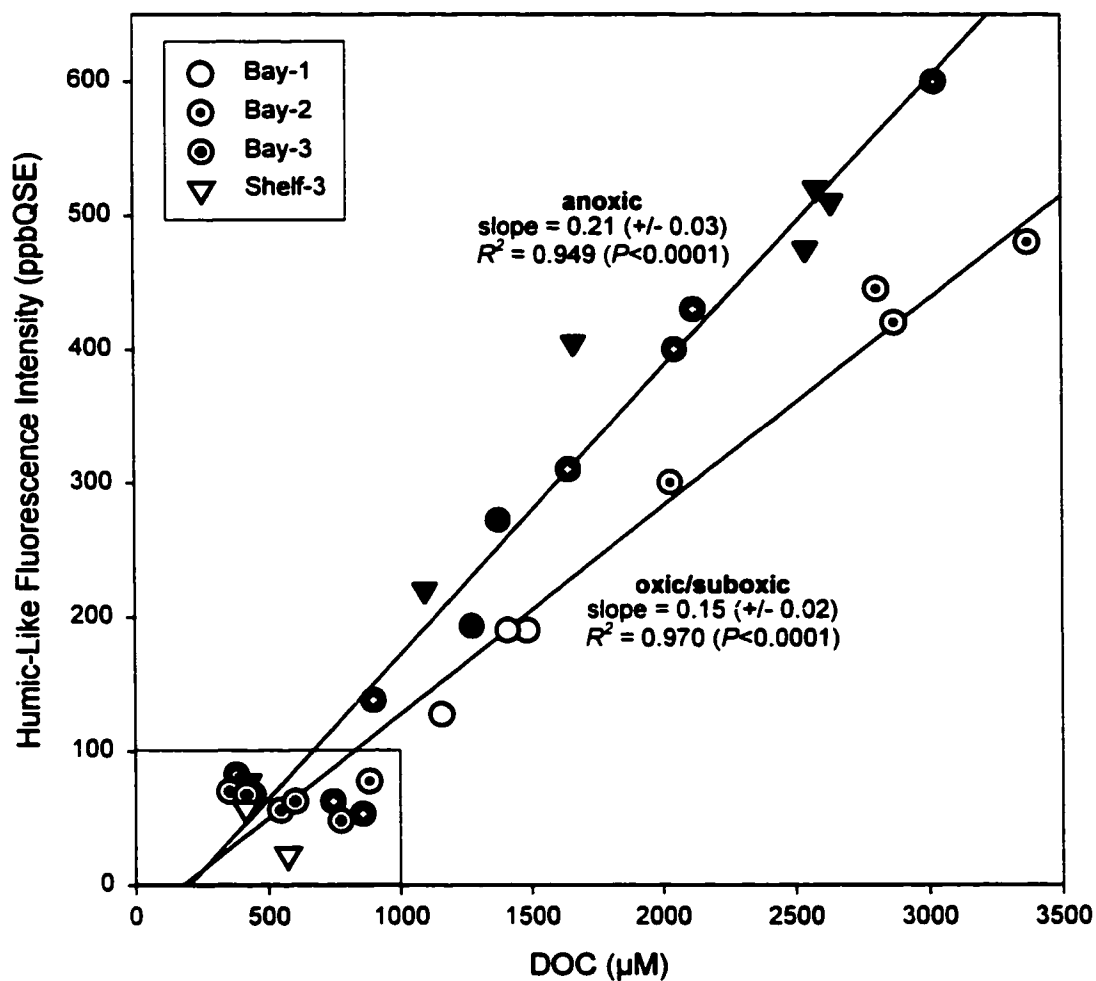


Figure 4.8. Maximum intensity of humic-like fluorescence versus DOC concentration of pore waters. White and black symbols are those collected from above and below the suboxic-anoxic boundary (see section 3.2. for definition), respectively. The boxed area contain data points that may have been influenced by bioturbation/irrigation.

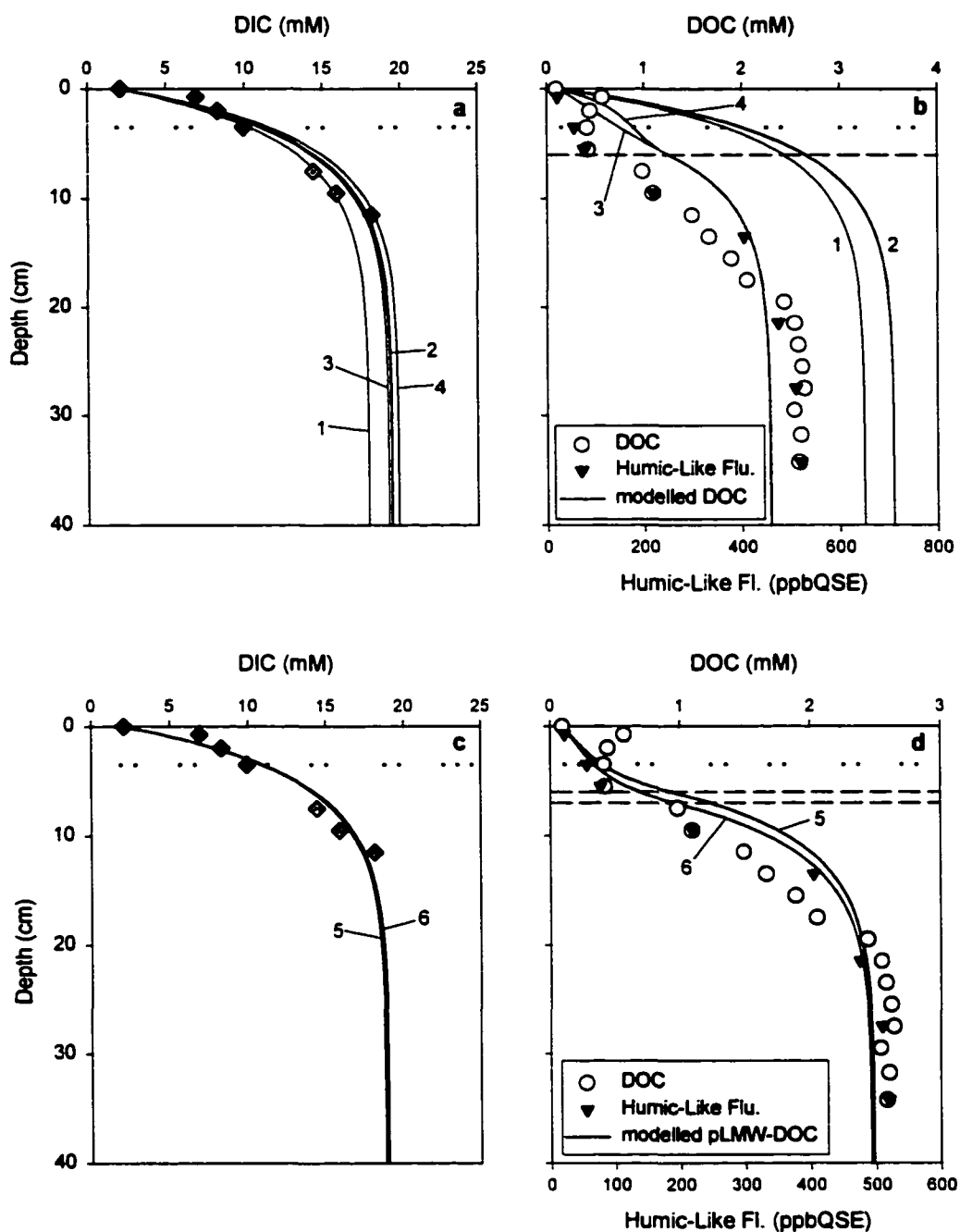


Figure 4.9. Measured profiles of DIC, DOC, and humic-like fluorescence (replication of those given in Fig. 4.6) and model-derived profiles of DOC, pLMW-DOC, and DIC (shown with curves) for station Shelf-3. Dotted and dashed horizontal lines indicate the suboxic-anoxic boundary and the position of L, respectively. (a,b): Model outputs for DIC and DOC calculated under 4 different settings (Cases 1-4; see Table 4.4). In (b), humic-like fluorescence profile (downwards triangle) is superimposed on the DOC profile for reference. (c,d): Model calculations of DIC and pLMW-DOC for Cases 5 and 6 (see Table 4.4).

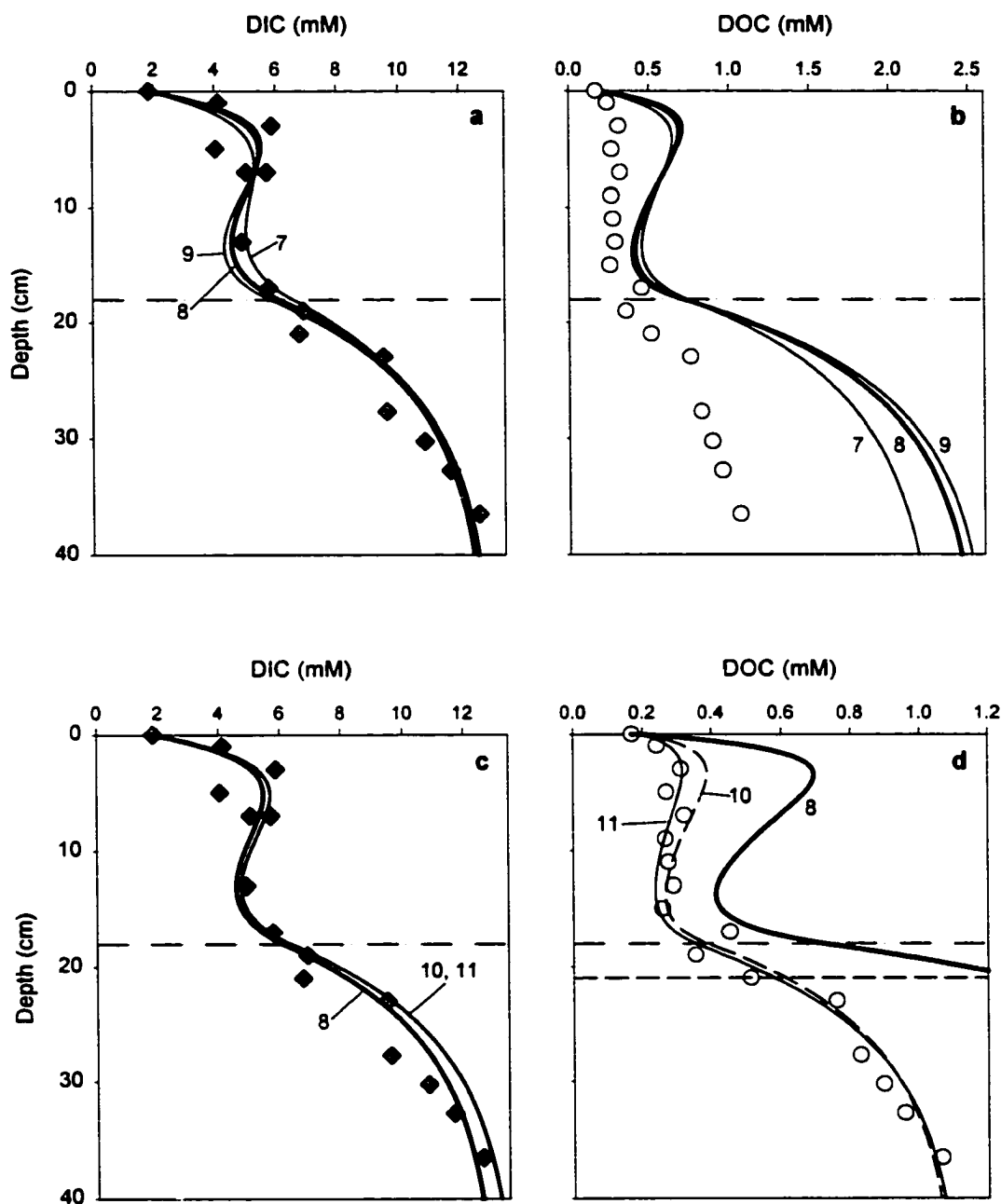


Figure 4.10. Measured and model-derived profiles of DIC and DOC for station Bay-3 (6/97). Dash-dot and dashed horizontal lines indicate the depth of irrigation, and position of L, respectively. (a,b): Model outputs for DIC and DOC calculated under three different conditions (Cases 7-9; Table 4.4). DOC reactivity is assumed to be uniform with depth. (c,d): Additional fitting parameters (a_r , L) are introduced to Case-8 to improve the fit to the DOC profile (Cases 10, 11; Table 4.4).

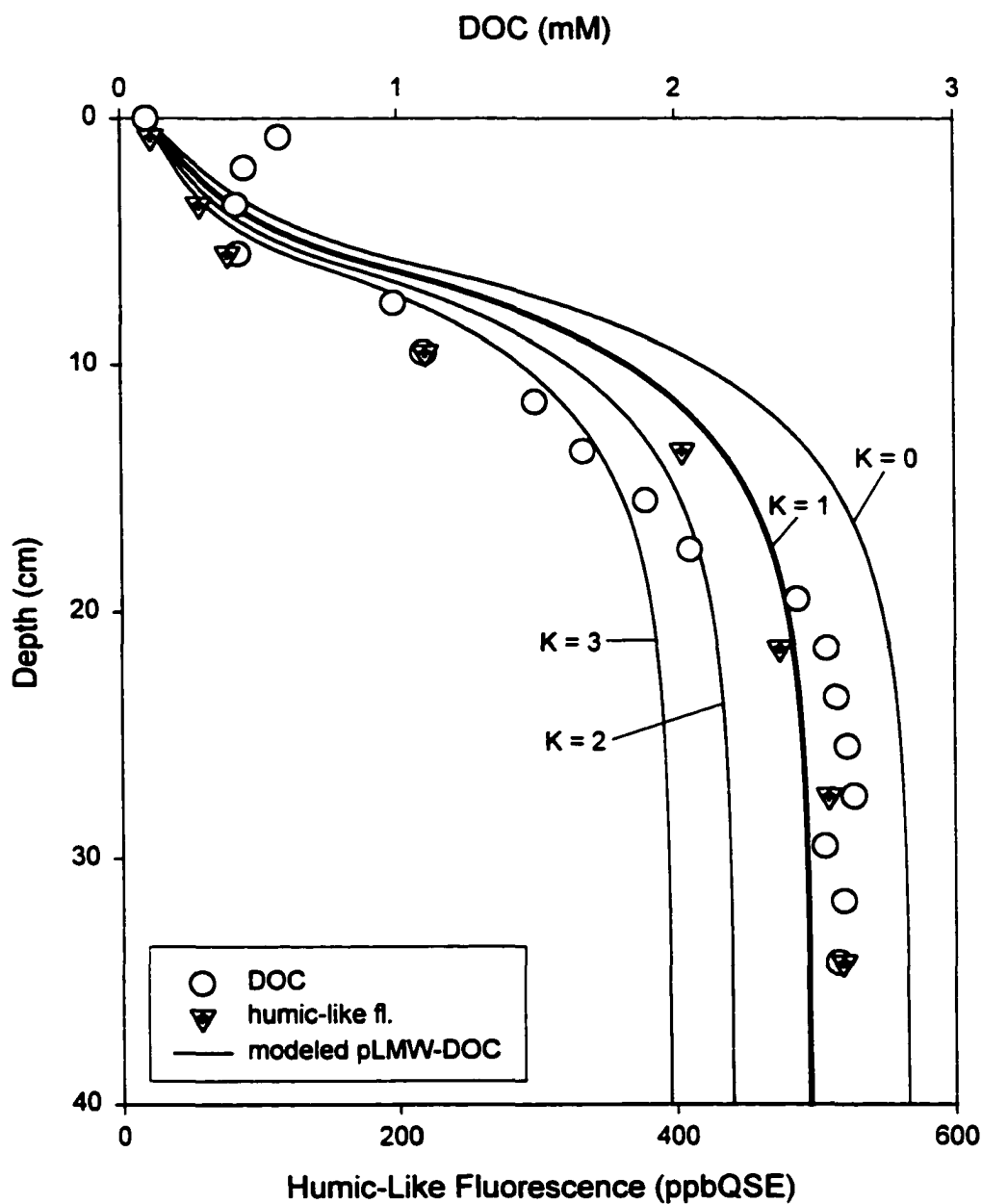


Figure 4.11. Measured profiles of DOC and humic-like fluorescence, and model-derived profiles of pLMW-DOC for station Shelf-3. pLMW-DOC profiles were calculated using K 's ranging between 0 and 3. The curve indicated with a bold line ($K = 1$) is Case-5 (Table 4.4) as presented in Fig. 4.9(d).

NOTE TO USERS

Page(s) not included in the original manuscript and are unavailable from the author or university. The manuscript was microfilmed as received.

116-120

This reproduction is the best copy available.

UMI[®]

APPENDICES

Appendix-1

k_p^x is defined to decrease exponentially with depth at all times:

$$k_p^x = k_p^0 \exp(-\lambda x). \quad (\text{A1})$$

Under this setting, one possible way to enhance k_p^x above the horizon L by a factor k_{pr} is to simply multiply the right hand side of Eq. A1 by k_{pr} when $x \leq L$. However, this results in preferential enhancement closer to the sediment-water interface. An alternative is to enhance the *average* value of k_p^x above horizon L by k_{pr} , such that the final effect is to add a constant, g , to k_p^x . This results in enhancing k_p^x evenly throughout the depth interval $0 \leq x \leq L$.

The enhancement constant, g , is calculated as follows. Let function $f(x)$ be the equation describing the depth-variation of k_p^x above L after enhancement:

$$f(x) = k_p^0 \exp(-\lambda x) + g \quad (\text{A2})$$

It then follows that:

$$\int_0^L f(x) dx = A \times k_{pr} \quad (\text{A3})$$

where A is the area under the curve given in Eq. A1 in the interval $0 \leq x \leq L$:

$$A = k_p^0 \int_0^L \exp(-\lambda x) dx = -\frac{k_p^0}{\lambda} (\exp(-\lambda L) - 1) \quad (\text{A4})$$

Solving Eq. A3 for g gives:

$$g = \frac{k_p^0}{\lambda L} [(1 - k_{pr}) \times (\exp(-\lambda L) - 1)]. \quad (\text{A5})$$

Appendix-2

Analyte	Stations ¹						Method	Precision	References and Comments
	Bay-1	Bay-2	Bay-3	Bay-4	Bay-5	Shelf-3			
DISSOLVED PHASE									
DIC	+		[+]			+	flow-injection and conductivity analysis	3 %	Hall and Aller (1992)
DOC	+	+	+	+	+	+	high-temperature catalytic oxidation	5 %	Determined using a Shimadzu 5000A TOC Analyzer following recommendations by Sharp et al. (1993)
NH ₄ , PO ₄	+	+	+	+	+	+	Spectrophotometry	3 %	Determined using an automated analyzer (Quick Chem AE, Lachat Instruments)
tot. Fe	+	+	[+]				Spectrophotometry	2 %	Determined using the method of Stookey (1970) with modifications described by Luther et al. (1996).
tot. Mn	+	+	[+]				graphite furnace atomic absorption spectrometry	3 %	Determined using the method of standard additions.
humic-like fluorescence	+	+	[+]			+	excitation-emission matrix spectroscopy	2 %	Coble et al. (1993) with modifications as described in Komada Chapter-2.
tot. H ₂ S			(2)			+ ³	Spectrophotometry	n.a.	Cline (1969)

(Continued on next page.)

Appendix-2 (continued)

Analyte	Stations ¹						Method	Precision	References and Comments
	Bay-1	Bay-2	Bay-3	Bay-4	Bay-5	Shelf-3			
SOLID PHASE									
Fe oxy-hydroxides	+	+	[+]				ascorbate and dithionite extractions followed by determination of total dissolved Fe	generally < 10 %	Determined in duplicate according to Kostka and Luther (1994). Dissolved Fe was determined according to Stookey (1970).
acid volatile sulfide (AVS)	+	+	[+]				acidification followed by trapping and quantitation of H ₂ S	generally < 20 %	Determined in triplicate according to Cutter and Oatts (1987) with modifications to the trapping and quantification procedures of H ₂ S as described by Luther et al. (1991).

1. Stations where the analysis was conducted are labeled with a + sign. At station Bay-3 where a total of 4 cores were collected, not all analyses were conducted on all cores. Those cases are indicated with a [+].
2. Analysis for total dissolved sulfide was conducted for the cores collected on 7/22/99 and 8/3/99, but was not detectable (to as deep as 30 cm in the 7/22/99 core, and throughout the 8/3/99 core). Detection limit of this method is 1 μM (Cline, 1969). Therefore, these data are not shown in Fig. 6.
3. Data courtesy of Dr. A. Draxler, NOAA, NMFS.

Appendix-3

Because the majority of the POC converted to HMW-DOC is rapidly remineralized to DIC via mLMW-DOC (Fig. 1), the rate of DIC production and its attenuation with depth should closely reflect the net reaction rate of POC and its attenuation with depth. Therefore, to determine λ and R^0 in Eq 5, an exponential curve was fit directly to the DIC profile:

$$C^x = (C^0 - C^\infty) \cdot \exp(-qx) + C^\infty \quad (\text{A6})$$

where C is the DIC concentration (with superscripts 0 and ∞ representing bottom water concentration and the asymptotic pore water concentration, respectively), and q is a depth-attenuation constant. By fixing C^0 to the measured bottom water value, the best-fit (least squares) of Eq.A6 to the observed profile was obtained when $q = 0.21 \text{ cm}^{-1}$ and $C^\infty = 18 \text{ mM}$. The production rate of DIC at the sediment-water interface, R_{DIC}^0 , was then determined by differentiating Eq. A6 and substituting the results to a diagenetic equation of the form:

$$D_s \frac{d^2 C}{dx^2} - \omega \frac{dC}{dx} + R_{\text{DIC}}^x = 0 \quad (\text{A7})$$

and solving for R_{DIC}^x at $x = 0$ (setting D_s and ω as given in Table 1). The result of this computation yielded $R_{\text{DIC}}^0 = 129,000 \text{ } \mu\text{M yr}^{-1}$ (0.35 mM d^{-1}).

BIBLIOGRAPHY

- Abood, K.A., Apicella, G.A., Wells, A.W., 1992. General evaluation of Hudson River freshwater flow trends. In: C.L. Smith (Editor), *Estuarine Research in the 1980s*. State University of New York Press, Albany, pp. 3-28.
- Achman, D.R., Brownawell, B.J., Zhang, L., 1996. Exchange of polychlorinated biphenyls between sediment and water in the Hudson River Estuary. *Estuaries* 19, 950-965.
- Adams, D.A., O'Connor, J.S., Weisberg, A.B., 1998. Sediment quality of the NY/NJ harbor system. EPA/902-R-98-001, U. S. Environmental Protection Agency.
- Aller, R.C., 1994. Bioturbation and remineralization of sedimentary organic matter: effects of redox oscillation. *Chem. Geol.* 114, 331-345.
- Alperin, M.J., Albert, D.B., Martens, C.S., 1994. Seasonal variations in production and consumption rates of dissolved organic carbon in an organic-rich coastal sediment. *Geochim. Cosmochim. Acta* 58, 4909-4930.
- Alperin, M.J., Martens, C.S., Albert, D.B., Suayah, I.B., Benninger, L.K., Blair, N.E., Jahnke, R.A., 1999. Benthic fluxes and porewater concentration profiles of dissolved organic carbon in sediments from the North Carolina continental slope. *Geochim. Cosmochim. Acta* 63, 427-448.
- Amon, R.M.W., Benner, R., 1996. Photochemical and microbial consumption of dissolved organic carbon and dissolved oxygen in the Amazon River system. *Geochim. Cosmochim. Acta* 60, 1783-1792.
- Arnarson, T.S., Keil, R.G., 2000. Mechanisms of pore water organic matter adsorption to montmorillonite. *Mar. Chem.* 71, 309-320.
- Arnosti, C., Holmer, M., 1999. Carbohydrate dynamics and contributions to the carbon budget of an organic-rich coastal sediment. *Geochim. Cosmochim. Acta* 63, 393-403.
- Bacon, M.P., Belastock, R.A., Bothner, M.H., 1994. ²¹⁰Pb balance and implications for particle transport on the continental shelf, U.S. Middle Atlantic Bight. *Deep-Sea Res. II* 41, 511-535.
- Barcelona, M.J., 1980. Dissolved organic carbon and volatile fatty acids in marine sediment pore waters. *Geochim. Cosmochim. Acta* 44, 1977-1984.
- Bauer, J.E., Reimers, C.E., Druffel, E.R.M., Williams, P.M., 1995. Isotopic constraints on carbon exchange between deep ocean sediments and sea water. *Nature* 373, 686-689.
- Bauer, J.E., Druffel, E.R.M., 1998. Ocean margins as a significant source of organic matter to the deep open ocean. *Nature* 392, 482-465.
- Benner, R., Opsahl, S., 2001. Molecular indicators of the sources and transformations of dissolved organic matter in the Mississippi river plume. *Org. Geochem.* 32, 597-611.
- Bergamaschi, B.A., Tsamakis, E., Keil, R.G., Eglinton, T.I., Montlucon, D.B., Hedges, J.I., 1997. The effect of grain size and surface area on organic matter, lignin and carbohydrate concentration, and molecular compositions in Peru Margin sediments. *Geochim. Cosmochim. Acta* 61, 1247-1260.
- Berlman, I.B., 1965. *Handbook of fluorescence spectra of aromatic molecules*. Academic Press, New York, 258 pp.
- Berner, R.A., 1976. Inclusion of adsorption in the modelling of early diagenesis. *Earth Planet Sci. Lett.* 29, 333-340.
- Berner, R.A., 1980. *Early Diagenesis*. Princeton University Press, Princeton.
- Bianchi, T.S., Lambert, C.D., Santschi, P.H., Guo, L., 1997. Sources and transport of land-derived particulate and dissolved organic matter in the Gulf of Mexico (Texas shelf/slope): The use of lignin-phenols and loliolides as biomarkers. *Org. Geochem.* 27, 65-78.
- Biscaye, P.E., Olsen, C.R., 1976. Suspended particulate concentrations and compositions in the

- New York Bight. In: M.G. Gross (Editor), *Middle Atlantic Continental Shelf and the New York Bight*. American Society of Limnology and Oceanography, New York City, pp. 124-137.
- Boehme, J.R., Coble, P.G., 2000. Characterization of colored dissolved organic matter using high-energy laser fragmentation. *Environ. Sci. Technol.* 34, 3283-3290.
- Bokuniewicz, H., Arnold, C.L., 1984. Characteristics of suspended sediment transport in the Lower Hudson River. *Northeast. Environ. Sci.* 3, 185-190.
- Bokuniewicz, H.J., Ellsworth, J.M., 1986. Sediment budget for the Hudson System. *Northeast. Geol.* 8, 156-164.
- Bopp, R.F., Robinson, D.W., Simpson, H.J., Biscaye, P.E., Anderson, R.F., Tong, H. Monson, S.J., Gross, M.L., 1995. Recent sediment and contaminant distributions in the Hudson Shelf Valley. NMFS 124, U. S. Dep. Commer., NOAA Tech. Rep. NMFS 124.
- Boudreau, B.P., 1997. *Diagenetic Models and Their Implementation*. Springer-Verlag, Heidelberg.
- Bowman, M.J., Wunderlich, L.D., 1977. *Hydrographic Properties*. MESA New York Bight Atlas Monograph, 1. New York Sea Grant Institute, Albany.
- Brunauer, S., Emmett, P.H., Teller, E., 1938. Adsorption of gases in multimolecular layers. *J. Am. Chem. Soc.* 60, 309-319.
- Burdige, D. J., in press. Dissolved organic matter in marine sediment pore waters. *In Biogeochemistry of Marine Dissolved Organic Matter*, Hansell, D. and Carlson, C, eds., Academic Press.
- Burdige, D.J., Martens, C.S., 1990. Biogeochemical cycling in an organic-rich coastal marine basin: 11. The sedimentary cycling of dissolved, free amino acids. *Geochim. Cosmochim. Acta* 54, 3033-3051.
- Burdige, D.J., Alperin, M.J., Homstead, J., Martens, C.S., 1992. The role of benthic fluxes of dissolved organic carbon in oceanic and sedimentary carbon cycling. *Geophys. Res. Lett.* 19, 1851-1854.
- Burdige, D.J., Homstead, J., 1994. Fluxes of dissolved organic carbon from Chesapeake Bay sediments. *Geochim. Cosmochim. Acta* 58, 3407-3424.
- Burdige, D.J., Gardner, K.G., 1998. Molecular weight distribution of dissolved organic carbon in marine sediment pore waters. *Mar. Chem.* 62, 45-64.
- Burdige, D.J., Zheng, S., 1998. The biogeochemical cycling of dissolved organic nitrogen in estuarine sediments. *Limnol. Oceanogr.* 43, 1796-1813.
- Burdige, D.J., Berelson, W.M., Coale, K.H., McManus, J., Johnson, K.S., 1999. Fluxes of dissolved organic carbon from California continental margin sediments. *Geochim. Cosmochim. Acta* 63, 1507-1515.
- Burdige, D.J., Skoog, A., Gardner, K., 2000. Dissolved and particulate carbohydrates in contrasting marine sediments. *Geochim. Cosmochim. Acta* 64, 1029-1041.
- Burdige, D.J., 2001. Dissolved organic matter in Chesapeake Bay sediment pore waters. *Org. Geochem.* 32, 487-505.
- Chen, R.F., Bada, J.L., Suzuki, Y., 1993. The relationship between dissolved organic carbon (DOC) and fluorescence in anoxic marine pore waters: Implications for estimating benthic DOC fluxes. *Geochim. Cosmochim. Acta* 57, 2149-2153.
- Chen, R.F., Bada, J.L., 1994. The fluorescence of dissolved organic matter in porewaters of marine sediments. *Mar. Chem.* 45, 31-42.
- Chen, R.F., 1999. In situ fluorescence measurements in coastal waters. *Org. Geochem.* 30, 397-409.
- Chin, W.-C., Orellana, M.V., Verdugo, P., 1998. Spontaneous assembly of marine dissolved organic matter into polymer gels. *Letters to Nature* 391, 568-572.
- Chin, Y.-P., Gschwend, P.M., 1991. The abundance, distribution, and configuration of porewater organic colloids in recent sediments. *Geochim. Cosmochim. Acta* 55, 1309-1317.

- Cline, J.D., 1969. Spectrophotometric determination of hydrogen sulfide in natural waters. *Limnol. Oceanogr.* 14, 454-458.
- Coble, P.G., Green, S.A., Blough, N.V., Gagosian, R.B., 1990. Characterization of dissolved organic matter in the Black Sea by fluorescence spectroscopy. *Nature* 348, 432-435.
- Coble, P.G., Schuitz, C.A., Mopper, K., 1993. Fluorescence contouring analysis of DOC Intercalibration Experiment samples: a comparison of techniques. *Mar. Chem.*, 41, 173-178.
- Coble, P.G., 1996. Characterization of marine and terrestrial DOM in seawater using excitation-emission matrix spectroscopy. *Mar. Chem.* 51, 325-346.
- Coble, P.G., Del Castillo, C.E., Avril, B., 1998. Distribution and optical properties of CDOM in the Arabian Sea during the 1995 Southwest Monsoon. *Deep-Sea Res. II* 45, 2195-2223.
- Collins, M.J., Bishop, A.N., Farrimond, P., 1995. Sorption by mineral surfaces: Rebirth of the classical condensation pathway for kerogen formation? *Geochim. Cosmochim. Acta* 59, 2387-2391.
- Cutter, G.A., Oatts, T.J., 1987. Determination of dissolved sulfide and sedimentary sulfur speciation using gas chromatography-photoionization detection. *Anal. Chem.* 59, 717-721.
- de Souza Sierra, M., M., Donard, O.F.X., Lamotte, M., 1997. Spectral identification and behaviour of dissolved organic fluorescent material during estuarine mixing processes. *Mar. Chem.* 58, 51-58.
- Del Castillo, C.E., Coble, P.G., Morell, J.M., López, J.M., 1999. Analysis of the optical properties of the Orinoco River plume by absorption and fluorescence spectroscopy. *Mar. Chem.* 66, 35-51.
- Duedall, I.W., O'Connors, H.B., Wilson, R.E., Parker, J.H., 1979. The Lower Bay Complex. MESA New York Bight Atlas Monograph, 29. New York Sea Grant Institute, Albany.
- Emerson, S., Jahnke, R., Heggie, D., 1984. Sediment-water exchange in shallow water estuarine sediments. *J. Mar. Res.* 42, 709-730.
- Emerson, S., Stump, C., Grootes, P.M., Stuiver, M., Farwell, G.W., Schmidt, F.H., 1987. Estimates of degradable organic carbon in deep-sea surface sediments from ¹⁴C concentrations. *Nature* 329, 51-53.
- Emerson, S., Hedges, J.I., 1988. Processes controlling the organic carbon content of open ocean sediments. *Paleoceanogr.* 3, 621-634.
- Findlay, R.H., Trexler, M.B., Guckert, J.B., White, D.C., 1990. Laboratory study of disturbance in marine sediments: response of a microbial community. *Mar. Ecol. Progr. Ser.* 62, 121-133.
- Findlay, S., Pace, M., Lints, D., 1991a. Variability and transport of suspended sediment, particulate and dissolved organic carbon in the tidal freshwater Hudson River. *Biogeochemistry* 12, 149-169.
- Findlay, S., Pace, M.L., Lints, D., Cole, J.J., Caraco, N.F., Peierls, B., 1991b. Weak coupling of bacterial and algal production in a heterotrophic ecosystem: The Hudson River estuary. *Limnol. Oceanogr.* 36, 268-278.
- Fox, L.E., 1983. The removal of dissolved humic acid during estuarine mixing. *Est. Coastal Shelf Sci.*, 16, 431-440.
- Geyer, W.R., 1995. Particle trapping in the Lower Hudson Estuary, Hudson River Foundation, unpublished report.
- Gieskes, J., Peretsman, G., 1986. Water chemistry procedures aboard Joides Resolution – some comments, Ocean Drilling Program, Texas A&M University.
- Gordon, A.S., Millero, F.J., 1985. Adsorption mediated decrease in the biodegradation rate of organic compounds. *Microb. Ecol.*, 11, 289-298.
- Graf, G., 1987. Benthic energy flow during a simulated autumn bloom sedimentation. *Mar. Ecol. Progr. Ser.* 39, 23-29.

- Gu, B., Schmitt, J., Chen, Z., Liang, L., McCarthy, J.F., 1995. Adsorption and desorption of different organic matter fractions on iron oxide. *Geochim. Cosmochim. Acta* 59, 219-229.
- Gu, B., Mehlhorn, T.L., Liang, L., McCarthy, J.F., 1996. Competitive adsorption, displacement, and transport of organic matter on iron oxide: I. Competitive adsorption. *Geochim. Cosmochim. Acta* 60, 1943-1950.
- Guilbault, G.G., 1973. *Practical Fluorescence*. Marcel Dekker, New York, 664 pp.
- Guo, L., Santschi, P.H., 2000. Sedimentary sources of old high molecular weight dissolved organic carbon from the ocean margin benthic nepheloid layer. *Geochim. Cosmochim. Acta* 64, 651-660.
- Hall, P.O.J., Aller, R.C., 1992. Rapid, small-volume, flow injection analysis for ΣCO_2 and NH_4^+ in marine and freshwaters. *Limnol. Oceanogr.* 37, 1113-1119.
- Hartnett, H.E., Keil, R.G., Hedges, J.I., Devol, A.H., 1998. Influence of oxygen exposure time on organic carbon preservation in continental margin sediments. *Nature* 391, 572-537.
- Harvey, G.R., 1984. Comment on the structure of marine fulvic and humic acids. *Mar. Chem.* 15, 89-90.
- Hatcher, P.G., Spiker, E.C., Szeverenyi, N.M., Maciel, G.E., 1983. Selective preservation and origin of petroleum-forming aquatic kerogen. *Nature* 305, 498-501.
- Hedges, J.I., 1992. Global biogeochemical cycles: Progress and problems. *Mar. Chem.* 39, 68-93.
- Hedges, J.I., Stern, J.H., 1984. Carbon and nitrogen determinations of carbonate-containing solids. *Limnol. Oceanogr.* 29, 657-663.
- Hedges, J.I., Keil, R.G., 1995. Sedimentary organic matter preservation: An assessment and speculative synthesis. *Mar. Chem.* 49, 81-115.
- Hedges, J.I., Keil, R.G., Benner, R., 1997. What happens to terrestrial organic matter in the ocean? *Org. Geochem.* 27, 195-212.
- Hedges, J.I., Hu, F.S., Devol, A.H., Hartnett, H.E., Tsamakis, E., Keil, R.G., 1999. Sedimentary organic matter preservation: a test for selective degradation under oxic conditions. *Am. J. Sci.* 299, 529-555.
- Hedges, J.I., Keil, R.G., 1999. Organic geochemical perspective on estuarine processes: sorption reactions and consequences. *Mar. Chem.* 65, 55-65.
- Hedges, J.I., Eglinton, G., Hatcher, P.G., Kirchman, D.L., Arnosti, C., Derenne, S., Evershed, R.P., Kögel-Knabner, I., de Leeuw, J.W., Littke, R., Michaelis, W., Rullkötter, J., 2000. The molecularly-uncharacterized component of nonliving organic matter in natural environments. *Org. Geochem.* 31, 945-958.
- Henrichs, S.M., 1992. Early diagenesis of organic matter in marine sediments: Progress and perplexity. *Mar. Chem.* 39, 119-149.
- Henrichs, S.M., 1995. Sedimentary organic matter preservation: an assessment and speculative synthesis - a comment. *Mar. Chem.* 49, 127-136.
- Henrichs, S.M., Farrington, J.W., 1979. Amino acids in interstitial waters of marine sediments. *Nature* 279, 319-322.
- Henrichs, S.M., Sugai, S.F., 1993. Adsorption of amino acids and glucose by sediments of Resurrection Bay, Alaska, USA: Functional group effects. *Geochim. Cosmochim. Acta* 57, 823-835.
- Holcombe, B.L., Keil, R.G., Devol, A.H., 2001. Determination of pore-water dissolved organic carbon fluxes from Mexican margin sediments. *Limnol. Oceanogr.* 46, 298-308.
- Howarth, R.W., Schneider, R., Swaney, D., 1996. Metabolism and organic carbon fluxes in the tidal freshwater Hudson River. *Estuaries* 19, 848-865.
- Jahnke, R.A., 1988. A simple, reliable, and inexpensive pore-water sampler. *Limnol. Oceanogr.* 33, 483-487.
- Kastens, K.A., Fray, C.T., Schubel, J.R., 1978. Environmental effects of sand mining in the

- Lower Bay of New York Harbor. 15, Marine Sciences Research Center, State University of New York Stony Brook, New York.
- Keil, R.G., Montluçon, D.B., Pahl, F.G., Hedges, J.I., 1994a. Sorptive preservation of labile organic matter in marine sediments. *Nature* 370, 549-552.
- Keil, R.G., Tsamakis, E., Fuh, C.B., Giddings, J.C., Hedges, J.I., 1994b. Mineralogical and textural controls on the organic composition of coastal marine sediments: Hydrodynamic separation using SPLITT-fractionation. *Geochim. Cosmochim. Acta* 58, 879-893.
- Keil, R.G., Mayer, L.M., Quay, P.D., Richey, J.E., Hedges, J.I., 1997. Loss of organic matter from riverine particles in deltas. *Geochim. Cosmochim. Acta* 61, 1507-1511.
- Keil, R.G., Tsamakis, E., Giddings, J.C., Hedges, J.I., 1998. Biochemical distributions (amino acids, neutral sugars, and lignin phenols) among size-classes of modern marine sediments from the Washington coast. *Geochim. Cosmochim. Acta* 62, 1347-1364.
- Keil, R.G., Fogel, M.L., 2001. Reworking of amino acid in marine sediments: Stable carbon isotopic composition of amino acids in sediments along the Washington coast. *Limnol. Oceanogr.* 46, 14-23.
- Kirchman, D.L., Suzuki, Y., Garside, C., Ducklow, H.W., 1991. High turnover rates of dissolved organic carbon during a spring phytoplankton bloom. *Nature* 352, 612-614.
- Komada, T., Reimers, C.E., 2001. Resuspension-induced partitioning of organic carbon between solid and solution phases from a river-ocean transition. *Mar. Chem.* 176, 155-174.
- Kostka, J.E., Luther, G.W., III., 1994. Partitioning and speciation of solid phase iron in saltmarsh sediments. *Geochim. Cosmochim. Acta* 58, 1701-1710.
- Krom, M.D., Sholkovitz, E.R., 1977. Nature and reactions of dissolved organic matter in the interstitial waters of marine sediments. *Geochim. Cosmochim. Acta* 41, 1565-1573.
- Laane, R.W.P.M., 1984. Comment on the structure of marine fulvic and humic acids. *Mar. Chem.* 15, 85-87.
- Laane, R.W.P.M., Koole, L., 1982. The relationship between fluorescence and dissolved organic carbon in the Ems-Dollart estuary and the western Wadden Sea. *Neth. J. Sea Res.* 15, 217-227.
- Li, Y.-H., Gregory, S., 1974. Diffusion of ions in sea water and in deep-sea sediments. *Geochim. Cosmochim. Acta* 38, 703-714.
- Limburg, K.E., Moran, M.A., McDowell, W.H., 1986. *The Hudson River Ecosystem*. Springer-Verlag, New York.
- Luther, G., W., III., Ferdelman, T.G., Kostka, J.E., Tsamakis, E.J., Church, T.M., 1991. Temporal and spatial variability of reduced sulfur species (FeS_2 , $\text{S}_2\text{O}_3^{2-}$) and porewater parameters in salt marsh sediments. *Biogeochemistry* 14, 57-88.
- Luther, G., W., III., Shellenbarger, P.A., Brendel, P.J., 1996. Dissolved organic Fe (III) and Fe (II) complexes in salt marsh porewaters. *Geochim. Cosmochim. Acta* 60, 951-960.
- Luther, G., W., III., Reimers, C.E., Nuzzio, D.B., Lovalvo, D., 1999. In situ deployment of voltammetric, potentiometric, and amperometric microelectrodes from a ROV to determine dissolved O_2 , Mn, Fe, S(-2), and pH in porewaters. *Environ. Sci. Technol.* 33, 4352-4356.
- Mannino, A., Harvey, H.R., 1999. Lipid composition in particulate and dissolved organic matter in the Delaware Estuary: Sources and diagenetic patterns. *Geochim. Cosmochim. Acta* 63, 2219-2235.
- Mannino, A., Harvey, H.R., 2000a. Biochemical composition of particles and dissolved organic matter along an estuarine gradient: Sources and implications for DOM reactivity. *Limnol. Oceanogr.* 45, 775-788.
- Mannino, A., Harvey, H.R., 2000b. Terrigenous dissolved organic matter along an estuarine gradient and its flux to the coastal ocean. *Org. Geochem.* 31, 1611-1625.
- Martin, W.R., McCorkle, D.C., 1993. Dissolved organic carbon concentrations in marine pore waters determined by high-temperature oxidation. *Limnol. Oceanogr.* 38, 1464-1479.

- Matthews, B.J.H., Jones, A.C., Theodorou, N.K., Tudhope, A.W., 1996. Excitation-emission-matrix fluorescence spectroscopy applied to humic acid bands in coral reefs. *Mar. Chem.* 55, 317-332.
- Mayer, L.M., Jumars, P.A., Taghon, G.L., Macko, S.A., Trumbore, S., 1993. Low-density particles as potential nitrogenous foods for benthos. *J. Mar. Res.* 51, 373-389.
- Mayer, L.M., 1994a. Relationships between mineral surfaces and organic carbon concentrations in soils and sediments. *Chem. Geol.* 114, 347-363.
- Mayer, L.M., 1994b. Surface area control on organic carbon accumulation in continental shelf sediments. *Geochim. Cosmochim. Acta* 58, 1271-1284.
- McKnight, D.M., Boyer, E.W., Westerhoff, P.K., Doran, P.T., Kulbe, T., Andersen, D.T., 2001. Spectrofluorometric characterization of dissolved organic matter for indication of precursor organic material and aromaticity. *Limnol. Oceanogr.* 46, 38-48.
- Meade, R.H., Sachs, P.L., Manheim, F.T., Hathaway, J.C., Spencer, D.W., 1975. Sources of suspended matter in waters of the Middle Atlantic Bight. *J. Sed. Petrol.* 45, 171-188.
- Metzger, S.G., Keppel, R.G., Geoghegan, P., Wells, A.W., 1992. Abundance of selected Hudson River fish species in previously unsampled regions: Effect on standing crop estimates. In: C.L. Smith (Editor), *Estuarine Research in the 1980's*. State University of New York Press, Albany, pp. 348-375.
- Meyers-Schulte, K.J., Hedges, J.I., 1986. Molecular evidence for a terrestrial component of organic matter dissolved in ocean water. *Nature* 321, 61-63.
- Miller, J.N. (Editor), 1981. *Standards in Fluorescence Spectrometry. Techniques in Visible and Ultraviolet Spectrometry, 2*. Chapman and Hall, New York.
- Miller, W.L., Zepp, R.G., 1995. Photochemical production of dissolved inorganic carbon from terrestrial organic matter: Significance to the oceanic organic carbon cycle. *Geophys. Res. Lett.* 22, 417-420.
- Miller, W.L., Moran, M.A., 1997. Interaction of photochemical and microbial processes in the degradation of refractory dissolved organic matter from a coastal marine environment. *Limnol. Oceanogr.* 42, 1317-1324.
- Mitra, S., Bianchi, T.S., Guo, L., Santschi, P.H., 2000. Terrestrially derived dissolved organic matter in the Chesapeake Bay and the Middle Atlantic Bight. *Geochim. Cosmochim. Acta* 64, 3547-3557.
- Mobed, J.J., Hemmingsen, S.L., Autry, J.L., McGown, L.B., 1996. Fluorescence characterization of IHSS humic substances: Total luminescence spectra with absorbance correction. *Environ. Sci. Technol.* 30, 3061-3065.
- Montluçon, D.B., Lee, C., 2001. Factors affecting lysine sorption in a coastal sediment. *Org. Geochem.* 32, 933-942.
- Moran, M.A., Shelton, W.M., Jr., Zepp, R.G., 2000. Carbon loss and optical property changes during long-term photochemical and biological degradation of estuarine dissolved organic matter. *Limnol. Oceanogr.* 45, 1254-1264.
- Morin, J., Morse, J.W., 1999. Ammonium release from resuspended sediments in the Laguna Madre estuary. *Mar. Chem.* 65, 97-110.
- Naudin, J.J., Cauwet, G., 1997. Transfer mechanisms and biogeochemical implications in the bottom nepheloid layer. A case study of the coastal zone off the Rhone River (France). *Deep-Sea Res.* 44, 551-575.
- Oades, J.M., 1972. Studies on soil polysaccharides III. Composition of polysaccharides in some Australian soils. *Austr. J. Soil Res.* 10, 113-126.
- Olsen, C.R., Larsen, I.L., Brewster, R.H., Cutshall, N.H., Bopp, R.F., Simpson, H.J., 1984. A geochemical assessment of sedimentation and contaminant distributions in the Hudson-Raritan Estuary. NOS OMS 2, National Oceanic and Atmospheric Administration, Rockville.
- Opsahl, S., Benner, R., 1997. Distribution and cycling of terrigenous dissolved organic matter in

- the ocean. *Nature* 386, 480-482.
- Parker, C.A., 1968. *Photoluminescence of Solutions*. Elsevier, New York, 544 pp.
- Parlanti, E., Worz, K., Geoffroy, L., Lamotte, M., 2000. Dissolved organic matter fluorescence spectroscopy as a tool to estimate biological activity in a coastal zone submitted to anthropogenic inputs. *Org. Geochem.* 31, 1765-1781.
- Phillips, D. (Editor), 1985. *Polymer Photophysics: Luminescence, Energy Migration and Molecular Motion in Synthetic Polymers*. Chapman and Hall, New York, 437 pp.
- Prahl, F.G., Carpenter, R., 1983. Polycyclic aromatic hydrocarbon (PAH)-phase associations in Washington coastal sediment. *Geochim. Cosmochim. Acta* 47, 1013-1023.
- Preston, M.R., Riley, J.P., 1982. The interactions of humic compounds with electrolytes and three clay minerals under simulated estuarine conditions. *Est. Coast. Shelf Sci.* 14, 567-576.
- Ransom, B., Kim, D., Kastner, M., Wainwright, S., 1998. Organic matter preservation on continental slopes: Importance of mineralogy and surface area. *Geochim. Cosmochim. Acta* 62, 1329-1345.
- Rashid, M.A., Buckley, D.E., Robertson, K.R., 1972. Interactions of a marine humic acid with clay minerals and a natural sediment. *Geoderma* 8, 11-27.
- Raymond, P.A., Bauer, J.E., 2001a. DOC cycling in a temperate estuary: A mass balance approach using natural ^{14}C and ^{13}C isotopes. *Limnol. Oceanogr.* 46, 655-667.
- Raymond, P.A., Bauer, J.E., 2001b. Riverine export of aged terrestrial organic matter to the North Atlantic Ocean. *Nature* 409, 497-500.
- Raymond, P.A., Bauer, J.E., 2001c. Use of ^{14}C and ^{13}C natural abundances for evaluating riverine, estuarine, and coastal DOC and POC sources and cycling: a review and synthesis. *Org. Geochem.* 32, 469-485.
- Reeburgh, W.S., 1983. Rates of biogeochemical processes in anoxic sediments. *Ann. Rev. Earth Planet. Sci.* 11, 269-298.
- Romankevich, E.A., 1984. *Geochemistry of Organic Matter in the Ocean*. Springer-Verlag, Berlin, 334 pp.
- Saliot, A., Brault, M., Boussuge, C., 1988. The lipid geochemistry of interstitial waters of recent marine sediments. *Geochim. Cosmochim. Acta* 52, 839-850.
- Sansone, F.J., 1986. Depth distribution of short-chain organic acid turnover in Cape Lookout Bight sediments. *Geochim. Cosmochim. Acta* 50, 99-105.
- Santschi, P.H., Guo, L., Baskaran, M., Trumbore, S., Southon, J., Bianchi, T.S., Honeyman, B., Cifuentes, L., 1995. Isotopic evidence for the contemporary origin of high-molecular weight organic matter in oceanic environments. *Geochim. Cosmochim. Acta* 59, 625-631.
- Santschi, P.H., Balnois, E., Wilkinson, K.J., Zhang, J., Buffle, J., 1998. Fibrillar polysaccharides in marine macromolecular organic matter as imaged by atomic force microscopy and transmission electron microscopy. *Limnol. Oceanogr.* 43, 896-908.
- Seitz, W.R., 1981. Luminescence spectrometry (fluorimetry and phosphoresimetry). In: I.M. Kolthoff (Editor), *Treatise on Analytical Chemistry*. Wiley, New York, pp. 159-248.
- Senesi, N., Miano, T.M., Provenzano, M.R., Brunetti, G., 1991. Characterization, differentiation, and classification of humic substances by fluorescence spectroscopy. *Soil Sci.* 152, 259-271.
- Sharp, J.H., Benner, R., Bennett, L., Carlson, C.A., Dow, R., Fitzwater, S.E., 1993. Re-evaluation of high temperature combustion and chemical oxidation measurements of dissolved organic carbon in seawater. *Limnol. Oceanogr.* 38, 1774-1782.
- Sholkovitz, E.R., 1976. Flocculation of dissolved organic and inorganic matter during the mixing of river water and seawater. *Geochim. Cosmochim. Acta* 40, 831-845.
- Sholkovitz, E.R., Boyle, E.A., Price, N.B., 1978. The removal of dissolved humic acids and iron during estuarine mixing. *Earth Planet. Sci. Lett.* 40, 130-136.
- Sholkovitz, E.R., Mann, D.R., 1984. The pore water chemistry of $^{239,240}\text{Pu}$ and ^{137}Cs in sediments

- of Buzzards Bay, Massachusetts. *Geochim. Cosmochim. Acta* 48, 1107-1114.
- Simon, N.S., 1989. Nitrogen cycling between sediment and the shallow-water column in the transition zone of the Potomac River and Estuary. II. The role of wind-driven resuspension and adsorbed ammonium. *Est. Coast. Shelf Sci.* 28, 531-547.
- Smith, S.V., Hollibaugh, J.T., 1993. Coastal Metabolism and the Oceanic Organic Carbon Balance. *Rev. Geophys.* 31, 75-89.
- Starikova, N.D., 1970. Vertical distribution patterns of dissolved organic carbon in sea water and interstitial solutions. *Oceanology* 10, 796-807.
- Stevenson, F.J., 1994. *Humus Chemistry: Genesis, Composition, Reactions*. Wiley, New York, 496 pp.
- Stookey, L.L., 1970. Ferrozine - A new spectrophotometric reagent for iron. *Anal. Chem.* 42, 779-781.
- Stumm, W., 1992. *Chemistry of the Solid-Water Interface*. Wiley-Interscience.
- Sugimura, Y., Suzuki, Y., 1988. A high-temperature catalytic oxidation method for the determination of non-volatile dissolved organic carbon in seawater by direct injection of a liquid sample. *Mar. Chem.* 24, 105-131.
- Tegelaar, E.W., De Leeuw, J.W., Derenne, S., Largeau, C., 1989. A reappraisal of kerogen formation. *Geochim. Cosmochim. Acta* 53, 3103-3106.
- Thimsen, C.A., Keil, R.G., 1998. Potential interactions between sedimentary dissolved organic matter and mineral surfaces. *Mar. Chem.* 62, 65-76.
- Thompson, S., Eglinton, G., 1978. The fractionation of a Recent sediment for organic geochemical analysis. *Geochim. Cosmochim. Acta* 42, 199-207.
- Thurman, E.M., 1985. *Organic Geochemistry of Natural Waters*. Developments in Biogeochemistry. Nijhoff/Junk, Dordrecht, 497 pp.
- Tipping, E., 1981. The adsorption of aquatic humic substances by iron oxides. *Geochim. Cosmochim. Acta* 45, 191-199.
- Tomaic, J., Zutic, V., 1988. Humic material polydispersity in adsorption at hydrous alumina/seawater interface. *J. Colloid Interface Sci.* 26, 482-492.
- Turchenek, L.W., Oades, J.M., 1979. Fractionation of organo-mineral complexes by sedimentation and density techniques. *Geoderma* 21, 311-343.
- Valiela, I., 1995. *Marine Ecological Processes*. Springer-Verlag, New York.
- Velapoldi, R.A., Mielenz, K.D., 1980. A fluorescence standard reference material: Quinine sulfate dihydrate. National Bureau of Standards, Washington, DC.
- Vodacek, A., Hoge, F.E., Swift, R.N., Yungel, J.K., Peltzer, E.T., Blough, N.V., 1995. The use of in situ and airborne fluorescence measurements to determine UV absorption coefficients and DOC concentrations in surface waters. *Limnol. Oceanogr.* 40, 411-415.
- Wainright, S.C., 1987. Stimulation of heterotrophic microplankton production by resuspended marine sediments. *Science* 238, 1710-1712.
- Wang, X.-C., Lee, C., 1993. Adsorption and desorption of aliphatic amines, amino acids and acetate by clay minerals and marine sediments. *Mar. Chem.* 44, 1-23.
- Wang, X.-C., Druffel, E.R.M., Griffin, S., Lee, C., Kashgarian, M., 1998. Radiocarbon studies of organic compound classes in plankton and sediment of the northeastern Pacific Ocean. *Geochim. Cosmochim. Acta* 62, 1365-1378.
- Zsolnay, A., Baigar, E., Jimenez, M., Steinweg, B., Saccomandi, F., 1999. Differentiation with fluorescence spectroscopy the sources of dissolved organic matter in soils subjected to drying. *Chemosphere* 38, 45-50.

CURRICULUM VITA

Tomoko Komada

Education

- 1996-2002 Ph.D. in Oceanography, Rutgers the State University of New Jersey.
Dissertation: Sorptive dynamics and fluorescence properties of organic carbon within coastal sedimentary environments.
- 1994-1996 M.S. in Oceanography, Rutgers, the State University of New Jersey. *Thesis:* Verification of the use of pH and P_{CO2} microelectrodes in determining the concentration gradients of total CO₂ in marine sediments.
- 1989-1993 B.A. in Chemistry, International Christian University, Tokyo.
Senior Project: Extraction and identification (by GC-MS) of organo-phosphorous and organo-chlorine pesticides in imported tropical fruits.

Employment

- 1994-2001 Graduate Assistant, Institute of Marine and Coastal Sciences, Rutgers University
- Spring 1999 Teaching Assistant, Oceanographic Methods and Data Analysis, Institute of Marine and Coastal Sciences, Rutgers University
- Fall 2000 Teaching Assistant, Chemical Oceanography, Institute of Marine and Coastal Sciences, Rutgers University

Publications

- Komada T., Reimers C. E., Boehme S. E. (1998)** Dissolved inorganic carbon profiles and fluxes determined using pH and P_{CO2} microelectrodes. *Limnology and Oceanography* 43, 769-781.
- Komada T., Reimers C. E. (2001)** Resuspension-induced partitioning of organic carbon between solid and solution phases from a river-ocean transition. *Marine Chemistry* 176, 155-174.